

N 67 11729 (THRU)
 (ACCESSION NUMBER)
102 (CODE)
 (PAGES)
CR 79508 (CATEGORY)
 (NASA CR OR TMX OR AD NUMBER)

GPO PRICE \$ _____

CFSTI PRICE(S) \$ _____

Hard copy (HC) 4.00Microfiche (MF) .75

ff 653 July 85



WYLE LABORATORIES
 TESTING DIVISION, HUNTSVILLE FACILITY

research

WYLE LABORATORIES - RESEARCH STAFF
Report WR 65-28

THE STABILITY OF CAPTIVE BALLOONS FOR
INSTRUMENT FLYING, INCLUDING ANALYSIS
OF MULTI-CABLE CONFIGURATIONS

by
R.C. Potter

Work Performed under Contract NAS8-5384

Prepared by: R.C.P.
R.C. Potter

Approved by Kenneth McK. Eldred
Kenneth McK. Eldred
Director of Research

Approved by R. W. White
R.W. White

November 1965

COPY NO. 19

SUMMARY

Recent requirements for accurate positioning of instruments in the atmosphere, near the ground but too high for simple structural support, has led to a revival in captive balloon flying. Such systems are normally flown with the balloon on several cables to provide for maximum stability. A balloon that moves only a small distance with a change in wind velocity is considered to have good stability, and will be more suitable for flying instruments than a balloon which shifts its position greatly with a small wind velocity change. This report presents the results of a study to determine design criteria and operational characteristics of multi-cable balloon configurations.

A single cable system is first analyzed to determine the relations between the various parameters; such as cable tension, length, weight, slope, position and the wind speed. The effects of neglecting either the aerodynamic drag of the cable or the weight of the cable, are examined. An example of a balloon flying on a single cable is then presented, and it is shown that the cable drag has little effect on the balloon stability with varying wind speed.

This single cable analysis is applied to examples of a single balloon flying on several cables. These systems are initially considered as being symmetrical so that they can be reduced to simple configurations in a single plane. The components of the forces in the cables of the balloon are determined, from the results of the single cable analysis, and these are then equated to the balloon excess lift and drag, to solve for the position of the balloon in a given configuration and at different wind speeds. The solution is simplified by assuming that no aerodynamic lift force due to the balloon exists, and the stability of four basic two-cable configurations is determined. This assumption, of no aerodynamic lift, is necessary, since otherwise, the simultaneous equations for the solution of the system are non-linear relationships and are not simple reducible. However, one particular system is solved, with the balloon aerodynamic lift included, by using a digital computer to search for the solution.

The results obtained for these different configurations are then used to examine the basic properties of multi-cable systems. The various parameters are examined to determine those which give maximum stability for instrument flying, and an optimum configuration of two long upstream cables and one short downstream cable is suggested. The importance of setting up this cable system symmetrically about the wind direction axis, to take full advantage of the configuration, is mentioned. The extra stability that can be achieved by a balloon with aerodynamic lift is determined. However, it is pointed out that the configuration must also be stable throughout the low wind speed range.

The problems of launching and handling multi-cable systems, to ensure that the correct configuration is attained, are discussed. This can prove difficult when balloons which generate aerodynamic lift are being launched in high speed winds. The resultant recommendations for designing multi-cable configurations are included in a final section.

An Appendix gives details of the computer programs developed; one for a single cable and a second for an approximate solution of a two cable system with balloon aerodynamic lift. The actual programs are presented, with examples and results, and are in a form suitable for the solution of other cable configurations.

A final Appendix is concerned with the particular balloon system presently used by NASA, MSFC, to obtain acoustic measurements of the noise field from large rocket engines. The presently used technique for flying the system is discussed and criticized. A better configuration is suggested and its stability characteristics are calculated and compared to the existing configuration.

TABLE OF CONTENTS

	PAGE NO.
SUMMARY	ii
TABLE OF CONTENTS	iv
LIST OF TABLES	v
LIST OF FIGURES	vi
LIST OF SYMBOLS	viii
1.0 INTRODUCTION	1
2.0 EQUILIBRIUM OF A BALLOON CABLE	3
2.1 Basic Cable Theory	3
2.2 Balloon Cable, Neglecting the Weight of the Cable	8
2.3 Balloon Cable, Neglecting the Cable Aerodynamic Drag	10
3.0 SINGLE CABLE CONFIGURATIONS	14
3.1 Single Cable, Neglecting Cable Aerodynamic Drag	14
3.1.1 Numerical Example	18
3.2 Single Cable, Including Cable Aerodynamic Drag	20
4.0 MULTI-CABLE CONFIGURATIONS	22
4.1 Simple Two Cable Array in the Wind Direction Axis	22
4.2 Two Cable Examples, with Constant Excess Lift Force	24
4.3 Two Cable Example, Including the Aerodynamic Lift of the Balloon	28
5.0 DESIGN OF MULTI-CABLE CONFIGURATIONS	30
6.0 CONCLUDING REMARKS	33
APPENDIX A Solution of Multi-Cable Configurations, Single Cable Behavior, and Computer Programs	35
A1 Solution for Two Cable Configuration	35
A2 Single Cable Behavior	38
APPENDIX B Marshall Space Flight Center Balloon	41
B1 Description of the MSFC Balloon System	41
B2 Balloon on a Single Cable	43
B3 Balloon on Several Cables	45
B4 Discussion and Concluding Remarks	46
REFERENCES	48
FIGURES	49

LIST OF TABLES

		PAGE NO.
TABLE I	Balloon A and Cable	19
TABLE II	Flow Diagram for POT 21	37
TABLE III	Calculation of Payload Weight for MSFC Balloon	44

LIST OF FIGURES

	PAGE NO.
Figure 1. Element of Cable.	49
Figure 2. Cable Parameter τ , from Neumark (Reference 1) .	50
Figure 3. Cable Parameter λ , from Neumark (Reference 1) .	51
Figure 4. Cable Parameter σ , from Neumark (Reference 1) .	52
Figure 5. Balloon on Single Cable.	53
Figure 6. Balloon A - Aerodynamic Forces.	54
Figure 7. Single Cable and Balloon Stability.	55
Figure 8. Single Cable and Balloon Stability.	56
Figure 9. Single Cable and Balloon Stability.	57
Figure 10. Balloon on Single Cable, Effect of Aerodynamic Drag of Cable.	58
Figure 11. Balloon on Single Cable, Effect of Aerodynamic Drag of Cable.	59
Figure 12. Simple Two Cable Array, in the Wind Direction Axis.	60
Figure 13. Two Cable Balloon Stability, Configuration A 1.	61
Figure 14. Two Cable Balloon Stability, Configuration A 1.	62
Figure 15. Stability of Configuration A2, Compared to Single Cable Example.	63
Figure 16. Two Cable Balloon Stability, Configuration A 2.	64
Figure 17. Cable Tension at Balloon, Configuration A 2.	65
Figure 18. Cable Angles at Balloon, Configuration A 2.	66
Figure 19. Two Cable Balloon Stability, Configuration B.	67
Figure 20. Cable Tension at Balloon, Configuration B.	68
Figure 21. Two Cable Balloon Stability, Configuration C.	69
Figure 22. Two Cable Balloon Stability, Configuration C.	70
Figure 23. Cable Tension at Balloon, Configuration C.	71
Figure 24. Cable Angle at Balloon, Configuration C.	72
Figure 25. Two Cable Balloon Stability, Configuration D.	73
Figure 26. Two Cable Balloon Stability, Configuration D.	74
Figure 27. Balloon Configuration D, Cable Tension at Balloon.	75

LIST OF FIGURES (CONTINUED)

	PAGE NO.
Figure 28. Configuration D, Cable Angles at Balloon.	76
Figure 29. Effect of Aerodynamic Lift of Balloon, Configuration D.	77
Figure 30. Three Cable Configurations.	78
Figure 31. Balloon Positioned Upstream of Rocket.	79
Figure 32. Computer Program POT 21, for Solution of Two-Cable Configuration with Aerodynamic Lift.	80
Figure 33. Typical Results for POT 21.	81
Figure 34. Computer Program POT 15, for Solution of Single Cable.	82
Figure 35. Typical Results for POT 15.	83
Figure 36. Single Cable Analysis.	84
Figure 37. Vertical Components of Tension Configuration A2, Y = 856 ft.	85
Figure 38. Sample Tabulation to Solve for Balloon Position.	86
Figure 39. MSFC Balloon Rigging.	87
Figure 40. Estimated Aerodynamic Lift and Drag Coefficients for MSFC Balloon.	88
Figure 41. Estimated Aerodynamic Forces of MSFC Balloon.	89
Figure 42. Calculated Behavior of MSFC Balloon on a Single Cable.	90
Figure 43. MSFC Balloon, 172.5 ft Base.	91
Figure 44. MSFC Balloon, 400 ft Base.	92
Figure 45. MSFC Balloon, 1200 ft Base.	93

LIST OF SYMBOLS

$a, b,$ and c	Chapter 2, Cable parameters
$a, b, c,$ and d	Chapter 4, Parameters in balloon equations
A	$= \frac{1}{2} \rho V^2 C_D d / w$, Cable parameter
A_D	Cross-sectional area of balloon for calculating aerodynamic drag.
A_L	Cross-sectional area of balloon for calculating aerodynamic lift.
B and D	Chapter 2, Parameters in cable equations.
c	$= T \cos \theta / w$, Cable parameter
C_D	Aerodynamic drag coefficient
C_L	Aerodynamic lift coefficient
d	Diameter of cable
D	Aerodynamic drag of the balloon
D_c	Aerodynamic drag of the cable
ℓ	Length of the cable
L	Lift of the balloon
L_b	Buoyant lift of balloon
n	$= wA$, Cable parameter
S	Cross-sectional area of balloon
T	Cable tension
V	Wind velocity
w	Weight per unit length of cable
W	Weight of payload and balloon
W_1	Weight of balloon
W_2	Weight of payload
$x, y,$ and z	Coordinate axes system
X	Chapter 4, Base distance of two cable system
X and Y	Horizontal and vertical positions of balloon relative to tethering point.
z	$= \cos \theta$, Chapter 2.

LIST OF SYMBOLS (CONTINUED)

θ	Angle of cable to horizontal axis
ρ	Gas density
ψ	$= 1/2 (\tan^{-1} 2A)$, Cable parameter
τ , σ , and λ	Chapter 2, Cable parameters
η	$= T_1 \cos \theta_1 / w$, Cable parameters
ξ	$= \tan \theta$
Σ	Volume of balloon

Subscripts and Suffixes

l	Point on cable at balloon
o	Point on cable at tether
'	General point on cable
h	Horizontal component
a	Atmospheric property
e	Balloon gas property
1 and 2	Chapter 4, Refer to the two cable systems.

1.0 INTRODUCTION

The flying of captive balloons is once again becoming a serious scientific technique after being neglected in the concentration on heavier-than-air machines. Free flying balloons have been used to examine the upper atmosphere and for meteorological experiments. Now the need to place instruments at fixed points near the ground, but at positions too high for a simple structure, has seen a revival in captive balloon flying. Typical examples are aerial photography and acoustic measurements of rocket noise, the latter requirement being the motivation behind this study.

Large solid propellant rockets are usually tested by firing them vertically upwards. This technique dispenses with the need for massive thrust stands and exhaust flow deflectors and solves the problems of erosion of the neighboring structure due to the exhaust gas. These firings offer the opportunity to obtain some good acoustic data of the noise field from a rocket motor, particularly since the majority of the noise is propagated upwards into a clear free field. This directional characteristic is typical of noise generated aerodynamically by the exhaust gas mixing with the atmosphere, where the principal radiation is directed at an acute angle to the rocket exhaust flow direction. With normal rocket tests, the exhaust flow is either deflected or horizontal, and so the majority of the noise is propagated into a cluttered far-field. Thus, the opportunity of obtaining basic data on rocket noise production and propagation into a clean far-field and for such a large rocket typical of those for the large space vehicles under development and construction, can not be neglected. Accordingly, a program of acoustic measurements using microphones positioned by captive balloons was initiated. For this purpose, it is essential that the instruments be positioned at the required point, that this point be known and, most important, that the position of the instruments did not change greatly with wind variations.

Once the acoustic measurement program was started, it became obvious that no general experience of flying balloons, on the several cables necessary for stability, existed. Captive balloons, such as used for aircraft protection during the Second World War, were simply winched out and allowed to wander across the sky. However, this technique was not suitable for the accurate positioning required for this acoustic measurement program. Consequently, a study was initiated to help produce fundamental data and design techniques for such multi-cable captive balloon configurations. The results of this study are presented in this report.

First, the basic equations of a single cable configuration are considered and these results are used to analyze various multi-cable configurations. It is necessary that certain simplifications be made to obtain solutions for the more complex cases, and these are justified and given with their limitations. Two basic programs for solving multi-cable configurations are then presented. The first, and more accurate method, requires that the aerodynamic lift of the balloon be zero; that is the excess lift, the lift of the balloon less its weight and the payload weight, remains constant at all wind velocities. Several configurations are examined using this method, and the basic rules of design

for multi-cable systems are determined. The second program, including the balloon aerodynamic lift, is used to study a single simple system. These programs are included in an Appendix, and will allow analyses of other balloon systems to be completed.

A final Appendix is concerned with the actual balloon used by NASA to position the microphones. An optimum cable configuration is determined and the operational characteristics of this system are presented.

2.0 EQUILIBRIUM OF A BALLOON CABLE

In this section, the basic forces acting on a balloon cable will be stated, and the equations expressing the cable shape and tension will be derived. Certain special cases, concerning the neglect of either the cable weight or its aerodynamic drag forces, will be included since these simplifications will generally be necessary if the results are to be applied to practical examples. A single cable will be considered, and it will be taken as flying in a vertical plane in the mean wind direction. The basic theory is due to Neumark (Reference 1), although certain parts were derived independently for this study. The application of the results requires the use of certain detailed integral expressions, which are tabulated in Reference 1 for a wide range of cable parameters. The theory is repeated here, since it forms the basis of the solution of the multi-cable configurations, and also because it indicates those relevant parameters that determine the cable configurations.

2.1 Basic Cable Theory

Figure 1 is a sketch of an element of a cable δl long, and shows those forces that act on the element. These forces are the cable tension T , which changes over the small length of the element by the amount δT , the weight of the cable $w\delta l$ where w is the weight per unit length, and the aerodynamic drag D . The cable is considered as a long infinite cylinder, and so the drag is taken as acting normal to the element. Various wind tunnel tests (Reference 2) have shown this approach is perfectly valid for cables similar to those used for balloons, where the length to diameter ratio is large and the component of aerodynamic force along the cable can be neglected. This aerodynamic drag will then be considered as two components, one vertical and the other horizontal, but first a value for the overall drag coefficient must be assigned.

The value of the drag coefficient for a cylinder normal to the airstream is 1.1 when the Reynolds number is less than the critical value, and 0.3 when the Reynolds number is greater than the critical value, (Reference 3). The critical Reynolds number for a cylinder, based on the cylinder diameter, lies within the range of 80,000 to 400,000. Taking the lower value, and putting the air density as 0.00238 slug/cu.ft. and the kinematic viscosity of air as 0.000168 ft²/sec, the critical velocity for a 0.5 inch diameter cylinder calculates as 322 fps. Since this velocity is much higher than any that the balloon cable will experience, the sub-critical drag coefficient of 1.1 will therefore be applicable. This figure is substantiated by Hoerner (Reference 2) who also presents details of the drag of yawed cables. Hoerner gives the drag coefficient for a cable, yawed so it forms an angle θ with the stream direction, as $C_D \sin^2\theta$, where C_D is the basic drag coefficient for a normal cylinder. This then produces drag coefficient components for the element of the cable of $1.1 \sin^2\theta \cos \theta$ vertically and $1.1 \sin^3\theta$ horizontally. Note that the vertical component will generally act down, as the balloon will be directed downstream of its tethering point by the wind.

Now equating the component forces on the cable element, in the equilibrium position,

$$(T + \delta T) \cos \delta \theta = T + w \delta \ell \sin \theta$$

$$(T + \delta T) \sin \delta \theta = \frac{1}{2} \rho V^2 1.1 \sin^2 \theta \delta \ell d + w \delta \ell \cos \theta$$

where the notation is as given before and shown in Figure 1, with the wind velocity V assumed horizontal, and where ρ is the air density and d the cable diameter.

In the limit of a very small element, these equations reduce to

$$\delta T = w \delta \ell \sin \theta \quad (1)$$

$$T \delta \theta = \frac{1}{2} \rho V^2 1.1 \sin^2 \theta \delta \ell d + w \delta \ell \cos \theta \quad (2)$$

The geometry of the cable element gives

$$\delta x = \delta \ell \cos \theta \quad (3)$$

$$\delta y = \delta \ell \sin \theta \quad (4)$$

Eliminating $\delta \ell$ from Equations (1) and (2) produces

$$\frac{\delta T}{T} = \frac{\sin \theta \delta \theta}{A \sin^2 \theta + \cos \theta} \quad (5)$$

where

$$A = \frac{\frac{1}{2} \rho V^2 1.1 d}{w} \quad (6)$$

The next step is to integrate Equation (5) between the bottom of the cable, indicated by a suffix o , and a point on the cable indicated by a prime. The point l is where the cable meets the balloon and a special case of the general point.

Then

$$\int_{\theta_o}^{\theta'} \frac{dT}{T} = \int_{\theta_o}^{\theta'} \frac{\sin \theta}{A \sin^2 \theta + \cos \theta} d\theta$$

$$\left[\log_e T \right]_{\theta_0}^{\theta'} = \int_{\theta_0}^{\theta'} \frac{\sin \theta}{-A \cos^2 \theta + A + \cos \theta} d\theta$$

$$= \int_{\cos^{-1} \theta_0}^{\cos^{-1} \theta'} \frac{dz}{Az^2 - z - A}$$

where $z = \cos \theta$

$$= \int \frac{dz}{a z^2 + b z + c}$$

where $a = A$, $b = -1$, and $c = -A$

The term $4ac$ is always negative, since A is always positive being a real quantity, so

$$4ac < b^2$$

Using Reference 4, the integration can be completed,

$$\left[\log_e T \right]_{\theta_0}^{\theta'} = \left[\frac{1}{(1 + 4A^2)} \log_e \left(\frac{2Az - 1 - (1 - 4A^2)^{1/2}}{2Az - 1 + (1 + 4A^2)^{1/2}} \right) \right]$$

Then putting $2A = \tan 2\psi$

$$\left[\log_e T \right]_{\theta_0}^{\theta'} = \left[\cos 2\psi \log_e \frac{\tan 2\psi z - 1 - \sec 2\psi}{\tan 2\psi z - 1 + \sec 2\psi} \right]$$

and substituting for z , and simplifying

$$= \left[\cos 2\psi \log_e \left(\frac{\cos \theta - \cot \psi}{\cos \theta + \tan \psi} \right) \right]_{\theta_o}^{\theta_1}$$

Hence, dropping the prime to indicate the general point, the tension T is proportional to the factor τ , where

$$\tau(\theta) = \left(\frac{\cos \theta - \cot \psi}{\cos \theta + \tan \psi} \right)^{\cos 2\psi} \quad (7)$$

Then if the suffix o refers to the ground point and the suffix 1 refers to the cable at the balloon

$$T = T_1 \frac{\tau}{\tau_1} \quad \text{and} \quad T_o = T_1 \frac{\tau_o}{\tau_1} \quad (8)$$

Neumark, in Reference 1, using a slightly different approach to the integration, obtained the same value for the tension proportionality factor τ . He has tabulated this and other factors in Reference 1, and they will be required to solve for this single cable configuration.

From Equations (2) and (8)

$$\delta \ell = \frac{T_1}{\tau_1} \frac{\tau \delta \theta}{w A \sin^2 \theta + w \cos \theta} \quad (9)$$

and integrating to obtain the length of the cable from the ground to the point under consideration,

$$\ell = \frac{T_1}{\tau_1} \int_{\theta_o}^{\theta_1} \frac{\tau}{w A \sin^2 \theta + w \cos \theta} d\theta$$

$$\text{Putting } \lambda(\theta) = \int_0^\theta \frac{n\tau}{n \sin^2 \theta + w \cos \theta} d\theta$$

where $n = wA$

$$\text{Then } l = \frac{T_1}{n\tau_1} (\lambda - \lambda_0) \quad (10)$$

Similarly from Equation (3)

$$x = \frac{T_1}{n\tau_1} (\sigma - \sigma_0) \quad (11)$$

$$\text{where } \sigma(\theta) = \int_0^\theta \frac{n\tau \cos \theta}{n \sin^2 \theta + w \cos \theta} d\theta$$

and the vertical height is given by

$$y = \frac{T_1}{w\tau_1} (\tau - \tau_0) \quad (12)$$

These factors are all in Neumark's notation of Reference 1, which is continued here for convenience. Neumark tabulated the factors τ , λ , and σ for various values of the factor n/w typical to balloon cables, and certain of these values are shown in Figures 2 to 4. These figures will allow quick calculations, but they also indicate that the functions change quite slowly with cable angle over a large range. Therefore, when solving for particular examples, the tables of Reference 1, which are very detailed, are to be preferred to these figures.

To solve for a particular case of a single cable, a value for the ratio n/w is taken appropriate to one of the tabulated sets of factors. Since the cable parameters are known, the appropriate values of A , ψ , and the wind velocity V can be calculated. Then these are used to determine the aerodynamic lift and drag of the balloon and so the values of the tension T_1 , and cable angle θ_1 , at the balloon can be calculated.

Now the values of T_1 , n , τ_1 and λ_1 , are known, as is the length of the cable. These

allow the value of λ_o to be found, and the corresponding factors, σ_o and τ_o to be determined. Substituting into the equations for y and x , gives the vertical and horizontal position of the balloon. This process is repeated for other values of the factor n/w to obtain the balloon performance as the wind velocity changes.

Alternative approaches can involve solving for the necessary cable length to fly the balloon at a given height, or over a given downstream point. The method here is again similar to that outlined above.

2.2 Balloon Cable, Neglecting the Weight of the Cable

The neglect of the cable weight can be a fair approximation when the aerodynamic forces are large, and only a light cable is considered. This is more normally applicable to aircraft towing cables rather than balloons. However, it could be important for certain stabilizing cables, which are more concerned with fixing the balloon in position rather than taking the lift forces of the system. In this case,

$$\tan 2\psi = 2A \rightarrow \infty \quad \text{when } w \rightarrow 0$$

so

$$2\psi \rightarrow \pi/2$$

$$\psi \rightarrow 45^\circ \quad \text{and} \quad \tau \rightarrow 1$$

Then $T = T_1 = \text{constant throughout the length of the cable.}$

λ and $\sigma \rightarrow \infty$ as $w \rightarrow 0$

$$\text{but } \lambda - \lambda_o \rightarrow \int_{\theta_o}^{\theta} \frac{1}{\sin^2 \theta} d\theta = \cot \theta_o - \cot \theta \quad (13)$$

$$\sigma - \sigma_o \rightarrow \int_{\theta_o}^{\theta} \frac{\cos \theta}{\sin^2 \theta} d\theta = \operatorname{cosec} \theta_o - \operatorname{cosec} \theta \quad (14)$$

The derivative of τ , with respect to θ , can be obtained from Equations (5) and (8) as,

$$\frac{d\tau}{d\theta} = \frac{\tau \sin \theta}{A \sin^2 \theta + \cos \theta}$$

Then

$$\frac{\tau - \tau_o}{w} \rightarrow \int_{\theta_o}^{\theta} \frac{1}{A w \sin \theta} d\theta \quad \text{as } w \rightarrow 0$$

$$= \frac{1}{n} \left(\log_e \tan \frac{\theta}{2} - \log_e \tan \frac{\theta_o}{2} \right) \quad (15)$$

Therefore $n\ell = T (\cot \theta_o - \cot \theta)$ (16)

$$nx = T (\operatorname{cosec} \theta_o - \operatorname{cosec} \theta) \quad (17)$$

$$ny = T \left(\log_e \tan \frac{\theta}{2} - \log_e \tan \frac{\theta_o}{2} \right) \quad (18)$$

where T is the tension at all points in the cable.

To solve for the cable shape relationship, it is necessary to eliminate θ between Equations (17) and (18).

From Equation (17)

$$\operatorname{cosec} \theta = \operatorname{cosec} \theta_o - \frac{nx}{T} \quad (19)$$

and from Equation (18)

$$\log_e \tan \frac{\theta}{2} = \frac{ny}{T} + \log_e \tan \frac{\theta_o}{2} = B$$

$$\tan \frac{\theta}{2} = \operatorname{cosec} \theta - \cot \theta = e^B$$

$$\operatorname{cosec} \theta - (\operatorname{cosec}^2 \theta - 1)^{1/2} = e^B$$

Squaring both sides and simplifying

$$\operatorname{cosec} \theta = \frac{1}{2} \left(e^B + \frac{1}{e^B} \right) = \cosh B \quad (20)$$

Substituting Equation (20) into Equation (19)

$$\cosh B = \operatorname{cosec} \theta_o - \frac{nx}{T}$$

which is an equation for a common catenary in x and y with a horizontal axis, since B is a direct linear function of y . The equation will not be further simplified, to determine the origin, since the more useful example for balloons will be with the air drag of the cable neglected.

2.3 Balloon Cable, Neglecting the Cable Aerodynamic Drag

In this case, consider the aerodynamic drag term being reduced to zero. Then the drag parameter n approaches zero.

$$n \rightarrow 0$$

$$\cot 2\psi \rightarrow \infty$$

So $\psi \rightarrow 0$

Which means the parameter τ apparently approaches infinity, from Equation (7).

However, in the limit where $\psi \rightarrow 0$

$$\cot \psi \rightarrow 2 \cot 2\psi = w/n$$

So putting this value into Equation (7) and noting that

$$\tan \psi \rightarrow 0$$

$$\cos 2\psi \rightarrow 1$$

$$\tau(\theta) \rightarrow \frac{\frac{w}{n} - \cos \theta}{\cos \theta}$$

and in the limit

$$\tau(\theta) = \frac{w}{n \cos \theta} \quad (22)$$

Since $w/(n \cos \theta)$ is infinitely large compared to 1.

Therefore $n\pi = w \sec \theta$.

Hence

$$\lambda(\theta) = \int_0^\theta \sec^2 \theta \, d\theta = \tan \theta$$

and

$$\sigma(\theta) = \int_0^\theta \sec \theta \, d\theta = \log_e \tan \left(\frac{\pi}{4} + \frac{\theta}{2} \right)$$

Also

$$T = \frac{T_1 \cos \theta_1}{\cos \theta} = \frac{T_o \cos \theta_o}{\cos \theta}$$

or

$$T \cos \theta = \text{constant} \quad (23)$$

This is the horizontal force on the system and is equal to the aerodynamic drag of the balloon.

Substituting these values into the equation for the cable length, and position,

$$\ell = \frac{T \cos \theta}{w} (\tan \theta - \tan \theta_o) \quad (24)$$

$$x = \frac{T \cos \theta}{w} \left[\log_e \left(\frac{\tan \left(\frac{\pi}{4} + \frac{\theta}{2} \right)}{\tan \left(\frac{\pi}{4} + \frac{\theta_o}{2} \right)} \right) \right] \quad (25)$$

$$y = \frac{T \cos \theta}{w} (\sec \theta - \sec \theta_o) \quad (26)$$

The relationship for the cable shape is obtained by eliminating θ from Equations (25) and (26).

First put $\frac{T \cos \theta}{w} = c$

Then from Equation (25)

$$e^D = \tan \left(\frac{\pi}{4} + \frac{\theta}{2} \right)$$

where $D = \frac{x}{c} + \log_e \tan \left(\frac{\pi}{4} + \frac{\theta_o}{2} \right)$

$$e^D = \frac{\cot \frac{\pi}{4} + \cot \frac{\theta}{2}}{\cot \frac{\pi}{4} \cot \frac{\theta}{2} - 1}$$

$$= \frac{1 + \cot \frac{\theta}{2}}{\cot \frac{\theta}{2} - 1}$$

$$= \frac{\sin \theta + 1 + \cos \theta}{1 + \cos \theta - \sin \theta}$$

Then

$$e^D + \frac{1}{e^D} = \frac{1 + \cos \theta + \sin \theta}{1 + \cos \theta - \sin \theta} + \frac{1 + \cos \theta - \sin \theta}{1 + \cos \theta + \sin \theta}$$

$$= 2 \sec \theta \quad \text{after simplification.}$$

Hence $\sec \theta = \cosh D$ (27)

Substitute Equation (27) into Equation (26),

$$\frac{y}{c} + \sec \theta_o = \cosh \left[\frac{x}{c} + \log_e \tan \left(\frac{\pi}{4} + \frac{\theta_o}{2} \right) \right] \quad (28)$$

This is the curve of a common catenary, with a vertical axis. (Note that neglecting the weight of the cable produces a common catenary with a horizontal cable.) The term $\sec \theta_o$ and the logarithmic function are included in the equation, since the cable origin

is at the ground point, where the cable is not horizontal. If x and y are measured from that point where the cable is horizontal, (or would be if extended underground,) the equation reduces to

$$\frac{y}{c} = \cosh \frac{x}{c} - 1 \quad (29)$$

where $c = T \cos \theta / w \quad (29)$

and $T \cos \theta$ is a constant $= T_h$, the tension at the bottom horizontal point of the catenary. Further, if the origin is positioned vertically at a distance c below the horizontal point of the complete catenary, the equation reduces to

$$y = \frac{T_h}{w} \cosh \left(\frac{x}{T_h/w} \right) \quad (30)$$

3.0 SINGLE CABLE CONFIGURATIONS

The single cable and balloon will be examined in the equilibrium position, where the balloon is stationary and directly downstream of the tethering point. In actual practice the balloon will generally wander, and typical examples of this have been noted by Waters (Reference 5). He measured the position of a balloon on a single cable with time, and, although the acceleration of the balloon was small, lateral velocities of up to 70 percent of the mean wind speed were recorded. The displacement in the horizontal axis in the wind direction was noted to reach over 125 feet for a cable 920 feet long. The displacement normal to the wind direction was much greater, being some 500 feet overall. The balloon oscillated with a definite time period, but attempts to describe the balloon motion as a simple harmonic motion generally underestimated the maximum accelerations and velocities in two component directions. This wander will obviously be important for the case of balloons flying instruments, when the exact location of the measurement point is required. Neumark (Reference 1) derived expressions for the cable derivatives, following the results he had developed for the cable configuration. These were extremely complicated expressions and produced values that were dependent on the assumption of constant cable length. This assumption becomes less acceptable when nylon line, which stretches considerably under load, replaces the wire cables previously used. However, the inclusion of this stretching effect in the mathematical derivation of stability derivatives of the cable will complicate the process even more. Therefore, for the present time, such work will have to be restricted to experimental examination of actual flying balloons.

However, for the analysis here, the exact location of the instruments will be generally the major concern of the experiments, and multi-cable systems will always be required, as the wandering motion of a single cable system cannot be tolerated. Therefore, the following sections will only consider the equilibrium stability of the balloon and cable systems.

3.1 Single Cable, Neglecting Cable Aerodynamic Drag

The equilibrium stability of a single cable and balloon, neglecting the cable aerodynamic drag, will be examined by studying a practical example. The cable parameters are shown in Figure 5, where the tension T , at the top of the cable, equals the component forces of the balloon. These are the aerodynamic drag of the balloon and the aerodynamic lift plus the excess lift of the balloon. In the figure, the suffix o refers to the tethering point on the ground and the suffix 1 is the position at the top of the cable. The angle θ is the angle that the cable makes to the horizontal at each point.

Since the aerodynamic drag of the cable is neglected, the cable shape is given by Equation (30), which is repeated here

$$y = \frac{T_h}{w} \cosh \left(\frac{x}{T_h/w} \right) \quad (30)$$

where T_h is the horizontal component of the cable tension, which is the same at all points in the cable and equal to the aerodynamic drag of the balloon

$$T_h = T_1 \cos \theta_1 = T_o \cos \theta_o = T \cos \theta = D \quad (31)$$

The position of the balloon, the top of the cable in fact, relative to the tethering point is quickly determined in terms of the relevant cable parameters, which will be the forces and cable angle at the balloon. These can be equated to the aerodynamic and buoyancy forces of the balloon to allow the position of the balloon to be determined with varying wind velocity.

From Equation (26) the height of the balloon above the tethering point Y can be obtained

$$Y = \frac{T_1 \cos \theta_1}{w} (\sec \theta_1 - \sec \theta_o) \quad (32)$$

Then, equating the vertical forces on the whole cable,

$$T_1 \sin \theta_1 = w\ell + T_o \sin \theta_o$$

$$\frac{T_1 \sin \theta_1}{T_1 \cos \theta_1} = \frac{w\ell}{T_1 \cos \theta_1} + \frac{T_o \sin \theta_o}{T_1 \cos \theta_1}$$

and using Equation (31)

$$\tan \theta_1 = \frac{w\ell}{T_1 \cos \theta_1} + \tan \theta_o$$

$$\text{Hence} \quad \tan \theta_o = \tan \theta_1 - \frac{w\ell}{T_1 \cos \theta_1} \quad (33)$$

$$\text{and} \quad \sec \theta_o = 1 + \tan^2 \theta_o^{1/2} \quad (34)$$

Substituting Equation (33) into Equation (34), and the result into Equation (32) gives

$$Y = \frac{T_1 \cos \theta_1}{w} \left\{ \sec \theta_1 - \left[1 + \tan \theta_1 - \left(\frac{w\ell}{T_1 \cos \theta_1} \right)^2 \right]^{1/2} \right\} \quad (35)$$

which is the vertical height of the balloon above the tethering point, completely in terms of the cable weight and length and the cable tension and angle at the top point.

Similarly, the horizontal distance of the balloon from the tethering point can be determined in the same parameters.

From Equation (30),

$$\frac{dy}{dx} - \tan \theta = \sinh \left(\frac{x}{T_h/w} \right)$$

Therefore,

$$x = \frac{T_h}{w} \sinh^{-1} (\tan \theta)$$

The horizontal distance of the balloon from its tethering point is given by

$$\begin{aligned} X &= x_1 - x_0 \\ &= \frac{T_1 \cos \theta_1}{w} \left[\sinh^{-1} (\tan \theta_1) - \sinh^{-1} (\tan \theta_0) \right] \end{aligned}$$

and substituting for $\tan \theta_0$

$$X = \frac{T_1 \cos \theta_1}{w} \left[\sinh^{-1} (\tan \theta_1) - \sinh^{-1} \left(\tan \theta - \frac{w\ell}{T_1 \cos \theta_1} \right) \right] \quad (36)$$

Equations (35) and (36) give the position of the top of a cable, when no aerodynamic drag of the cable is considered, and are in terms of the forces at the top of the cable. These equations are sufficient for solving for the case of a single balloon on a single cable. The values of the excess lift and drag of the balloon are calculated from its characteristics. This will include any aerodynamic lift due to velocity. Then these values are used to solve for the tension in the cable T_1 , and the angle of the cable at the balloon θ_1 . Using the weight per unit length and the length of the cable, the

equilibrium position of the balloon is found by substituting into Equations (35) and (36). The position of the balloon with varying wind speed, which affects the aerodynamic drag and lift of the balloon, can then be determined.

The stability of a system can be defined as the way the balloon moves in space with varying wind speed. A good stable system, suitable for positioning instruments at a given point, would have very little movement as the wind changes. The stability of various balloon and single cable configurations will now be considered, as the basic parameters of the system are varied.

The position of the balloon is given by Equations (35) and (36). Putting

$$\eta = \frac{T_1 \cos \theta_1}{w\ell} \quad \text{and} \quad \xi = \tan \theta \quad (37)$$

these equations can be written as

$$\frac{X}{\ell} = \eta \left[\sinh^{-1} \xi - \sinh^{-1} \left(\xi - \frac{1}{\eta} \right) \right] \quad (38)$$

$$\text{and} \quad \frac{Y}{\ell} = \eta \left\{ (1 + \xi^2)^{1/2} - 1 + \left[\left(\xi - \frac{1}{\eta} \right)^2 \right]^{1/2} \right\} \quad (39)$$

Then equating the forces at the balloon

$$\frac{D}{w\ell} = \eta \quad (40)$$

and

$$\frac{L - W}{w\ell} = \eta \xi \quad (41)$$

where

D is the aerodynamic drag of the balloon,

$L - W$ is the excess lift

L is the lift of the balloon

and

W is the weight of the balloon W_1 , and the payload W_2 .

The balloon forces, which equal the cable tension and direction, are given by,

Drag $D = 1/2 \rho A_D V^2 C_D$

Lift $L = L_b + 1/2 \rho A_L V^2 C_L$

where ρ is the density of the atmosphere

A_D is the equivalent aerodynamic cross-sectional drag area

A_L is the equivalent aerodynamic cross-sectional lift area

C_D is the drag coefficient

C_L is the lift coefficient

V is the wind velocity over the balloon

and L_b is the buoyant lift of the balloon.

For a given balloon and cable, the aerodynamic forces can be calculated for each wind velocity. The total forces at the end of the cable are found, and the equations for the functions η and ξ are solved. These values are then used in Equations (38) and (39) to solve for the equilibrium position of the balloon, at that velocity. The stability of the system with wind velocity is then determined by plotting the position of the balloon with varying wind speed.

3.1.1 Numerical Example

The properties of the balloon and cable used in the example, called Balloon A, are listed in Table I. These various values were substituted into the equations and the position of the balloon was obtained. The aerodynamic forces of the balloon are given in Figure 6, for the four values of lift coefficient used, (0.0, 0.2, 0.4, and 0.6), and for the drag coefficient and area. This figure shows how the aerodynamic forces can become considerable at the larger lift coefficients and velocities. The total buoyant lift of the balloon is 223 pounds, and the balloon and cable weigh 118 pounds, leaving an excess lift of 105 pounds without including the payload. The aerodynamic lift reaches almost 600 pounds at a lift coefficient of 0.6 and a wind velocity of 50 fps. Note that, the aerodynamic forces were calculated using a constant drag coefficient and area, while the lift forces are for a varying lift coefficient. This approach is not strictly correct, since no allowance for the drag, due to the balloon aerodynamic lift, has been included. However, for this preliminary examination, it simplified the calculations.

The results obtained for this balloon and cable are illustrated, in part, in Figures 7, 8, and 9. Each figure is for a different payload, and shows the resultant position of the balloon as a function of the cable length. For optimum performance for flying instruments, the balloon is required to have a minimum movement with a change in

TABLE I
BALLOON A AND CABLE

Volume of balloon	Σ	3400	cubic ft
Equivalent cross-section area for lift	A_L	266	ft ²
Equivalent cross-section area for drag	A_D	154	ft ²
Drag coefficient	C_D	0.3	
Weight of balloon	W_1	100	pounds
Density of atmosphere	ρ_a	0.00238	slugs/ft ³
Density of balloon gas	ρ_e	0.00034	slugs/ft ³
Length of cable		1200	ft
Weight per unit length of cable	w	0.015	pounds/ft

The Lift Coefficient C_L was varied from 0 to 0.6.

The Payload Weight W_2 was varied from 0 to 80 pounds.

The Wind Speed V was varied from 0 to 50 fps.

wind velocity. A system with good characteristics will be one where x/ℓ remains small, and Y/ℓ stays near 1.0 for all wind velocities. These figures show that the effect of both the aerodynamic lift and the payload can be considerable. The balloon with a high lift coefficient of 0.6 produces a very stable system, and the payload has very little effect. However, the payload becomes more important at the lower lift coefficients, when the excess lift is smaller. Further, the results of these three figures show that at wind velocities less than 20 fps, for this particular configuration, neither the lift coefficient or the payload has much effect on the balloon stability. Therefore, if the balloon were restricted to this wind velocity range, then any effort to produce a high aerodynamic lift would be wasted, since it will have little effect on the resultant position and motion of the balloon with wind velocity. However, if the system were to be operated at much higher wind speeds, then obviously this point will be more important.

The use of aerodynamic lift, as a stability technique, will generally be more suitable than increasing the excess lift by increasing the balloon size. The balloon must be carefully designed, so that the induced drag does not become too great and reduce the stability.

However, the larger cables required for the higher loads could be a limitation on the stability of the system. At higher wind speeds, for very high flying balloons, the use of tapered cables, or successively larger cables rising, will be necessary to keep the cable weight to a minimum.

In conclusion, the system of this particular example is suitable for very low wind speeds, but, at velocities above 20 fps and with no aerodynamic lift, it is not sufficient. The balloon will have to be replaced by a larger or a lighter balloon, to provide a larger excess lift force, so that a more stable system is produced. This brings out one further point, in that a lighter balloon will be more susceptible to damage, especially as it will also be operated in higher wind speeds, which will make it more prone to damage when being launched.

The balloon system used here is obviously very unsuitable for instrumentation location, and will have to be restricted to low wind velocities, or assisted by careful flying to obtain the maximum aerodynamic lift.

3.2 Single Cable, Including Cable Aerodynamic Drag

In this section, calculations for the same Balloon A and cable as used in Section 3.1 are completed, but include the effect of the cable aerodynamic drag. The values of the cable parameter functions given by Neumark in Reference 1 were substituted in the equations of Section 2.0. The use of these tables involves accurate interpolation at the bigger angles, and this must be done very carefully, since the final answers depend on the small differences between the values of these functions for the top and bottom of the cable. The results for the height were rather scattered and only an estimate of the varying position with velocity could be obtained.

The cable was assumed to be 0.25 inch in diameter, and a drag coefficient of 1.1 was used to estimate its aerodynamic drag. The function n is then given by

$$\begin{aligned} n &= \frac{1}{2} \rho V^2 d C_D \\ &= 0.0000272 V^2, \text{ for this particular cable.} \end{aligned}$$

The weight per unit length of the cable is 0.15 pound/ft, so

$$n/w = 0.00187 V^2$$

For the values of the factor n/w given by Neumark, the maximum velocity calculated is 37.1 fps, so the results in this example are limited to wind velocities below this value.

The procedure outlined in Section 2.0 using Equations (10), (11), and (12) was followed to obtain the solutions for the balloon stability when the payload was held constant at 45 pounds and the aerodynamic lift coefficients were 0.0 and 0.6. The results for the resultant balloon position are given in Figures 10 and 11, where they are compared to the values for when the aerodynamic drag of the cable is ignored. In these figures the actual dimensions of the horizontal and vertical positions, relative to the tethering point are given. These figures show that the inclusion of the cable aerodynamic drag causes a less stable system with wind velocity. The greatest difference in the two sets of results is for when the lift coefficient is zero and is 150 feet for the horizontal distance at a wind speed of 23 fps. However, in comparison with the results of Figures 7, 8, and 9, it would appear that the addition of aerodynamic lift by the balloon, at a lift coefficient of 0.2 would more than cancel out this effect for this particular configuration.

4.0 MULTI-CABLE CONFIGURATIONS

The solution of a multi-cable configuration will be complicated, unless certain assumptions are made. Normally, the configuration will be divided into several simple systems, each in two dimensions, which can be solved more easily. The components of the drag and the lift of the balloon will easily fit into this arrangement, but the determination of the aerodynamic forces on the cables will be very involved for cables yawed across the wind direction. Therefore, since the analysis of the previous section has shown that these forces have only a small effect on the resultant position of the balloon, they will be neglected. However, it must be remembered that the aerodynamic drag of the cables will cause the system to be less stable and a small allowance must be made for this effect.

For maximum stability, the configuration will be set up symmetrically about the wind direction axis. This will be assumed to be the case for all configurations considered in this section, since it will allow the systems to be reduced to simple two dimensional arrays. One array will be in the wind direction, and the other normal to it, to prevent balloon wandering. In the following subsections, various two-cable configurations will be analyzed to allow the most stable configuration to be determined.

4.1 Simple Two Cable Array in the Wind Direction Axis

The array considered is shown in Figure 12. The equations relating the drag, lift, cable parameters, and position, can be obtained by equating the forces at the top of the cable, Equations (37) to (40).

Horizontal Forces at the Balloon,

$$D = a \eta_1 - b \eta_2 \quad (42)$$

Vertical Forces at the Balloon,

$$L - W = a \eta_1 \xi_1 + b \eta_2 \xi_2 \quad (43)$$

The height y for each cable is the same

$$\begin{aligned} \eta_1 c &= \left\{ (1 + \xi_1^2)^{1/2} - \left[1 + \left(\xi_2 - \frac{1}{\eta_2} \right)^2 \right]^{1/2} \right\} \\ &= \eta_2 d \left\{ (1 + \xi_2^2)^{1/2} - \left[1 + \left(\xi_2 - \frac{1}{\eta_2} \right)^2 \right]^{1/2} \right\} \quad (44) \end{aligned}$$

and the distance between the tethering points is constant.

$$\begin{aligned}
 X &= X_1 + X_2 \\
 &= c \eta_1 \left[\sinh^{-1} \xi_1 - \sinh^{-1} \left(\xi_1 - \frac{1}{\eta_1} \right) \right] \\
 &\quad + d \eta_2 \left[\sinh^{-1} \xi_2 - \sinh^{-1} \left(\xi_2 - \frac{1}{\eta_2} \right) \right] \quad (45)
 \end{aligned}$$

where

$$\begin{aligned}
 a &= W_1 l_1 \\
 b &= W_2 l_2 \\
 c &= l_1 \\
 d &= l_2
 \end{aligned}$$

and the subscripts here refer to the two cables.

Equations (42) to (45) are four simultaneous equations in η_1 , η_2 , ξ_1 , and ξ_2 , and so an exact solution exists. However, since they are non-linear, the solution cannot be found by simple substitution. In Appendix A1, a computer program to solve these equations by trial of selected values is given. However, this program requires a considerable running time on the computer, and it is still necessary to interpolate for a solution when the final results are obtained. Since it is required to examine several configurations, and determine which gives the best stability, this approach is not the most suitable. The main difficulty of handling these equations is that the forces at the balloon vary with wind velocity. Simplification of the configuration parameters, by assuming that the aerodynamic lift coefficient of the balloon is zero, allows the resultant position of the balloon to be determined by matching the cable parameters, at a given height, to give the total excess lift. Because the aerodynamic lift of the balloon is then zero, this excess lift remains a constant with wind velocity, and at each height the horizontal position of the balloon can be determined, and the necessary drag and wind velocity to hold the system in position can then be found. This approach was used in the following section to determine the stability characteristics of various two cable configurations.

A simple computer program was written to give the tension, its vertical and horizontal components, and the direction of the top end of the cable, for various heights and

horizontal distances. These values were produced in a tabular form as described in Appendix A2. Then, for a given two cable configuration, a height Y was chosen and the program completed for each cable. The various horizontal distances X_1 for one cable were matched with corresponding horizontal distances X_2 for the second cable, to give the required base. The total excess lift to hold the configuration in each position was obtained by adding to two vertical components of tension, and the configuration was solved when this value matched the given excess lift of the system. The drag force was calculated from the horizontal components of tension and, using the aerodynamic characteristics of the balloon, the wind speed necessary to hold the configuration in this position was obtained. The height was then reduced and the process repeated to determine a new horizontal position and wind speed. Eventually, the height was such that one cable had some slack on the ground, and so the stability determination was stopped, since now the balloon effectively swung on a single cable. A typical example of the solution is given in Appendix A2.

The key to the solution is the simplification resulting from the assumption of a constant excess lift. This assumption allows the cable parameters to be matched, at each height, to equal this known lift force. The examples of Section 4.2 are all calculated using this technique. However, it was also required that the effect of balloon aerodynamic lift be examined and so, in Section 4.3, an example of a single configuration is examined, using the full equations with the solution determined by the method of Appendix A1.

4.2 Two Cable Examples, with Constant Excess Lift Force

In the following examples, the same balloon, called Balloon B, is used in each case. The total buoyant lift was determined as 500 pounds for a 24 ft diameter spherical balloon. Putting the balloon and its fittings as weighing 225 pounds and the payload weight as 200 pounds, gives an excess lift force of 75 pounds. This value will be kept constant for all the examples of this section. This force must support the cables and will be equal to the total vertical components of the tensions at the top of the cables.

The cross-sectional area of the balloon S calculates as 486 square feet, and the drag is given by,

$$D = 1/2 \rho V^2 S C_D$$

The velocity is obtained from the total drag force by rearranging and substituting in the relationship

$$V = 2.44 D^{1/2} \quad (46)$$

for air at standard density, and with the drag coefficient C_D as 0.3.

Equation (46) will be used to determine the wind velocity, once the total drag force has been found by matching the two cable parameters to give the required total lift.

4.2.1 Configuration A, Two Equal Cables, Tethered in the Wind Direction Axis

This configuration is sketched in the inset of Figure 13, where the dimensions of the first example, called A1, are given. The two cables are 1200 ft long, and weigh 0.02 pound/ft. The base distance for the tethering points was set at 1000 ft. Figures 13 and 14 show the results for the balloon position with a varying wind velocity in the direction of the tethering base line. As the wind speed increases, the balloon quickly moves from the central equilibrium position. In Figure 14, the performance of the configuration is compared to an example where the same balloon is flown as a single cable, the same as one of those used in Configuration A1. This latter figure shows the additional stability of the two cable system, but also indicates the low wind velocity range. When the wind speed exceeds 10 fps for this configuration, the downwind cable is so slack that it falls on the ground. The cable then is only acting as extra payload, of just less than its total weight of 24 pounds, and the balloon is swinging on the upstream cable, as for the single cable example.

To provide a more stable configuration, the base distance was increased to 1600 ft for the same balloon and cables, and the process of determining the position of the balloon with wind speed was repeated. The resultant values are plotted in Figures 15 to 18. Here the wind velocity could increase to nearly 15 fps before the downstream cable goes slack. Figure 15 shows the better stability with wind than for the single cable system. Figure 16 is a plot of the balloon position, with the various wind speed points marked. It shows how the system is very stable up to a wind speed of 10 fps, above which the balloon moves significantly with a small change in wind velocity. Figures 17 and 18 present the cable tension and angles at the balloon. The tensions do not become excessive within the 15 fps range, and the results show how the tension of the downstream cable falls with the increasing windspeed.

This study of the first configuration shows how the use of a downstream cable provides an initial stability to the configuration. However, once the wind velocity increases so that this cable goes slack, then the system behaves as a single cable configuration with very little stability. The tethering points must be set far apart, to allow such a system to be used in the highest wind conditions, so as to provide a high tension in both cables. For a real system, the downstream cable does not need to be as massive as the upstream cable, which will have to be designed to take the whole lifting force alone. The use of a lifting balloon, to increase the aerodynamic lift, will form a more stable system, but a very high lift coefficient will be required if a sufficient lifting force is to be developed at low wind speeds, before the downstream cable goes slack.

4.2.2 Configuration B, Two Equal Cables, Tethered Normal to the Wind Direction Axis.

In this configuration, the two cables are again equal, but they are arranged so that the tethering baseline is normal to the wind direction. Because of the natural wander of a balloon and cable system, as mentioned in Section 3.0, it will be necessary to provide lateral stability by cables normal to the direction of the wind. The cables are as for the previous examples; 1200 feet long and 0.02 pound/ft weight. The base distance, now normal to the wind direction, was set at 1000 feet, and the resultant stability with varying wind speed was calculated. The results are shown in Figure 19 where they are compared to the values for a single cable configuration as before. In Figure 20 the tensions at the top of the cables, for the respective systems, are shown; that for the single cable being divided by two, to allow a direct comparison.

The results of Figure 15 show that the stabilities of both systems are almost identical. Because the two cable systems allow a shorter effective cable length, the final deflection of the two cable system is reduced. However, these calculations show that for a wind speed up to 20 fps, the horizontal deflection for the two cable system is greater. The tensions in the cables, Figure 20, show similar results.

On the basis of these results, it is argued that three-dimensional arrays, with equal side tethering, with respect to the wind direction, can be treated as an equivalent two-dimensional array in the wind direction.

4.2.3 Configuration C, Two Unequal Cables Tethered in the Wind Direction Axis, With Both Cables Upstream of the Balloon.

This system is sketched in the inset of Figure 21, and consists of two unequal cables. One is short and heavier than the other, and both are set to be upstream of the balloon. This system is not feasible when there is no wind, since the balloon will move over the nearer tethering point, to assume an equilibrium position between the two tethering points. However, the reasoning behind this system was that a slight wind would carry the balloon downstream, where it would adopt a fairly stable position. The shorter cable was made thicker, since it was believed that it would take the lift force and that the long thin cable would hold the configuration stable. The configuration of this example consisted of one cable 800 feet long weighing 0.04 pound/ft, and a longer cable, 1800 feet long weighing 0.005 pound/ft. They were set with the tethering points 1484 feet apart. This figure was chosen as typical for the setup considered, and, in fact, arose for fitting together the two cables at the selected altitude starting point of 774 ft. The tension in the short cable was set to give a vertical component of 60 pounds, and the tension in the longer, lighter cable was chosen to have a vertical component of 15 pounds. The distance between the tethering points was then found at the given value. If another distance had been chosen, then the system would not have fitted these design loads for a low wind velocity.

In practice, the system performance was not exactly as expected. Figures 21 and 22 show the position of the balloon with increasing wind speed. The balloon moves

horizontally at first, holds a reasonably stable position over a wind speed range of 12 to 20 fps, and then starts to fall. The balloon remains within a 20 foot square for wind speeds of 12 to 25 fps, which is very stable, considering the length of cables. Figures 23 and 24 show the tensions and angles of the cable at the balloon. The tension in the short cable quickly falls to 32 pounds, the weight of the cable, at a wind velocity near 25 fps. Then the short cable rests on the ground, and the position of the balloon is determined by the long cable alone. The tension in this cable has risen rapidly to near 150 pounds at the small angles of inclination of this configuration that occur at this wind speed.

The design is seen to be basically wrong, because the lighter cable has to take a greater load once the wind speed is above 18 fps. This cable should obviously be at least as heavy as the shorter cable, if the configuration is to be operated in wind speeds greater than a slight breeze.

4.2.4 Configuration D, Two Unequal Cables, Tethered in the Wind Direction Axis, With the Shorter Cable Downstream of the Balloon.

This system is sketched in the inset of Figure 25, and shows the same two cables used in Configuration C, to allow a direct comparison. This system is similar to Configuration A, but with unequal cables. Because the configuration is unsymmetrical, the system has a different stability when the wind direction reverses, and so the negative wind velocity performance was also calculated. The tables of cable performance were matched again for various heights, on the basis of a base distance of 2000 ft, and a lift force of 75 pounds, and the resultant values of the wind velocity and balloon position are shown in Figures 25 and 26.

This configuration is immediately seen to be the most stable of all those considered. The balloon remained within a 20 foot square for a range of wind velocities for - 5 to +20 fps. At higher velocities, the shorter cable becomes slack, and the balloon is effectively supported on the long cable, as before. The opposite effect is observed at negative wind velocities, and the balloon then swings down on the shorter cable. The tensions and the angles at the top of the cables are shown in Figures 27 and 28. The tension in the long cable does not rise with increasing wind velocity as quickly as for Configuration C, but this is only because the shorter cable remains taut over a greater wind velocity range. Eventually, it reaches the same high value as before, when the shorter, heavier cable becomes slack.

Once again the wrong assumptions concerning the cable weights were made. The long cable had to take a greater strain as the wind velocity increased, and it became the key cable for positioning the balloon. Any large increase in wind velocity reduced the load in the short cable, and so it was not likely to break in a gust.

This final configuration is the most stable; the position of the balloon, and the cable tensions and angles all change slowly with an increasing wind, and stay within a narrow range for a wide range of the wind velocity.

4.3 Two Cable Example, Including the Aerodynamic Lift of the Balloon

For this example, the Configuration D was used again, but this time the balloon was allowed to generate aerodynamic lift. The method of Appendix A1 was used to obtain the solution and the resultant stability curves, when the aerodynamic lift coefficients were 0.4, 0.2, and 0.0 are shown in Figure 29. The complete program was run with the lift coefficient zero, to allow a comparison with the results obtained in Section 4.2.4. Examination of the results showed that the position of the balloon calculated, for when the lift coefficient was zero, only differs by a maximum of two ft in either axis from the previously calculated values. Since the method used in this section does depend upon examination and interpolation of a series of results, this must be regarded as very good agreement, and, further, it would not be fair to re-examine the results to produce better agreement.

Only the three complete calculations were run, with the cables as for Configuration D and the balloon lift coefficients at 0.0, 0.2, and 0.4, because of the time necessary to complete the computations, and also because the results were immediately obvious from this sample analysis. The use of the aerodynamic balloon lift more than doubled the range of wind velocity over which the balloon system could be operated, and, in fact, the examples with aerodynamic lift are inherently stable in any wind velocity. The condition for this stability will now be derived.

As the lift force increases, the cables are drawn tight, and eventually they will become straight between the tethering points and the balloon. So long as the lift forces always remain greater than a fixed fraction of the drag force, then the two cables will remain taut, and the downstream cable will not go slack. Consider the system with the cables taut, and let the tensions in the cables at the balloon be T_1 and T_2 , where the suffixes 1 and 2 refer to the upstream and the downstream cables respectively. Then if the cables make angles θ_1 and θ_2 with the horizontal at the balloon, the components of the tension can be equated to the total lift L and drag D of the balloon.

$$L = T_1 \sin \theta_1 + T_2 \sin \theta_2 \quad (47)$$

$$D = T_1 \cos \theta_1 - T_2 \cos \theta_2 \quad (48)$$

Multiplying Equation (48) by $\tan \theta_1$ and subtracting from Equation (47),

$$L - D \tan \theta_1 = T_2 (\sin \theta_2 + \cos \theta_2 \tan \theta_1) \quad (49)$$

The downstream cable will go slack when the tension T_2 is zero or negative. This condition is given by,

$$\frac{L}{D} \leq \tan \theta_1 \quad (50)$$

In fact, the cable will go slack before the tension becomes zero, since once it is unable to support the weight of the cable, some will fall on the ground. This will occur when,

$$T_2 \leq w_2 l_2 / \sin \theta_2 \quad (51)$$

and the condition for this to occur is now,

$$L - D \tan \theta_2 \leq w_2 l_2 \left[1 + \left(\frac{\tan \theta_1}{\tan \theta_2} \right) \right] \quad (52)$$

The free lift force of the balloon is included in L , as well as the aerodynamic lift force, and it will generally be as great as the rhs of the inequality (52). Therefore, the approximate expression (50) can be used to estimate for inherent stability, by considering the aerodynamic lift force only.

For the example considered here, when the aerodynamic lift coefficient was 0.4, in the limit, the ratio of the Lift to Drag becomes 1.333 including only the aerodynamic forces. For the other example with the lift coefficient of 0.3, this ratio is 0.667. The configuration is such that the tangent of the angle θ_1 when the configuration is pulled taut, is

$$\tan \theta_1 = 719/1650 = 0.436$$

Since this value is much less than the Lift-Drag ratio, both configurations with aerodynamic lift will be inherently stable with increasing wind speed.

For a real balloon system, the drag coefficient will depend, in part, on the lift coefficient. Therefore, this example is not a true representation since the drag coefficient was kept constant for all cases. However, these results do indicate the stabilizing effect of aerodynamic lift of the balloon.

5.0 DESIGN OF MULTI-CABLE CONFIGURATIONS

On the basis of the preceding analysis and the examples in Section 4.0, the rules for design of a multi-cable balloon array can be determined. First it is essential to determine the objective of the balloon flying program. If, as is the general case considered here, the objective is to place instruments at a given point, then the exact conditions under which the system will be flown must be formulated. For example the exact range of the wind velocity to be used must be considered, or else specified for a given system. Then the configuration will be restricted to operation within these limits.

The analyses were all restricted to examples for the static equilibrium case only. The equations for the dynamic stability derivatives were not derived, since it was determined that they would be very complicated, even on the assumption of constant cable length. Further, this assumption could not be justified in determining the reaction of a given system to a sudden gust loading, since the configuration will immediately react by allowing the cables to stretch. The examination of the actual balloon system used by NASA, reported in Appendix B, indicates that the use of a single length of cable, to attach the balloon to the top of the multi-cable system, provides a shock absorber action. Any sudden gusts cause the balloon to move sharply on this single length of cable, while the cable system and the hanging instruments remain fairly stable.

The balloons will be operated at various ground altitudes, and the changes in the atmospheric properties can cause the excess lift of the system to be reduced. The effect of changes in the air temperature and pressure must be considered when designing a configuration. However, the changes in excess lift will not normally be critical for small changes in the air properties, since most balloons will contain an expansion section, which will allow the balloon to be inflated to a larger volume in atmospheric low density conditions. This expansion should allow the excess lift to remain near the design figure.

The analysis of the various configurations considered here allows certain design points to be specified. However, it must always be remembered that the aerodynamic drag of the cables was neglected in these studies, and, for real systems, it will always cause the system to be less stable than the calculated values.

The first point that can be specified, is that for the most stable system, a three dimensional array lined up in the wind direction will be required. The prevailing wind conditions will help in determining the basic layout, but the tethering points should be made mobile, if at all possible. A study of the ground conditions, such as mud, swamp, or dry land, and including the possible effects of the climate, should determine the limits on moving the tethering points.

The cable system must eliminate the balloon wander, and the use of equal cables set on each side of the wind direction axis will help in this respect. The system will then be

reduced, for analysis purposes, to a single plane system in the wind direction axis. The use of three cables, in this plane, is obviously redundant and a simple equivalent two cable system, such as considered in Section 4.2, will result. Either one, or both, of these cables will represent a double cable system, to provide the lateral stability of the configuration, and so the complete system will consist of either three or four cables. The obvious conclusion is to use a classic three cable arrangement, which could, perhaps, have been guessed as the most suitable by a logical examination of the problem. However, the preceding analyses and examples do allow more definite details of the system to be determined. The configuration will be symmetrical about the wind direction, and the upstream cable (or cables) will be considerably longer than the downstream cables (or cable). The two possible configurations are sketched in Figure 30.

The effect of the wind drag of the balloon is to cause a high tension to the upstream cable (s). The pattern of Figure 30a has two long upstream cables, and consequently these will each be near half the weight of the single upstream cable of Figure 30b. The former configurations, including the single short downstream cable, will probably be easier to handle in the field because of the reduced weight of the long cables. For the configuration in Figure 30b, the upstream cable could be excessively heavy to handle over rough ground. The first configuration will have more lateral stability as the wind speed increases, since the tension in the two upstream cables will rise. However, the second configuration will be more stable at very low wind speeds since the configurations will be designed so that the majority of the lift force is taken by the downstream cables at low wind speeds. But if the wind speed should increase such that the downstream cables go slack, then this second configuration will be very unstable. This instability will be serious since it will coincide with the occurrence of the highest and most critical loading of the system. For the first system, this loss of lateral stability will occur if the wind direction reverses. On the basis of this analysis, the configuration of Figure 30a is recommended as the most suitable.

Most practical configurations will also have a vertical cable below the balloon, which will be used for handling and attaching instruments to. In the normal flying position, this cable will not be used to locate the balloon, and so will be considered as part of the payload weight in any calculations.

A given system will be made more stable at high wind velocities by providing aerodynamic lift due to the balloon. This lift will depend on the aerodynamic characteristics of the balloon, and the effect of induced drag must not be forgotten. Provided that the lift force on the configuration is normally much greater than the drag force, then the system will be inherently stable. The approximate condition for this stability is given by the angle, whose tangent is the lift force over the drag force, being always greater than the angle of the upstream cable at the balloon when the cable system is pulled taut. This was seen with the example of Section 4.3, where the balloon quickly adopted a position with both cables stretched tight as the wind speed increased.

The problems of launching and handling high lift balloons must next be considered, because of the dangers of damage due to contact with the ground, and the difficulties

of getting the system to adopt the correct configuration. The optimum system for launching the balloon would be to let up the balloon, set at its correct lift configuration by paying out all the stabilizing cables simultaneously. However, an alternative system would involve launching the balloon trimmed to provide the minimum aerodynamic lift, and to reduce the loads on the cables and winches during the critical launch period. The balloon will then initially fly far downstream of the required position with the aerodynamic lift. The balloon should then be adjusted to increase the lift coefficient, and, by paying out the downstream stabilizing cables, allowed to move upstream. This is assuming that the upstream cables are already set at the required length. The balloon must not be winched upstream on the cables, as this will shorten them below the design length.

It will probably prove more suitable to lay out the required length of the upstream stabilizing cables, and to launch the balloon on the handling cable, with the upstream cables fixed at the correct length. The balloon is swung up on these cables, and finally the downstream cables are fixed when the balloon acquires the required altitude. The objectives should be to get the balloon up and away from the ground as quickly as possible, and to ensure that the upstream cables are never run out more than the required length. This will avoid winching the balloon upstream once it is set up in the air. The real key to flying the configuration will be to ensure that the long upstream cables are properly positioned, with respect to the wind direction, and that the correctly calculated length of cable is used.

In the case of balloons used for acoustic measurements of rocket noise, the balloons will generally have to be positioned upstream of the rocket, otherwise the cables could stretch across the exhaust gas flow. This will not be as bad as it seems on first sight, since the balloon could either be positioned to one side of the rocket, or the upstream cables could be made sufficiently long that the balloon cannot actually swing into the flow. Further, as a final point, if one cable should break, the balloon will swing to one side of the exhaust gas. Figure 31 illustrates these points.

A final note concerns the use of multi-balloon arrays. These are configurations where two or more balloons are flown with linked cables. A preliminary examination indicates that such a system should be more stable than a system using a single balloon. More cables will be required, but the more complex configuration will allow different wind conditions to be supported by different combinations of the cables. However, the problems of handling such a system could be excessive, and the difficulties of controlling all the cables simultaneously will require an increase in manpower and organization. Therefore, it would appear to be most suitable to fly single unlinked balloons, which can be positioned individually. Although it will probably take longer to launch the necessary number of balloons, the overall system will be more versatile. For example, it will only be necessary to bring down a portion of the instrumentation for repairs or adjustments, and also the system will be more adaptable to ground variations. Also, if it is necessary to string up several vertical arrays of instruments near each other, the use of an extra large single balloon, with the instruments hanging from the tethering cables, seems more appropriate.

6.0 CONCLUDING REMARKS

A basic analysis of a single balloon cable, both including and neglecting the aerodynamic forces on the cable due to the wind, has been presented in this report. The relationships for the equilibrium configuration of the cable were applied to the study of multi-cable configurations, and the following points were determined.

- a. The aerodynamic drag of the cable can generally be neglected, as having a small effect on the stability of the cable and balloon system. This result simplifies the basic analysis of the configuration; however, it must be remembered that the additional effect of the aerodynamic drag on the balloon systems will reduce the stability below the calculated values.
- b. The analysis of multi-cable configurations can be completed by reducing the system to suitable two-dimensional arrays. These arrays are determined by studying the equilibrium position of the configuration with zero wind velocity, and then projecting the cables to the given planes. The behavior of the system in these planes will then be considered for various velocity components, to produce the complete stability of the system with wind velocity. This method is only suitable for symmetrical arrays in practice, so that the movement in one chosen plane can be considered as independent of the motion in the other chosen plane.
- c. The best configuration, for the stable flying of instruments, will be with the main axis of the configuration in the direction of the wind. For optimum stability and simplicity, the arrangement will be two long cables set upstream of the balloon, and one shorter cable downstream of the balloon. The two upstream cables also provide the lateral stability by being placed symmetrically at equal but opposite angles to the wind direction axis.
- d. Each cable configuration, without balloon aerodynamic lift, will have an upper velocity limit, above which the downstream cable will go slack, and the balloon will swing on the upstream cables as for a single cable system.
- e. Aerodynamic lift due to the balloon will provide more stability, and will extend the wind velocity range of operation of the configuration. However, care must be taken to ensure that the induced drag does not become too large, and that the tensions in the cables increase beyond the design case. If the base distance of the configuration is great enough, then it is possible to design a system which is inherently always stable at all wind speeds.
- f. The difficulties of handling the balloon systems have been mentioned, particularly the problem of launching the balloons with aerodynamic lift. A technique involving control by the upstream cables is recommended.

- g. Multi-balloon systems will be more simply flown and operated singly and not tied together in an array. Although this array would probably be more stable, the complications of flying the arrangement will require more sophisticated methods of controlling the cables.

APPENDIX A

SOLUTION OF MULTI-CABLE CONFIGURATIONS, SINGLE CABLE BEHAVIOR, AND COMPUTER PROGRAMS

A.1 Solution for Two Cable Configuration

The basic equations for solution of a two cable system, set with the tethering points axes in the wind directions, are given in Section 4.1 and repeated here,

$$D = a \eta_1 - b \eta_2 \quad (42)$$

$$L - W = a \eta_1 \xi_1 + b \eta_2 \xi_2 \quad (43)$$

The height Y for each cable is the same

$$\begin{aligned} Y &= \eta_1 c \left\{ (1 + \xi_1^2)^{1/2} - \left[1 + \left(\xi_1 - \frac{1}{\eta_1} \right)^2 \right]^{1/2} \right\} \\ &= \eta_2 d \left\{ (1 + \xi_2^2)^{1/2} - \left[1 + \left(\xi_2 - \frac{1}{\eta_2} \right)^2 \right]^{1/2} \right\} \end{aligned} \quad (44)$$

and the distance between the tethering points is fixed

$$\begin{aligned} X &= X_1 + X_2 \\ &= c \eta_1 \left[\sinh^{-1} \xi_1 - \sinh^{-1} \left(\xi_1 - \frac{1}{\eta_1} \right) \right] \\ &\quad + d \eta_2 \left[\sinh^{-1} \xi_2 - \sinh^{-1} \left(\xi_2 - \frac{1}{\eta_2} \right) \right] \end{aligned} \quad (45)$$

For a given wind velocity, the lift L and the drag D can be calculated; therefore, there are four simultaneous equations with four unknowns η_1 , η_2 , ξ_1 , and ξ_2 .

Thus, a solution for the height Y and position of the balloon X_1 can be obtained. In practice, since the equations are nonlinear, a solution cannot be obtained by a simple substitution. The difficulty of solving for such cable configurations was avoided in Section 4.2 by considering a balloon with no aerodynamic lift. Then, no matter what

the wind speed was, two cables could be matched, for the same height Y , using the total vertical components of the tensions to equal the lift force. The drag force was then obtained, and the wind velocity found. The program used to calculate the cable shape and tension components is given in the second part of this Appendix.

However, when the balloon has an aerodynamic lift force dependent on velocity, then the vertical lift force is not known until the wind velocity is fixed. Therefore, the following digital computer program was written to allow a solution to be found for the above set of equations by inspection. At each wind velocity chosen, the aerodynamic forces of the balloon were calculated, and a range of possible values for the functions ξ_1 , and η_1 was defined. Taking these values in pairs the program first calculates the corresponding values of the functions ξ_2 and η_2 .

$$\eta_2 = \frac{a \eta_1 - D}{b} \quad (A1)$$

$$\xi_2 = \frac{L - W - a \eta_1 \xi_1}{a \eta_1 - D} \quad (A2)$$

If these latter two results are positive, then these four values are used to calculate the two heights of the cable Y_1 and Y_2 , and these values are compared. If they agree to within a predetermined amount the program continues to calculate the two horizontal distances X_1 and X_2 . These values are added to give a value for the total horizontal distance X . If this value agreed, within a defined error, with the actual base distance of the configuration to be solved, then the program prints out the values of the calculated distances X_1, Y_1 , and Y_2 , as well as certain other parameters, such as the angles of the first cable at the balloon. By suitably choosing the limits on the agreement of the calculated lengths, only a few results are eventually written for the thousands of pairs of original values used. These results are then examined and for each value of the drag force, an interpolation gives the point where the two heights, Y_1 and Y_2 , are equal. The corresponding value of the total base distance X and the base distance of the first cable X_1 are then determined. The values for the total base distances, one for each value of the drag force, are then examined and interpolated to find the point where the base distance X equals the given value for the configuration. The position of the balloon, as X_1 and Y , is then determined from the individual values obtained for each value of the drag force.

Table II is a flow diagram of the program, and Figure 32 is the actual computer program used for the example of Section 4.3. Examination of the program will show that every effort was made to reduce the amount of work, by having checks at each stage of the

TABLE II
FLOW DIAGRAM OF PROGRAM POT 21

PROGRAM POT 21	
1.	For each wind velocity, calculate the aerodynamic forces of the balloon, and calculate the excess lift.
2.	Take value of the drag component of Number 1 cable $(T_1 \cos \theta_1)_1$.
3.	Take value of the angle of Number 1 cable (θ_1)
4.	Calculate η_1 , ξ_1 , η_2 , and ξ_2 .
5.	Calculate Y_1 and Y_2 .
6.	Compare Y_1 and Y_2 , if within prescribed limits continue, otherwise back to 3 for next angle.
7.	Calculate X_1 and X_2 , and add to give X .
8.	Compare X with given base distance; if within prescribed limits compare, otherwise back to 3 for next angle.
9.	Write out X , X_1 , Y_1 , and Y_2 .
10.	Go back to 3 for next angle, unless all angles used, then continue.
11.	Go back to 2 for next drag component, unless all drag components used, then continue.
12.	Go back to 1 for next velocity, unless all velocities used, then PAUSE

computation to eliminate unsuitable answers. Even so, a typical program to calculate the equilibrium point for the configuration at nine different wind speeds required 1.25 hours of computer time on the Wyle Laboratories CDC 3200 digital computer. Figure 33 shows some typical outputs from the program. First the conditions of the balloon and cable systems are given, and then the calculated results for zero wind speed. These are followed by two sets of results for a wind speed of 20 fps with the balloon aerodynamic lift coefficient set at zero and 0.4, respectively. In each example the estimated equilibrium cases are noted along side.

A large number of pairs of variables was taken; some 24,000 at each wind velocity. Errors of up to ± 2 ft in the balloon position were observed for the example where the Configuration D with no aerodynamic lift was compared to the results obtained by the

method of matching the two cables. The use of this program POT 21 was limited to the single configuration of Section 4.3 and the MSFC balloon of Appendix B.

A2 Single Cable Behavior

When the aerodynamic lift of the balloon was eliminated, by considering non-lifting balloons, the solution of multi-cable configurations was found by matching cable parameters. The configuration was always considered as, or reduced to, a simple two cable system set in the mean wind direction, and the aerodynamic drag of the cable was further neglected. This approach allowed quick and accurate solutions to the several two-cable configurations used in Section 4 to determine the basic characteristics of such systems.

In this section, the basic equations are rearranged to give the required parameters, and the computer program developed to obtain the tabulated values is presented. Basically, a list of the cable tension, its components, angle of the top of the cable, and the horizontal distance from the tethering point, for a given height to the top of the cable is required. Then the results for the two cables of the chosen example were matched on the basis of the tethering locations, and the position of the balloon determined when the vertical components of tension added to give the required lift. The drag force was then quickly attained, and the resultant wind velocity found. This process was repeated at various balloon heights to obtain the complete stability curve of the system with velocity.

Expanding and squaring equation(35) gives

$$\left[\frac{Y w}{T_1 \cos \theta_1} - \sec \theta_1 \right]^2 = \left[\frac{T_1 \sin \theta_1 - w \ell}{T_1 \cos \theta_1} \right]^2 + 1$$

which after further expansion and simplification reduces to

$$T_1 = \frac{w(\ell^2 - y^2)}{2(\ell \sin \theta - y)} \quad (A3)$$

The horizontal distance of the top of the cable to the tethering point is given by Equation(36), which is repeated here,

$$X = \frac{T_1 \cos \theta_1}{w} \left[\sinh^{-1} (\tan \theta_1) - \sinh^{-1} \left(\tan \theta_1 - \frac{w \ell}{T_1 \cos \theta_1} \right) \right] \quad (36)$$

Then a computer program was written which accomplished the following calculations.

For a given height Y and cable length ℓ and weight per unit length w , the angle at the top of the cable θ_1 was varied. For each value of the angle θ_1 the program calculated,

1. The tension T_1 using Equation (A3)
2. The horizontal distance X using Equation (36)
3. The vertical and horizontal components of the tension as $T_1 \sin \theta_1$ and $T_1 \cos \theta_1$.

These values were then tabulated, and used to match two cables to solve for the configuration at that height.

A lower limit on the cable angle θ_1 occurs when the value of the factor

$$(\ell \sin \theta - y) \quad (A4)$$

in Equation (A3) is reduced to zero, and then goes negative. At this point, the tension T_1 , which was increasing with angle decreasing, becomes infinite. Angles of θ_1 , below this value, are not physically possible for the given cable length and height Y , since at this limit, the cable is stretched tight between the tethering point and the balloon.

An upper limit of cable angle also occurs where the cable, while making the required angle at its top, only achieves this, at the chosen height, by some cable falling slack on the ground. This limit is determined by the factor

$$\left(\tan \theta_1 - \frac{w \ell}{T_1 \cos \theta_1} \right) \quad (A5)$$

being negative.

The program was designed to start with the angle θ_1 at 89 degrees, and to check if the factor (A5) was positive. If it were negative the program continued to the next smaller value of the angle θ_1 . When the factor (A5) was determined as positive, the program calculated the tension, its components, and the horizontal distance. The program stopped when the value of the factor (A4) became zero or went negative. Then the value of the height Y was changed and the program started again with the angle θ_1 equal to 89 degrees. This program was written in Fortran 4 and is shown in Figure 34. Figure 35 is a typical output, and is for the cable used in example A2 of Section 4.2.1.

The complete behavior can be determined by taking a suitable range of heights for the top position of the cable. The results obtained for a cable 1600 ft long, and weighing 0.01 pound/ft, are given in Figure 36. This figure shows the horizontal base length of the cable plotted against the angle that the cable makes at the balloon, for various heights of the top of the cable, as the solid lines running across the graph. The right hand side of the figure is limited by that point where the cable becomes slack, so some must lie on the ground. The left hand side is limited by the cable becoming stretched tight. The solid line marked (Lift = 25 pounds) is for a constant vertical component of 25 pounds tension, and represents the behavior of such a cable when a balloon, with an excess lift of 25 pounds, is flown on it. The right hand limitation occurs when the vertical lift component of cable tension equals 16 pounds, which is the weight of the cable. The left hand broken line is for infinite cable tension. The lines of constant tension converge at the points where θ_1 equals 90 degrees and zero degrees.

Figure 37 is a graphical solution for one position of Configuration A2. This setup uses two identical cables as for the example of the output for the single cable program and is for the height used in this example of Figure 35. The values of the vertical component of the tension are plotted in Figure 37 for the various horizontal distances possible under this configuration and at the given height of 856 feet. The horizontal distance for the second similar cable is obtained by subtraction from the base distance. The total vertical force is found by simple addition of the two components, and the resultant position of the configuration obtained by equating this total force component to the balloon lift of 75 pounds. In practice, it is simplest to work using a table rather than a graph, as shown in Figure 38, which is for the same example. The figures are rounded to the nearest whole integer, and the accuracy can be seen by examining the actual numbers. Because the vertical tension component of the second cable is varying so slowly at the equilibrium point, the exact position of the balloon is quickly determined. The calculation is completed to give the required drag and wind velocity.

APPENDIX B

MARSHALL SPACE FLIGHT CENTER BALLOON

The sound field produced by large solid rocket engines, firing vertically upwards, is being measured as part of the acoustic measurement program of NASA, MSFC. The results are obtained using an array of microphones, hung from a balloon and positioned near the exhaust flow. For a recent firing, two such arrays were erected and measurements obtained for two vertical axes. The basic system used is described below, where the dimensions and normal flying procedure are given. These values are used, with the programs developed in the main body of this report, to calculate the flying characteristics of the balloon and cable system. The existing configuration is criticized and an alternative arrangement, with better stability, is recommended.

B1 Description of the MSFC Balloon System

The balloon used for this acoustic measurement program is a commercial aerofoil kite balloon, and the normal operating configuration is shown in Figure 39. The balloon flies on a 100 ft length of 0.25 inch diameter nylon cable, to which are attached three 5/32 inch diameter nylon stabilizing cables. (These latter cables are labeled a in Figure 39.) This extra 100 ft length of cable allows the balloon some wander, which acts as a shock absorber to sudden wind velocity changes or gusts, and so increases the stability of the microphone system. A 0.25 inch diameter nylon cable, (b in Figure 39), is used to launch the balloon, and a similar cable (c in Figure 39) is used to support the microphone array, which hangs from the apex where the three stabilizing cables meet. A final 5/32 inch diameter cable (d in Figure 39) acts as a ripcord to save the balloon, should it break away. The three stabilizing cables are spread at equal angles, and a nominal base distance of 200 ft is used, although this distance is varied to suit the particular terrain. The balloon is normally flown at an altitude of 1000 to 1100 ft. A second configuration, where one of the 5/32 inch diameter cables is omitted and the launch cable acts as a stabilizing cable, is used to fly the balloon at an altitude of 600 ft.

The balloon flies at a very high angle of incidence, near 40 degrees, at zero wind speed. Then, as the wind increases, the forces on the horizontal stabilizing fins cause the tail of the balloon to lift and the angle of incidence to decrease. Despite the resultant decrease in the aerodynamic lift coefficient, the total aerodynamic lift force of the balloon increases as the wind speed increases. At a wind speed of 40 fps, the balloon finally attains a near horizontal position. The high incidence at low wind speeds decreases as the wind speed increases, although the drag force increases. This mode of flying is designed to provide a stable system with the balloon flown on one cable, downstream of the tethering point, like a kite. At the slowest wind speeds, the top fin is left off, since it is blanketed by the balloon at angles of incidence greater than approximately 15 degrees. This reduces the drag force, and also the weight of the balloon, which provides a greater excess lift force.

The additional stabilizing cables were provided because the stability of the system on a single cable was not generally satisfactory. However, the characteristics of the balloon and the flying techniques used are such that the advantages of the additional cables are not fully achieved. The balloon is normally winched out on the 0.25 inch diameter cable, and then the stabilizing cables are adjusted to place the balloon and the microphone array at the required position. In the configuration used at the lower altitudes, the 0.25 inch diameter winch cable replaces one of the stabilizing cables. The result of the adjustments is that the cable system normally adopts an attitude where the balloon is effectively flying on one cable alone. The other two stabilizing cables are nominally taut, but they only restrict excessive sideways wander of the balloon, and have little effect on any initial movement from the equilibrium position. This instability is not helped by the small distances, compared to the height of the balloon, between the tethering points.

The values for the balloon and cable dimensions used in the calculations are listed below

<u>Balloon</u> - Length	37 ft 6 in
Maximum dia.	13 ft 9 in
Volume	3400 cu ft
Excess Lift	100 lbs

The value for the excess lift is the value given by the manufacturer of the balloon. The calculated value, based on the given volume of the balloon and using helium at atmospheric pressures and temperatures, gives a calculated lift of 138 pounds. The additional 38 pounds is therefore considered as the weight of the balloon rigging and the fin assembly.

Cables -

0.25 in. dia. nylon cable, 0.008 pound/ft
 5/32 in. dia. nylon cable, 0.006 pound/ft

The weight of the cables in Figure 39 therefore calculates as,

Cable	Length (ft)	Weight (pounds)
a	1100	6.6 (each)
b	1000	8.0
d	1100	6.6

Microphone Cable -

The electric cable for each microphone was estimated as 0.003 pound/ft weight and each microphone and bracket was estimated to weigh 0.8 pound. From these values the total

weight of the payload was calculated, as shown in Table III, to be 40.0 pounds. This payload is allowed for in the following calculations, by setting the excess lift at 60.0 pounds.

Balloon Aerodynamic Forces -

Examination of the manufacturer's specification, and analysis of the balloons flying characteristics, suggests the following figures for the aerodynamic force parameters.

$$\text{Area for lift calculation } A_L = 366 \text{ ft}^2$$

$$\text{Area for drag calculations } A_D = 142 \text{ ft}^2$$

The coefficient of lift was estimated to be,

1.0 at a wind speed of 0 fps

0.5 at a wind speed of 20 fps

0.3 at a wind speed of 40 fps

A quadratic equation was fitted to these results to give the following estimated relationship for calculating the lift coefficient,

$$C_L = 0.000375 V^2 - 0.0325V + 1.0 \quad (B1)$$

The drag coefficient was estimated as given by a simple linear relationship between the values of,

0.6 at a wind speed of 0 fps

0.3 at a wind speed of 40 fps

This is,

$$C_D = 0.6 - 0.0075 V \quad (B2)$$

These expressions for the aerodynamic force coefficients are shown in Figure 40, and the resultant calculated aerodynamic forces for the MSFC balloon are given in Figure 41.

B2 Balloon on a Single Cable

An initial analysis will be completed by considering the balloon as flying on a single cable. The aerodynamic values estimated above will be used, and the balloon buoyant lift of 100 pounds will be used. A payload of 40 pounds will be included, and the balloon stability will be calculated by assuming that it is flying on a 1/4 inch diameter nylon

TABLE III
CALCULATION OF PAYLOAD WEIGHT FOR MSFC BALLOON

Microphone (0.8 pound each)	Length of Cable (0.003 pound (ft)	Cable Weight Plus Microphone	Total Weight (lb)
1	900	3.5	20.7
2	800	3.2	
3	700	2.9	
4	600	2.6	
5	500	2.3	
6	400	2.0	
7	300	1.7	
8	200	1.4	
9	100	1.1	
1000 ft long 0.25 in. dia. support cable			8.0
1100 ft long 5/32 in. dia. ripcord			6.6
Rings and fittings			4.7
TOTAL			40.0

cable, 0.008 pound/ft weight, 1100 ft long. The values for the balloon and cable were substituted into Equations (38) to (41) using the aerodynamic forces calculated above. The position of the balloon with varying wind speed was determined, and the results are shown in Figure 42. Examination of these results indicates the good stability of the system, once the initial movement at low wind speeds is completed. The results were calculated for two other values of the zero wind velocity excess lift, since the experience with flying the balloon indicated that the system was only just capable of supporting the cable and microphone system with the balloon at 1200 ft altitude. This suggested that the actual free lift of the balloon was less than the calculated 60 pounds with a payload of 40 pounds. Therefore, the results for a zero wind speed excess lift of 40 and 20 pounds were determined, and these values are also shown on Figure 42. In fact, because of the magnitude of the aerodynamic lift force developed, the effect of changing the zero wind speed excess lift is small. The results show how the wind causes the balloon to move rapidly downstream at first, as the wind velocity increases. Then, as the aerodynamic lift force increases, the downstream movement is slowed, and eventually for the highest speeds, near 40 fps, the balloon actually starts moving upstream. The height of the balloon remains fairly constant; for the 60 pound excess lift case, the balloon only drops some 50 feet in altitude.

These results indicate the superior stability of a kite balloon on a single cable, over a balloon with no aerodynamic lift, (compare with the results of Figure 10), but show that the movement of the balloon can still be excessive at low wind velocity, and could be critical in a shifting wind condition.

B3 Balloon on Several Cables

The MSFC balloon is flown with three stabilizing cables, as described earlier in Section B1. The values given there, including the estimated aerodynamic characteristics, were then used in conjunction with the program described in Appendix A1, to solve for the stability of the system with the balloon flown on two cables.

The first example considered was with the stabilizing cable tethering points fixed at the corners of an equilateral triangle with sides 200 ft long. One cable was assumed to be directly upstream, and the system was reduced to the two cable configurations by combining the two downstream cables into a single double weight cable. By considering the cables stretched taut, the length of the equivalent downstream cable was calculated to be 1095 ft, and the base distance to be 172.5 ft. The equilibrium position, with no wind, would be with the base distance for the upstream cable X_1 as 115 ft, and the base distance for the heavier, shorter downstream cable as 57.5 ft. These values were then substituted into the program of Appendix A1, (Figure 32), with a slight modification to allow for the varying aerodynamic lift and drag coefficients, as given by Equations (B1) and (B2). The resultant calculated stability of the system is shown in Figure 43, where the full lines are for both cables taut, and the broken line is for when the downstream cable is slack, and the balloon is swinging on the upstream cable alone. The values for the latter condition were obtained by fairing the results obtained with both cables taut, to the results of Figure 42 for the single cable example.

The calculations indicated that the configuration is most unsatisfactory. The balloon is held by the two cables in a wind with a speed up to 8 fps, above which the downstream cable becomes slack. However, a certain amount of lateral stability will still be caused by the two downstream cables, but the full advantages to the multi-cable configuration are not achieved with this small base distance, which is typical of those used with the actual balloon system.

The base distance was next increased to 400 ft, for the two-dimensional two-cable system, to determine the effect of increasing the distance between the tethering points. This example is equivalent to the tethering points being positioned at a distance of 464 ft apart. The cables were considered to be 1100 ft long, and the length of the double weight equivalent cable calculated as 1075 ft. These values were used with the program of Appendix A1, and the results obtained for the stability are shown in Figure 44. Examination of this figure indicates that the configuration is much more stable than that previously considered. The two cables are taut up to a wind speed of 27 fps where the downstream equivalent cable becomes slack and the balloon swings on the single upstream cable as before. Up to 20 fps, the balloon remains practically stationary, with the horizontal displacement at 20 fps being only 14 ft from the equilibrium position with zero wind. These results indicate the obvious increased stability obtained by lengthening the tethering base distances by a factor of just over two.

A final example was considered where the base distance of the two-dimensional two-cable array was increased to 1200 ft. The height of the balloon was fixed as 1100 ft with the cables taut and straight. This gives the length of the upstream cable as 1360 ft and the double downstream cable as 1170 ft. The system is representative of a system of three stabilizing cables as suggested by the discussion in Section 5 of this report. The longer upstream cable is supposedly equivalent to two long light cables set 30 degrees to the system centerline, upon which the two cable representation is constructed. Therefore, in this example, the upstream cable is twice the weight of the single downstream cable. As explained in Section 5, this system should provide good lateral stability, and also the largest loads will be taken by two cables, rather than the single upstream cable of the previous two examples considered here. The values were again substituted into the program and the results obtained are plotted in Figure 45.

This figure shows the very good stability of the system. The equilibrium position at zero wind velocity is with the base distance of the upstream cable slightly shorter than the nominal distance of 800 ft. This occurs because of the extra weight of the upstream cable. An increasing wind causes the balloon to shift slightly downstream and to rise due to the aerodynamic lift. The system then remains very stable up to the maximum wind speed considered of 40 fps. The total horizontal movement of the balloon calculated as 12 ft and the total vertical movement was found to be 7 ft.

B 4 Discussion and Concluding Remarks

The examination of the balloon configuration and flying technique used by NASA, MSFC has shown that the optimum configuration is not normally used. The calculated performance of the system indicates that it is very unstable. The full advantage of the stabilizing

wires is not attained, and the balloon flies as if on a single cable for any wind speed greater than a light breeze. This configuration is so bad that the automatic stabilizing effects, due to the aerodynamic force being greater than the aerodynamic drag force, are not realized.

In order to achieve a better stability, it is recommended that the system be flown with a greater distance between the tethering points. With the balloon at 1100 ft altitude, it is recommended that the balloon be operated with the distance between the tethering points increased to at least 500 ft, which should allow stable operation in wind speeds up to 25 fps.

The altitude of the balloon is determined by the requirements of the measurement program, but to take full advantage of the stabilizing cables, the height should be kept to a minimum. The effect of the aerodynamic lift of the balloon is important, and far outweighs any performance gains by reducing the excess lift. Therefore, every effort should be made to ensure that the maximum aerodynamic lift force is attained. The aerodynamic drag force should obviously be reduced, as also must the effect of the aerodynamic drag of the cables and the payload. This latter force can be quite large from the microphones normally carried, and so this part of the system should be examined to ensure no extraneous drag is introduced.

The problems of handling, as described in the discussion section of the main report, also apply here. It is apparent that difficulties will occur with a simple procedure such as presently used, which incorporates launching the balloon on a single cable. The difficulties of winching the balloon into the correct operating position have been mentioned. However, it will be even more complicated to attempt to launch the balloon by simultaneously paying out the stabilizing cables. Therefore, if care is taken to ensure that the two upstream cables are located correctly and the required length is marked out, it may prove possible to launch the balloon by alternately letting out the two stabilizing cables and the main launch cable. Then, when the two upstream cables are extended to the correct length, the launch cable can be moved downstream to act as the third stabilizing cable.

REFERENCES

1. Neumark, S., "Equilibrium Configurations of Flying Cables of Captive Balloons, and Cable Derivatives for Stability Calculations", Brit. Royal Aircraft Establishment, Report Aero. 2653, 1961.
2. Hoerner, S.F., "Fluid Dynamic Drag", Hoerner, 1965.
3. Goldstein, S. (editor), "Modern Development in Fluid Dynamics", Oxford, 1957.
4. Dwight, H.B., "Tables of Integrals and Other Mathematical Data", The MacMillan Co., 1961.
5. Waters, M.H.L., "Some Observations on the Wander of a Kite Balloon", Brit. Royal Aircraft Establishment, Tech. Note, Mech. Eng. 305, 1959.

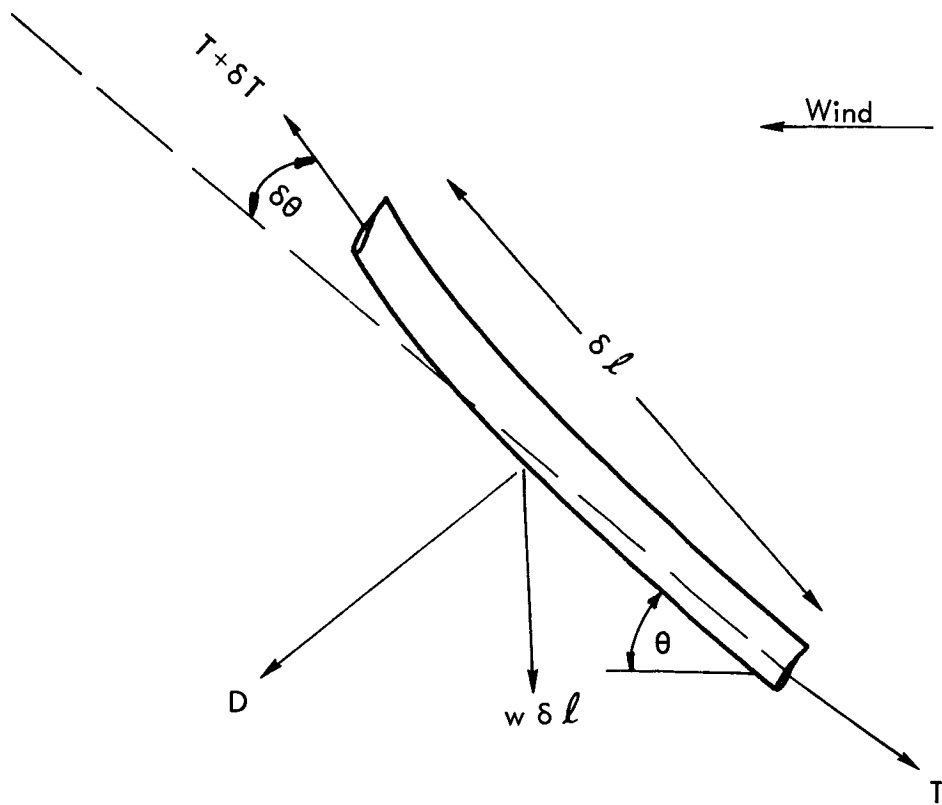


Figure 1. Element of Cable.

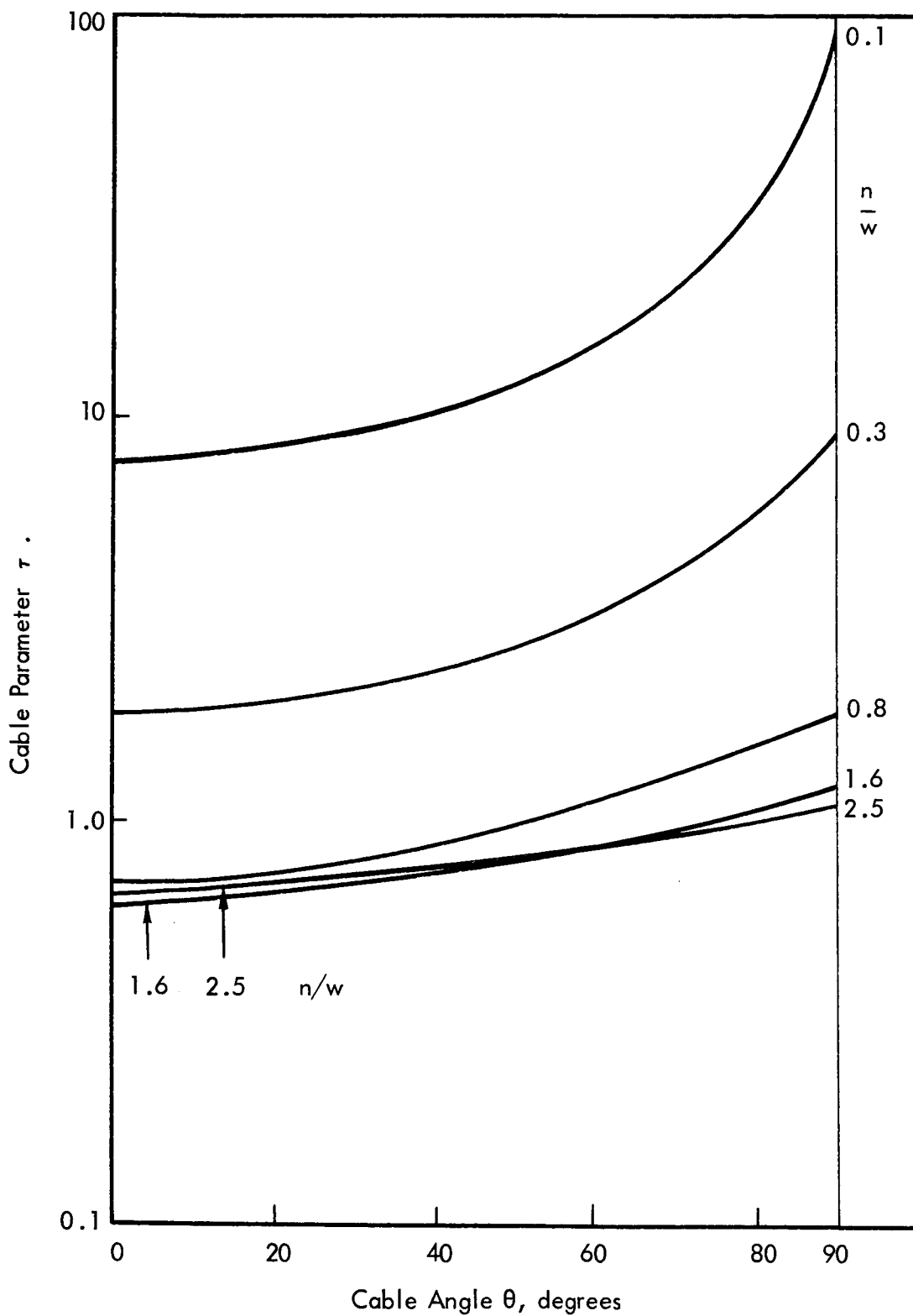


Figure 2. Cable Parameter τ , from Neumark (Reference 1).

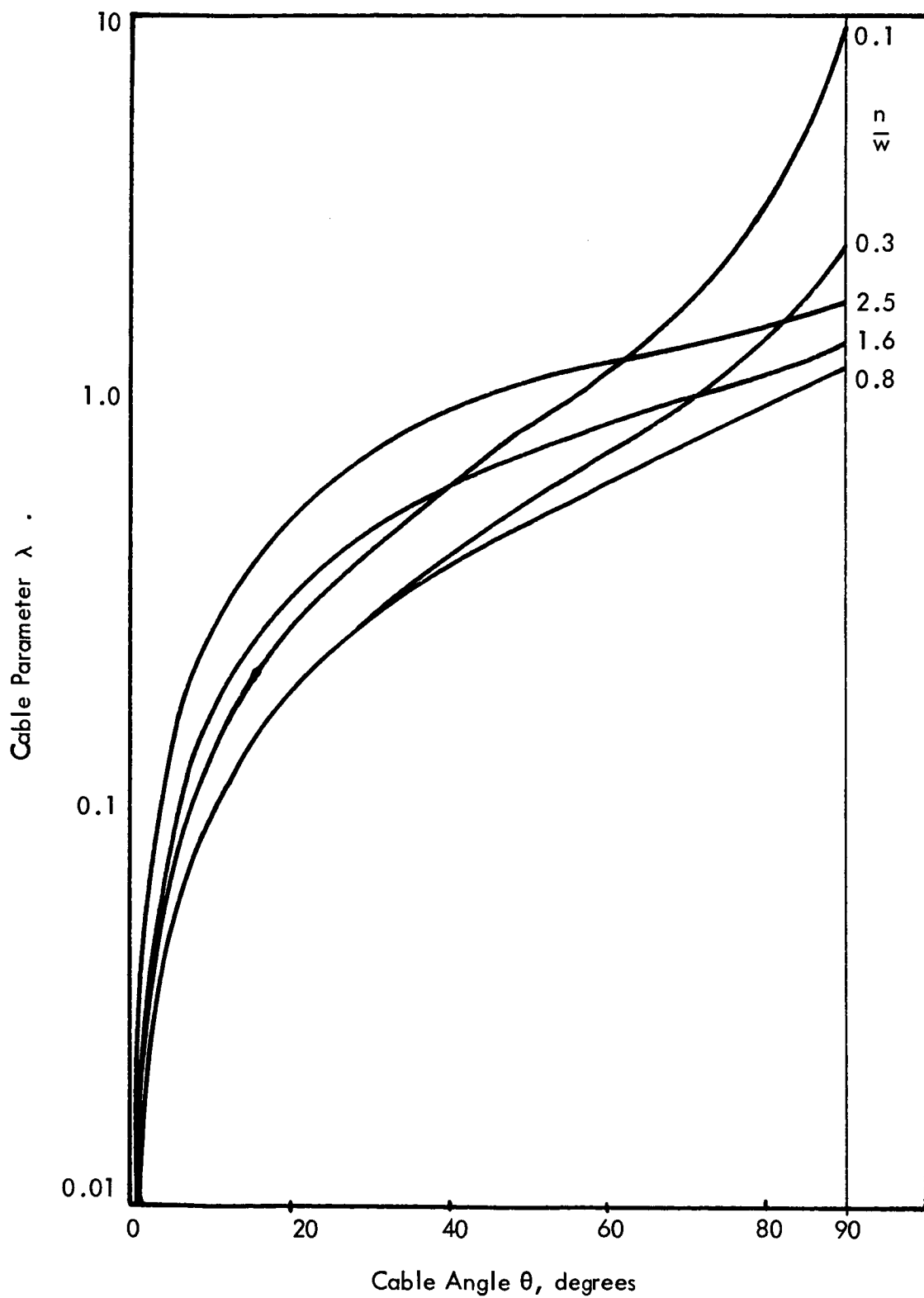


Figure 3. Cable Parameter λ , from Neumark (Reference 1).

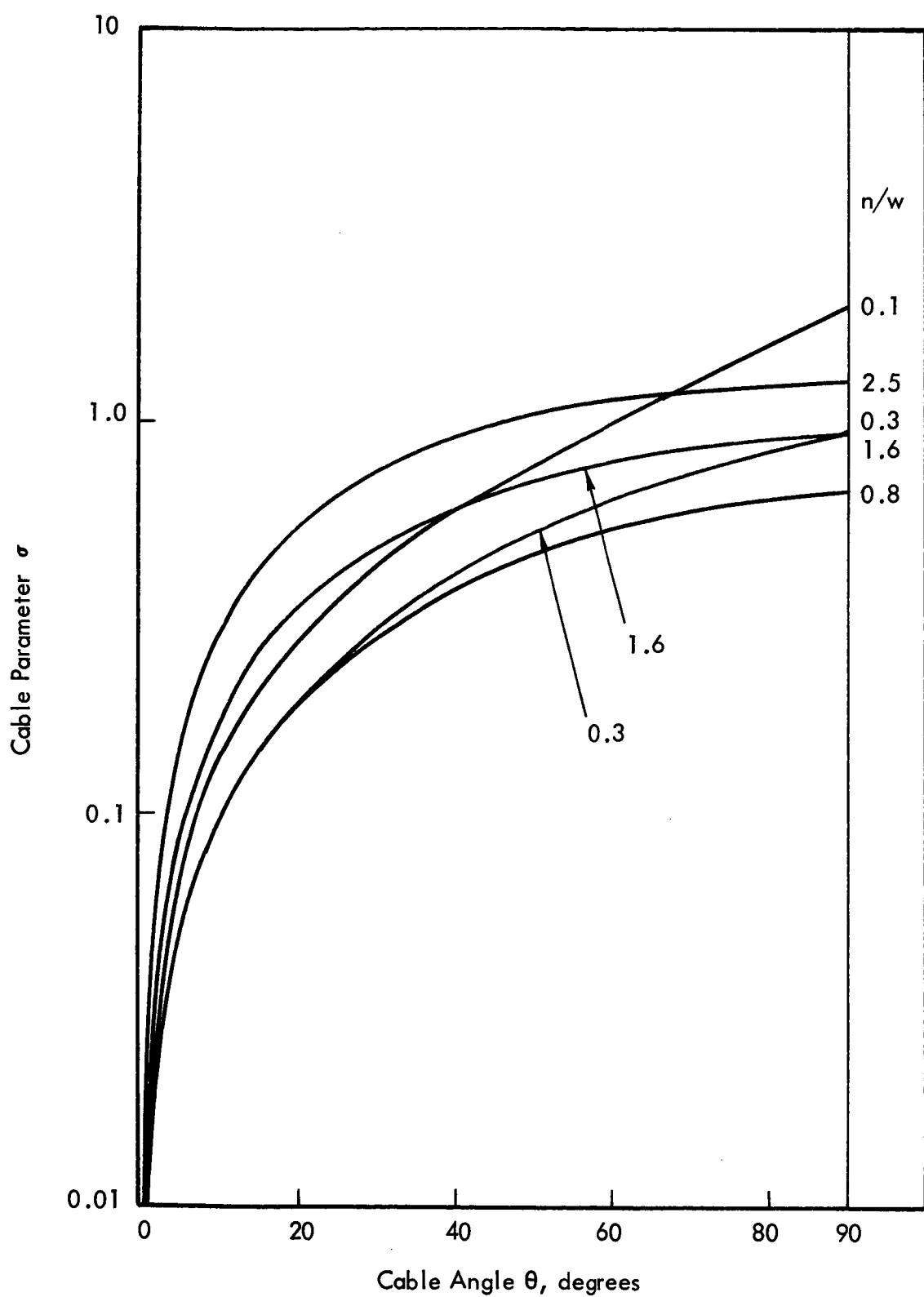


Figure 4. Cable Parameter σ , from Neumark (Reference 1).

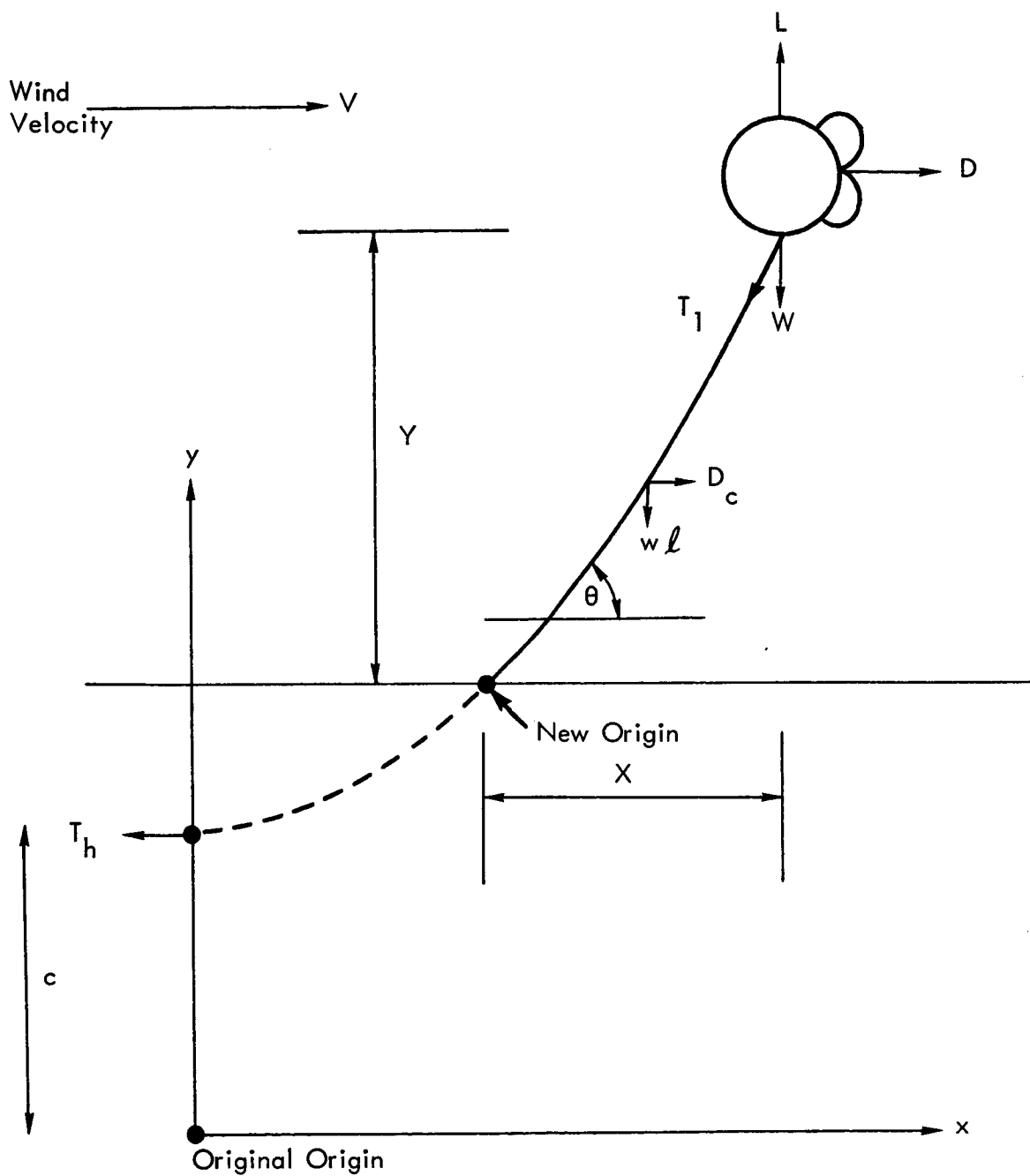


Figure 5. Balloon on Single Cable.

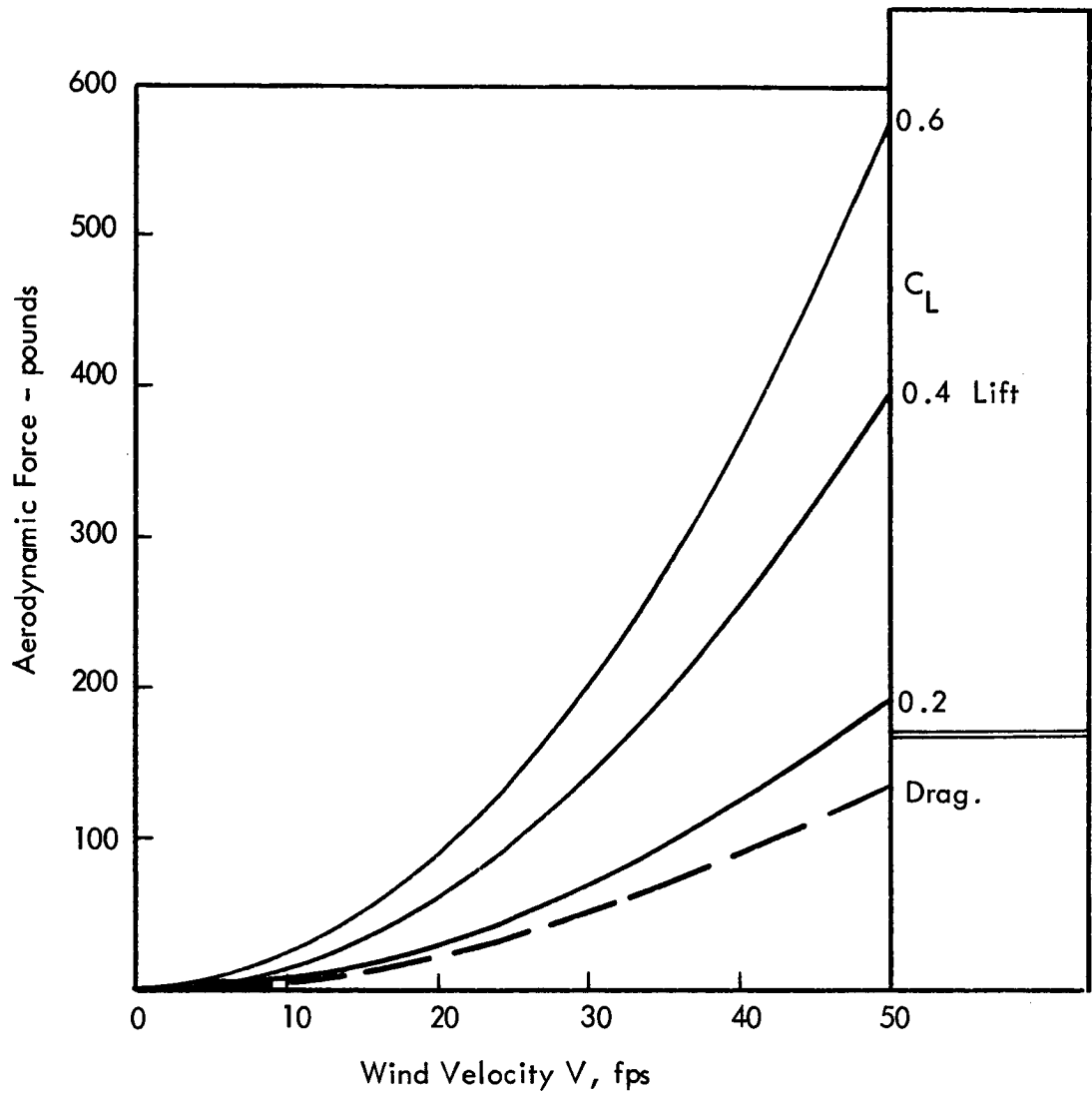
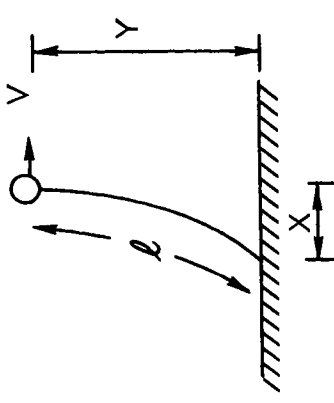


Figure 6. Balloon A - Aerodynamic Forces.



55

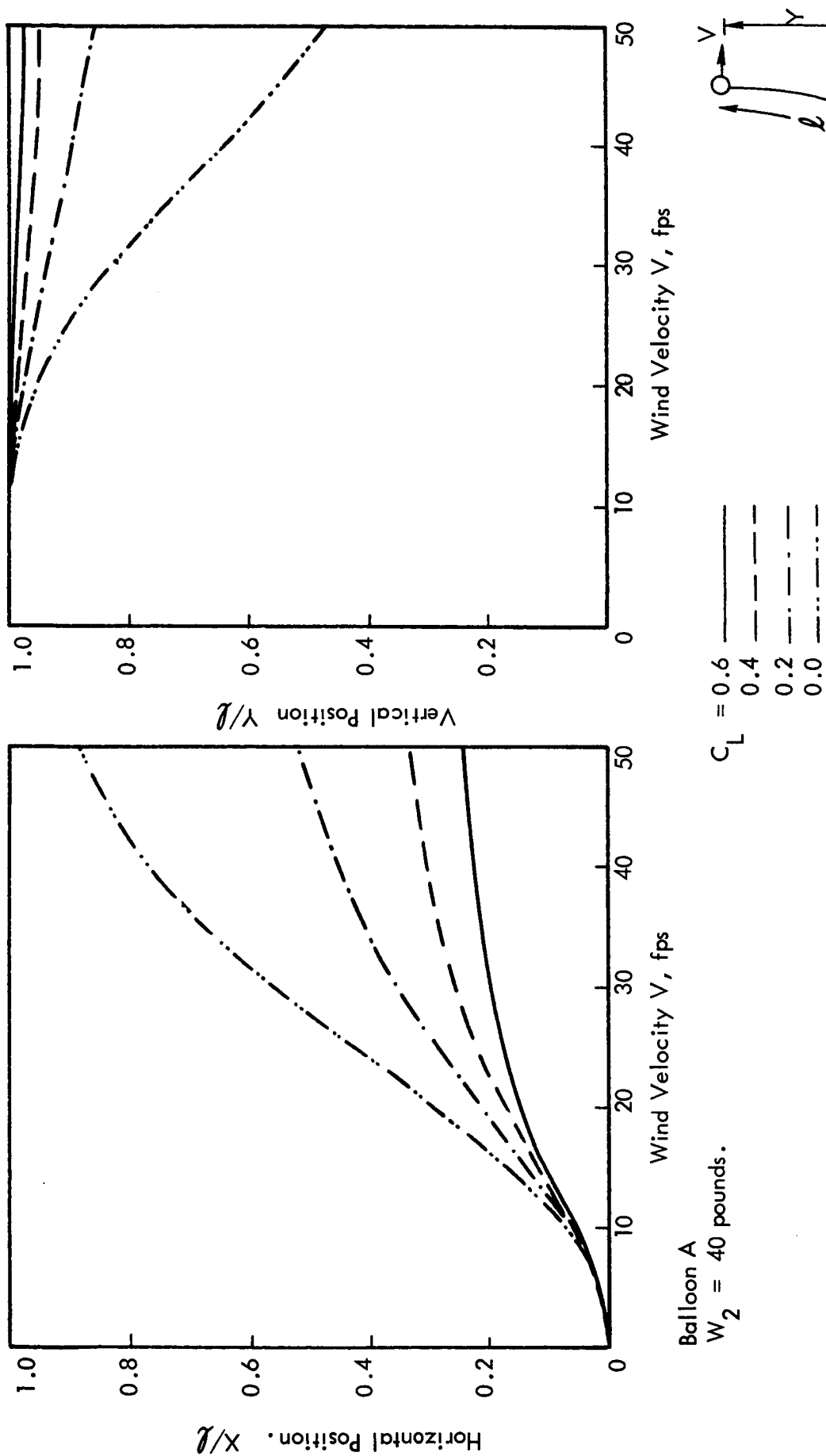


Figure 8. Single Cable and Balloon Stability.

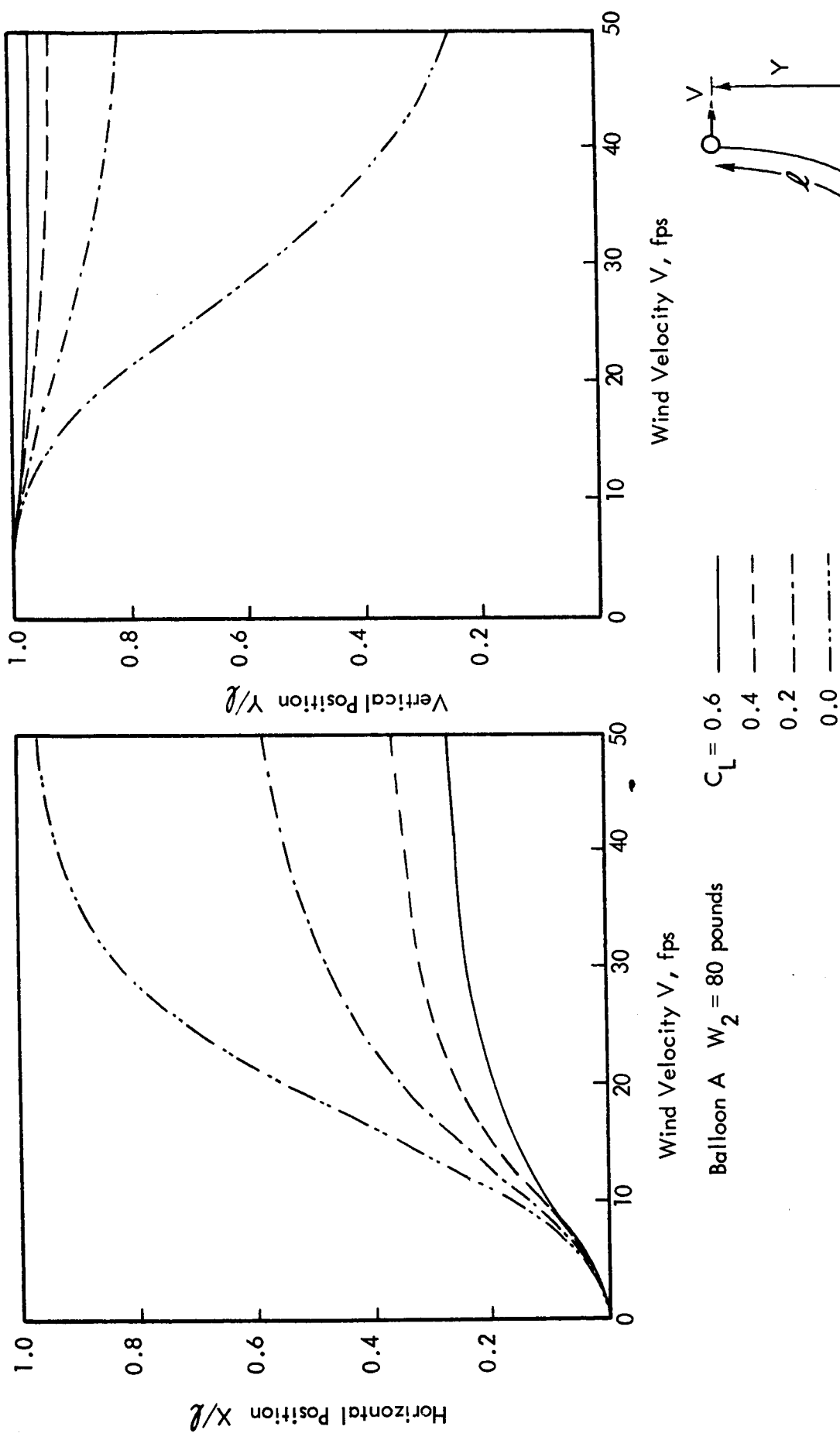


Figure 9. Single Cable and Balloon Stability.

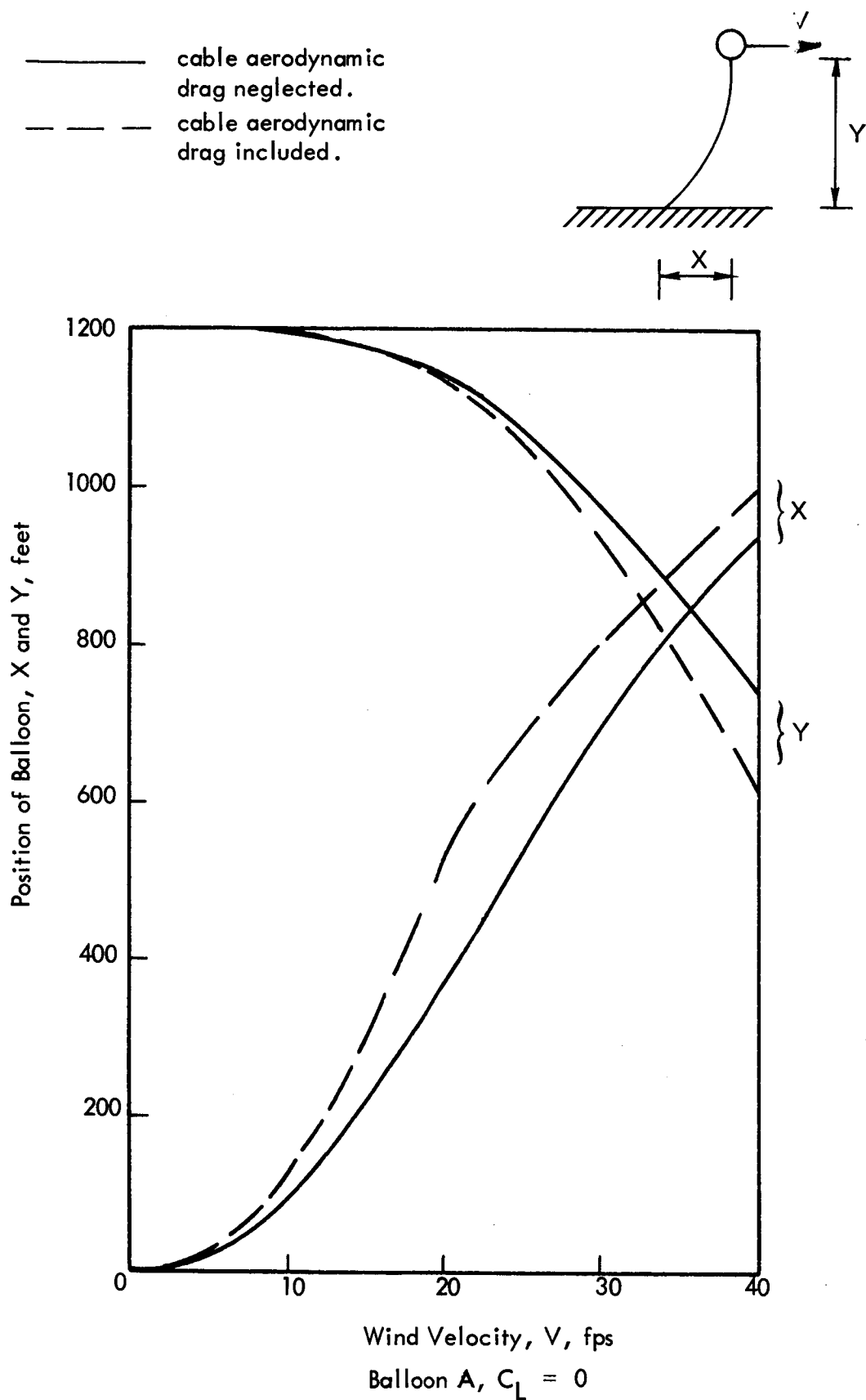


Figure 10. Balloon on Single Cable, Effect of Aerodynamic Drag of Cable.

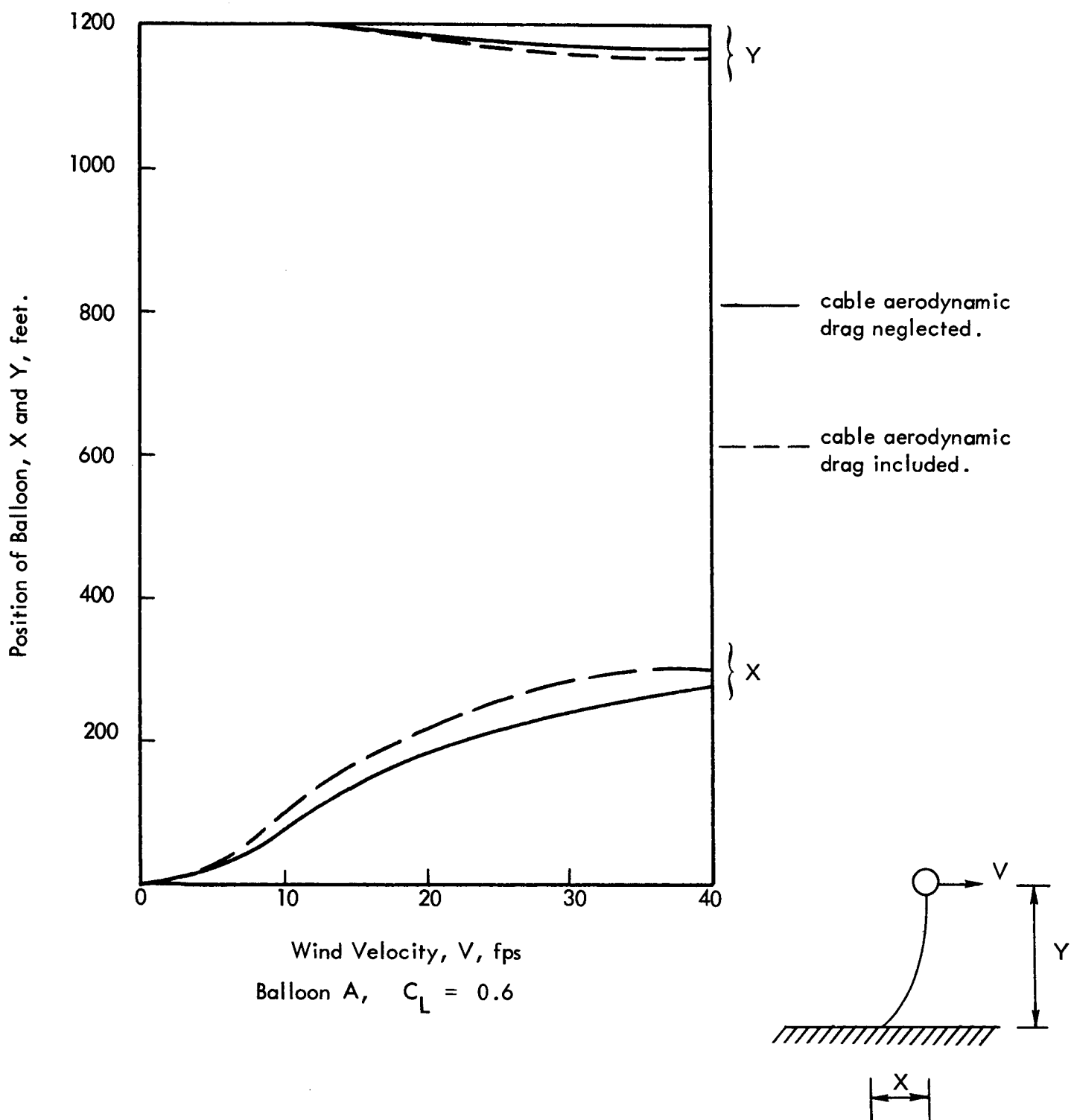


Figure 11. Balloon on Single Cable, Effect of Aerodynamic Drag of Cable.

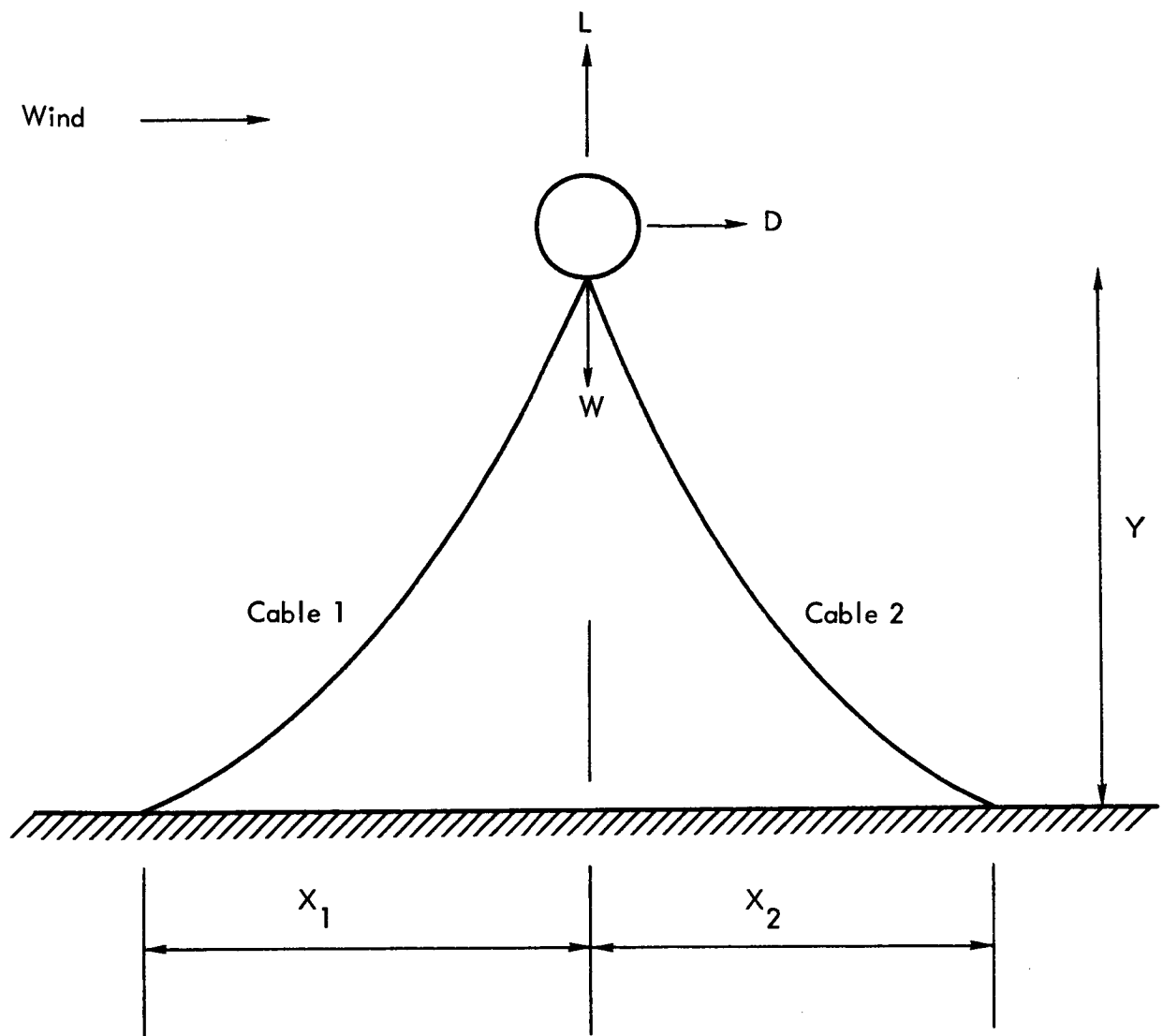
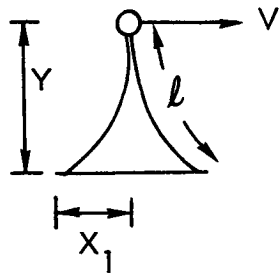
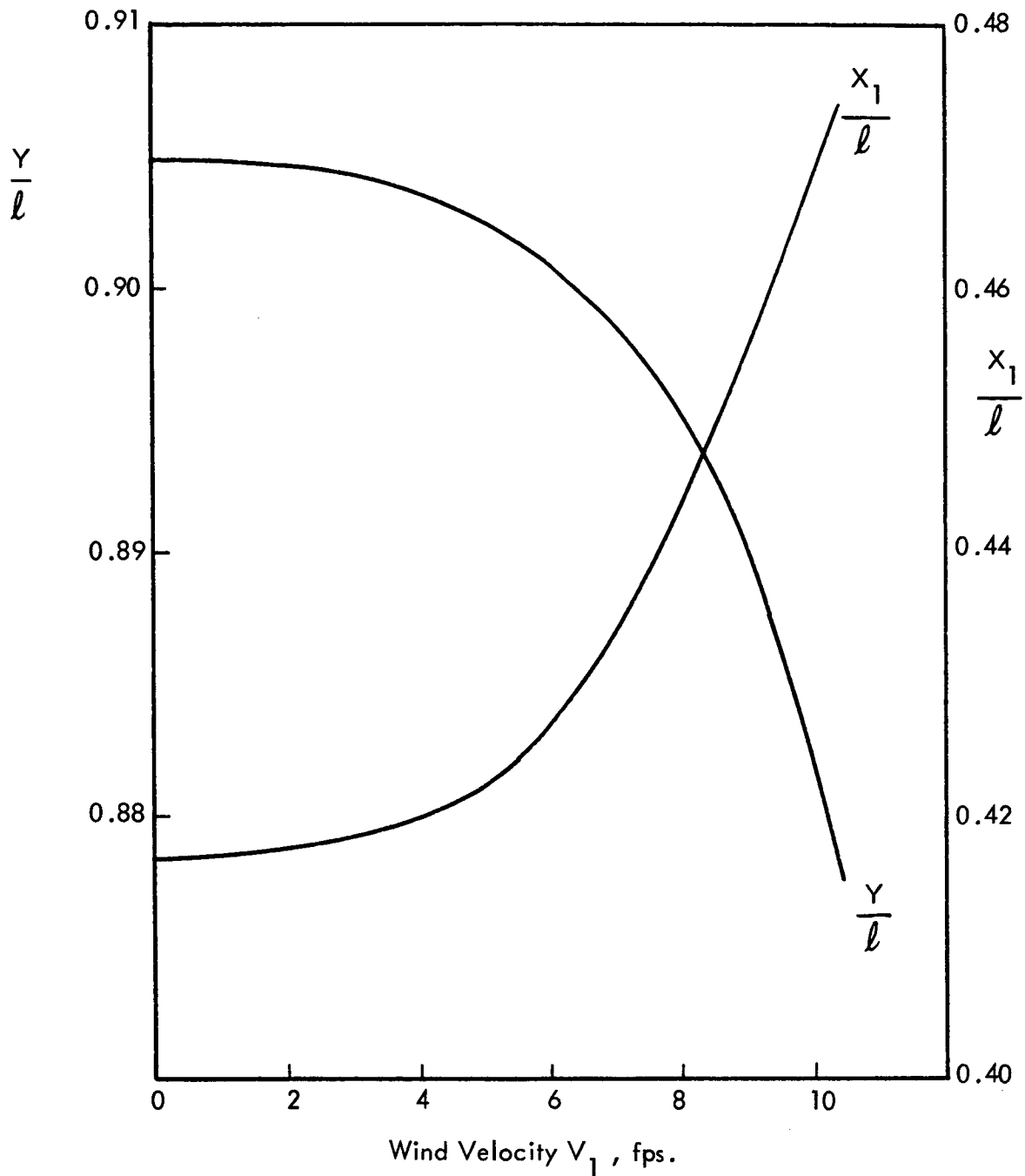
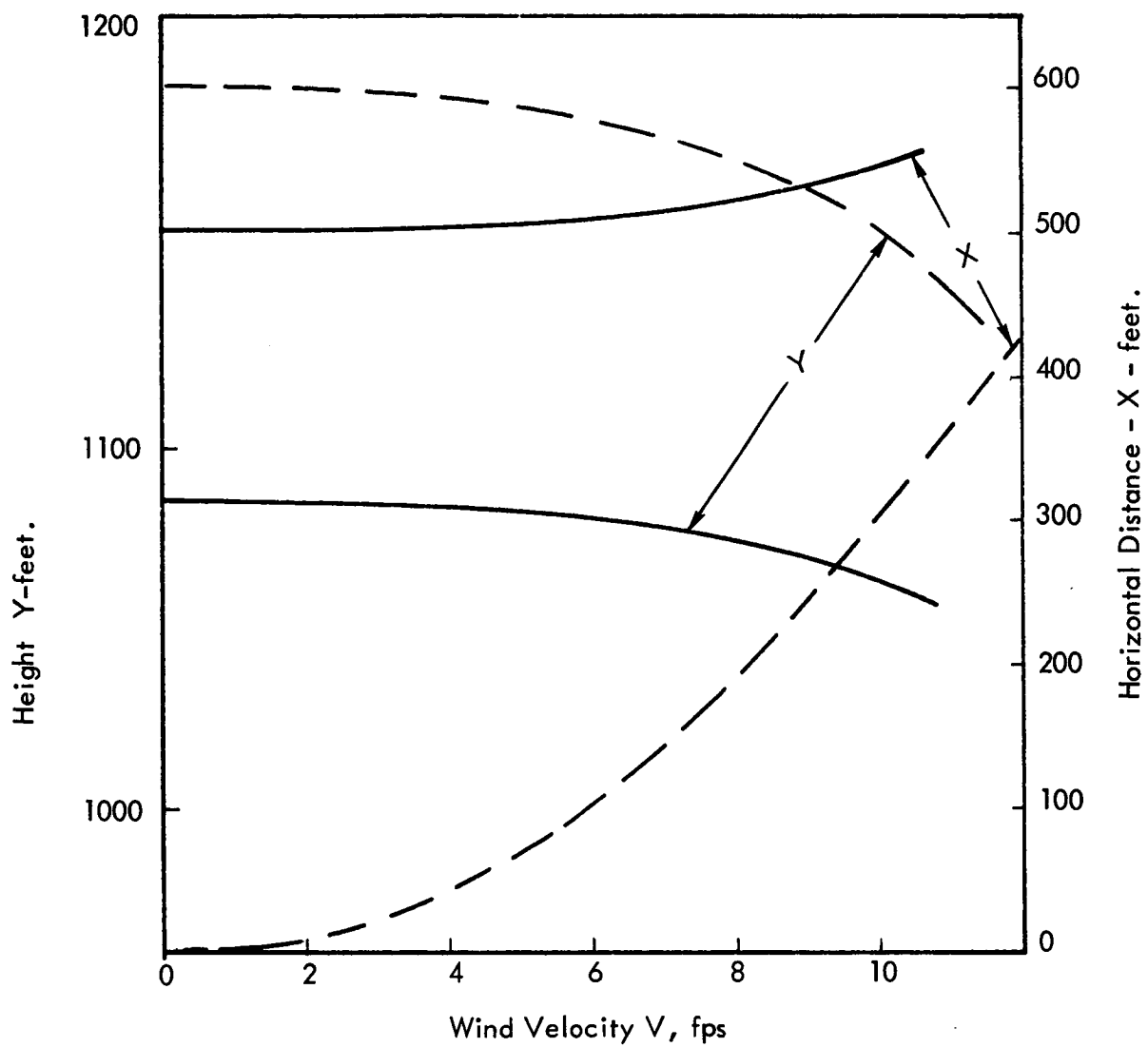


Figure 12. Simple Two Cable Array, in the Wind Direction Axis.

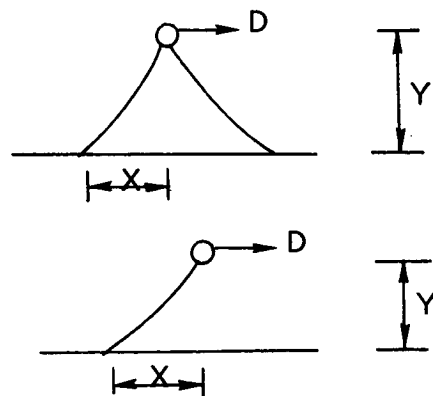


Cables both 1200 ft. long, 0.02 pound/ft.
 Base 1000 ft.
 Excess lift 75 pounds at balloon.

Figure 13. Two Cable Balloon Stability, Configuration A 1.

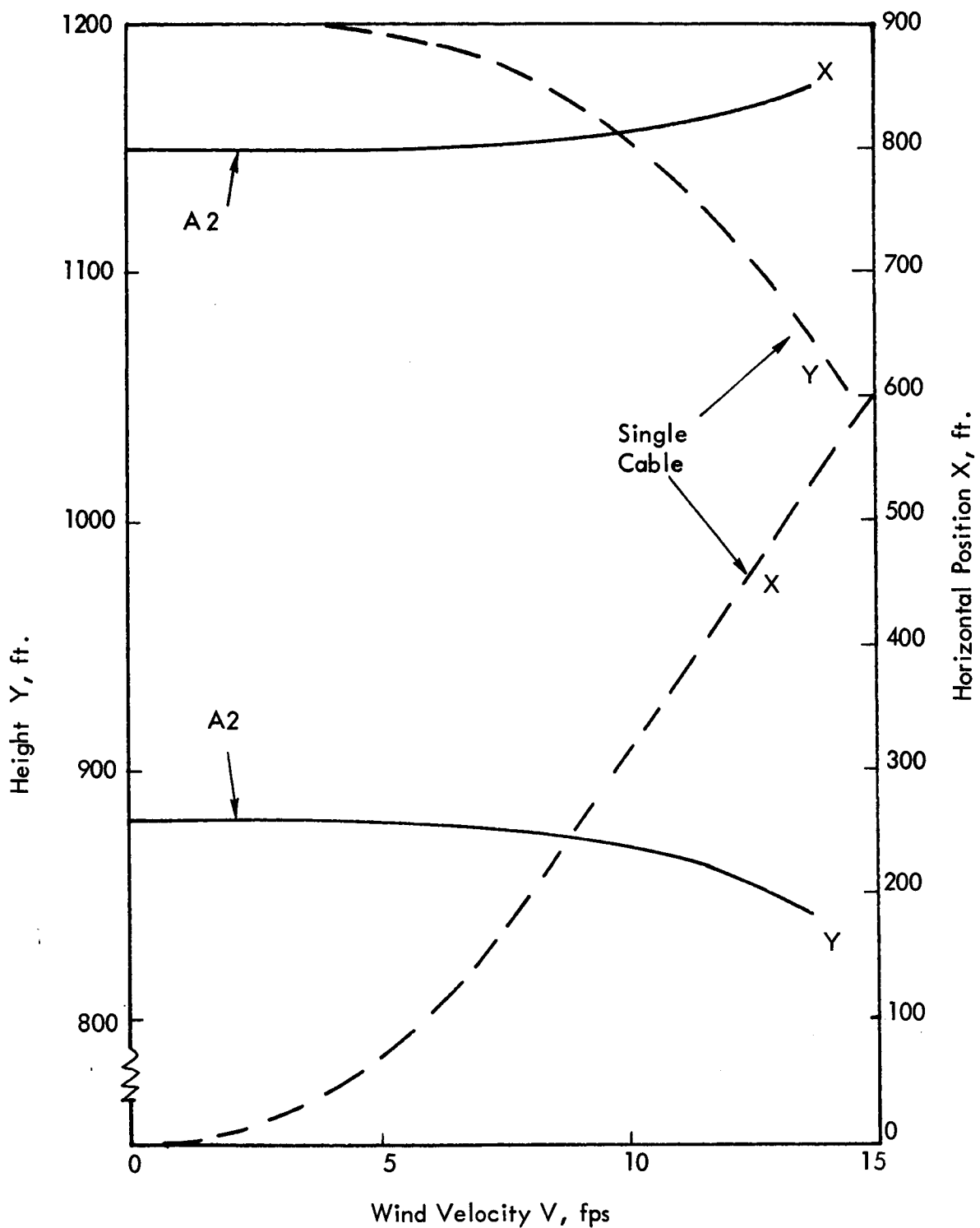


— Configuration A1
 Two cables
 - - - One cable



All cables 1200 ft. long, 0.02 pound/ft. Base 1000 ft. Excess Lift 75 pounds at balloon.

Figure 14. Two Cable Balloon Stability, Configuration A1.



Cables and Balloon as for Configuration A1, but base = 1600 ft.

Figure 15. Stability of Configuration A2, Compared to Single Cable Example.

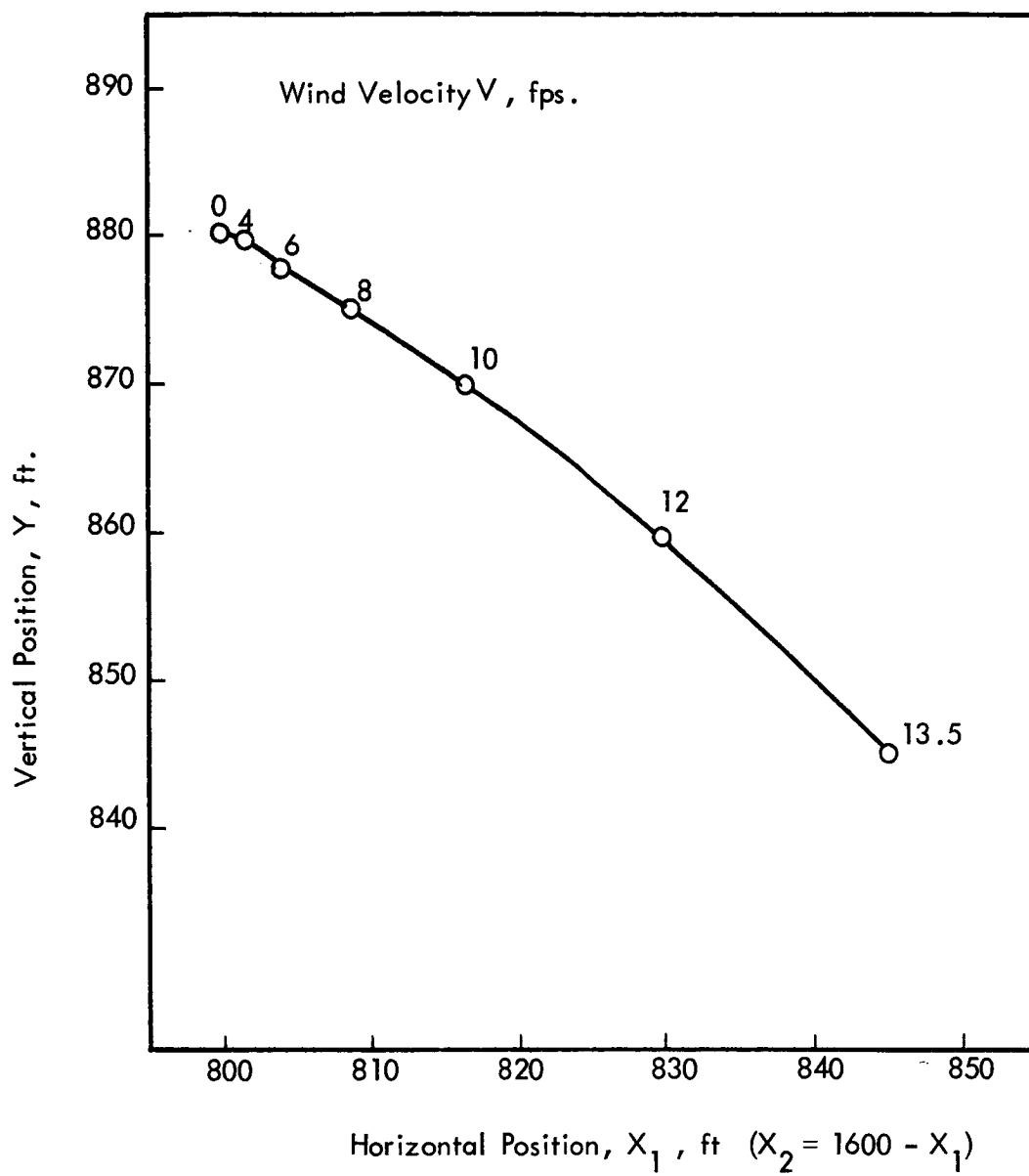


Figure 16. Two Cable Balloon Stability , Configuration A2.

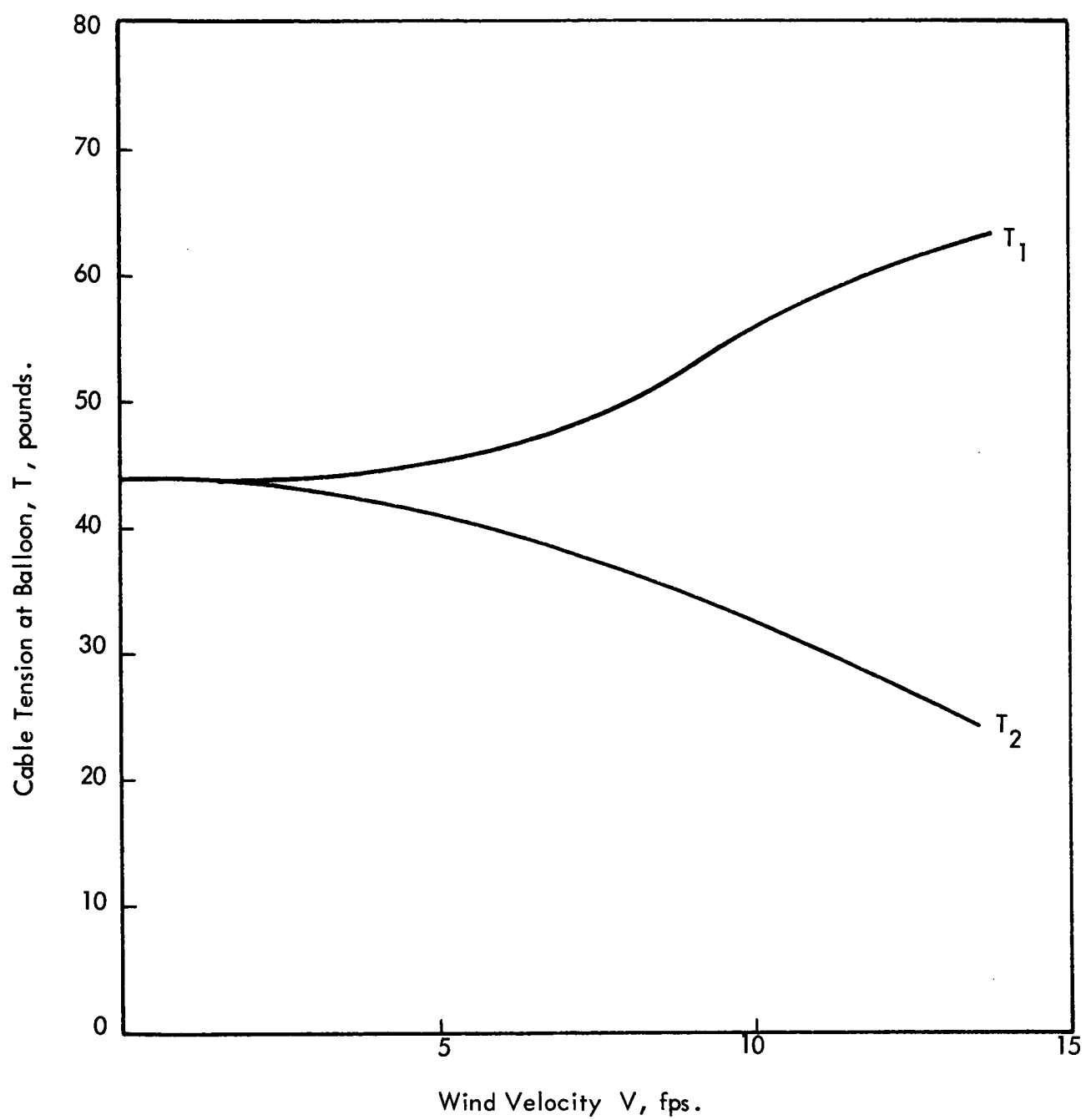


Figure 17. Cable Tension at Balloon, Configuration A2.

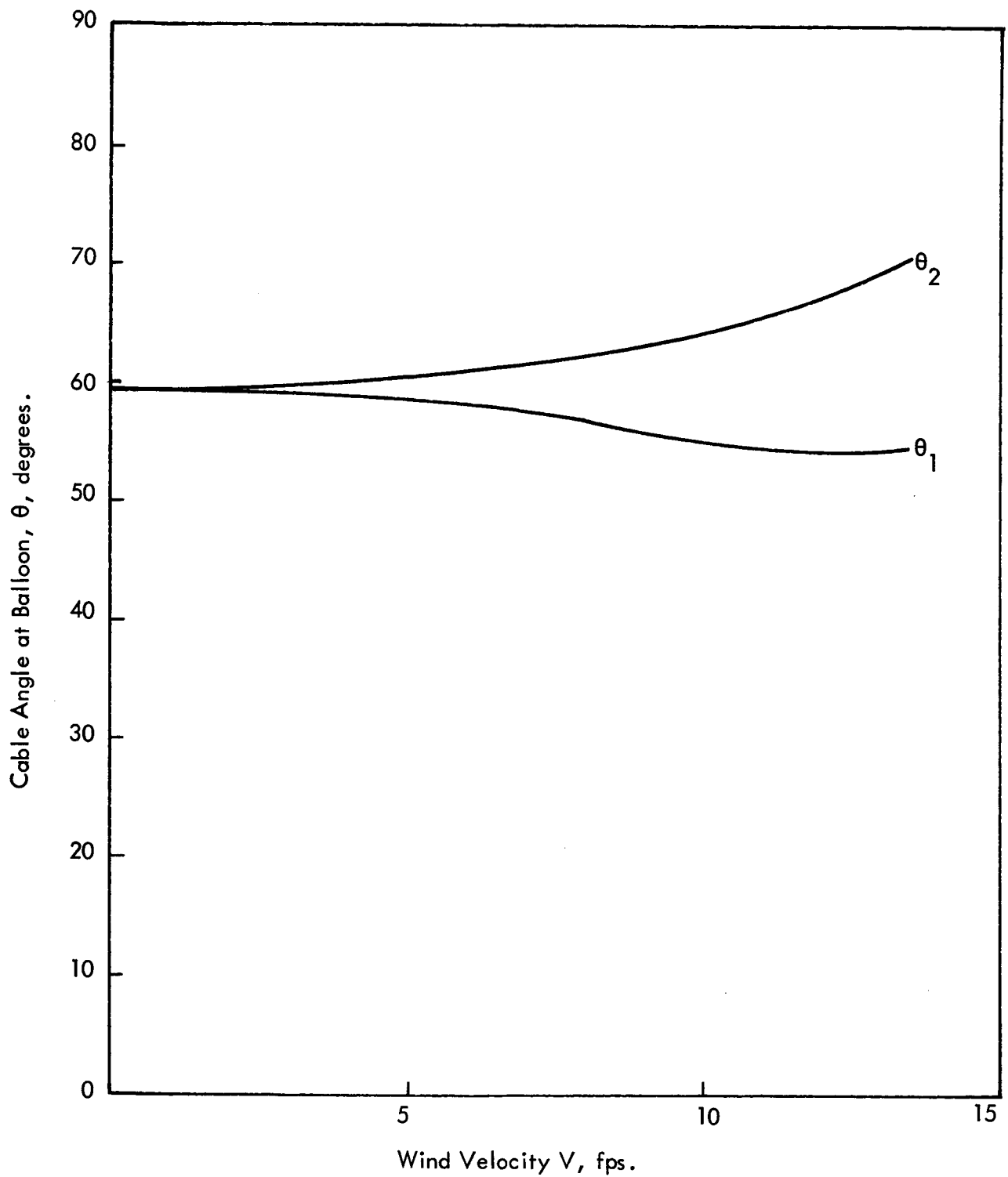
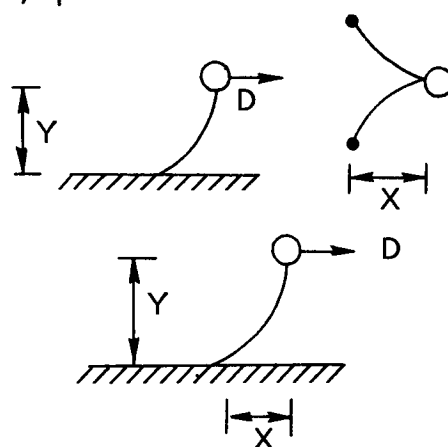
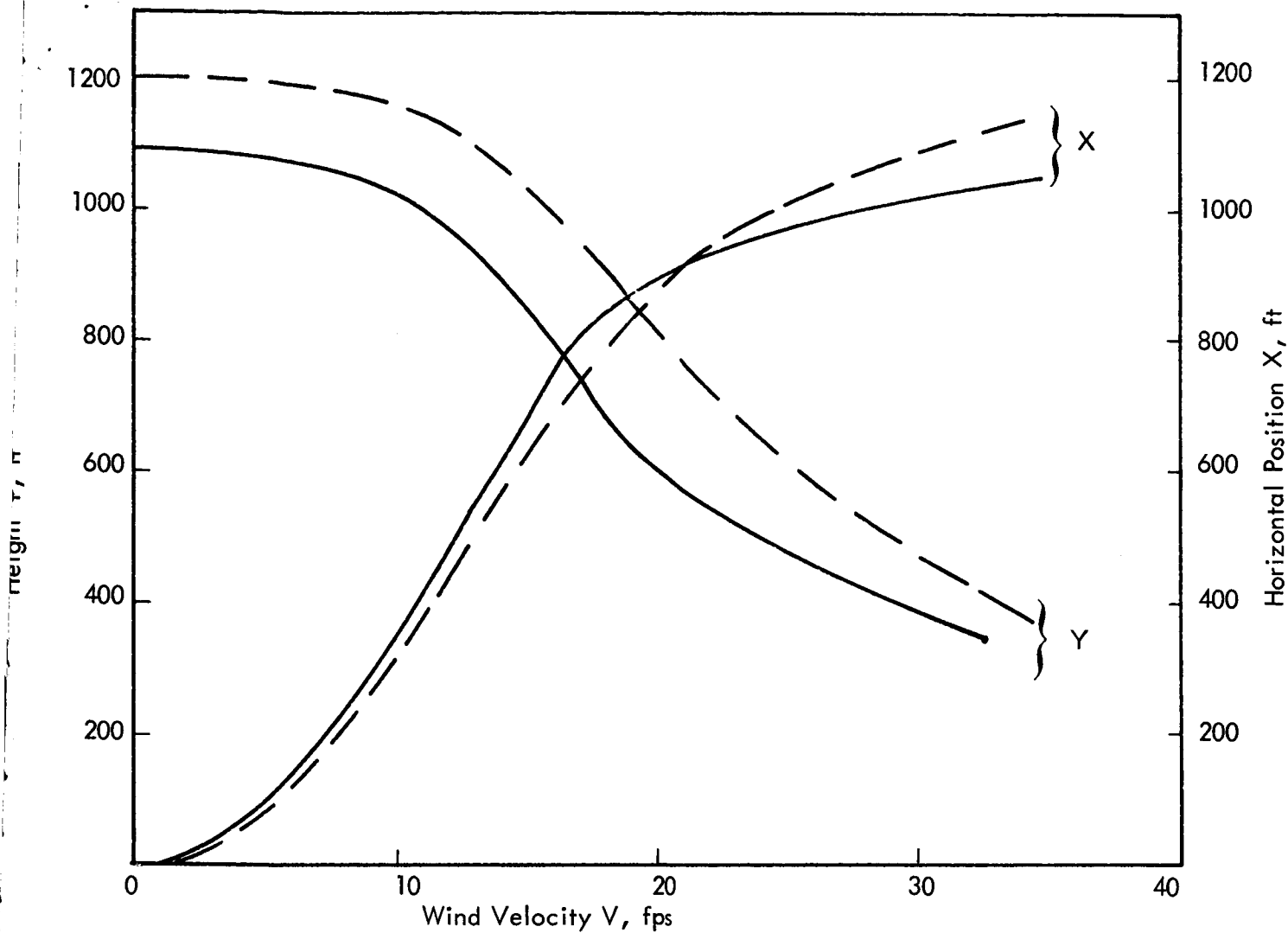


Figure 18. Cable Angles at Balloon, Configuration A2.



All Cables 1200 ft long, 0.02 pounds/ft. Excess lift = 75 lbs.

Figure 19. Two Cable Balloon Stability, Configuration B.

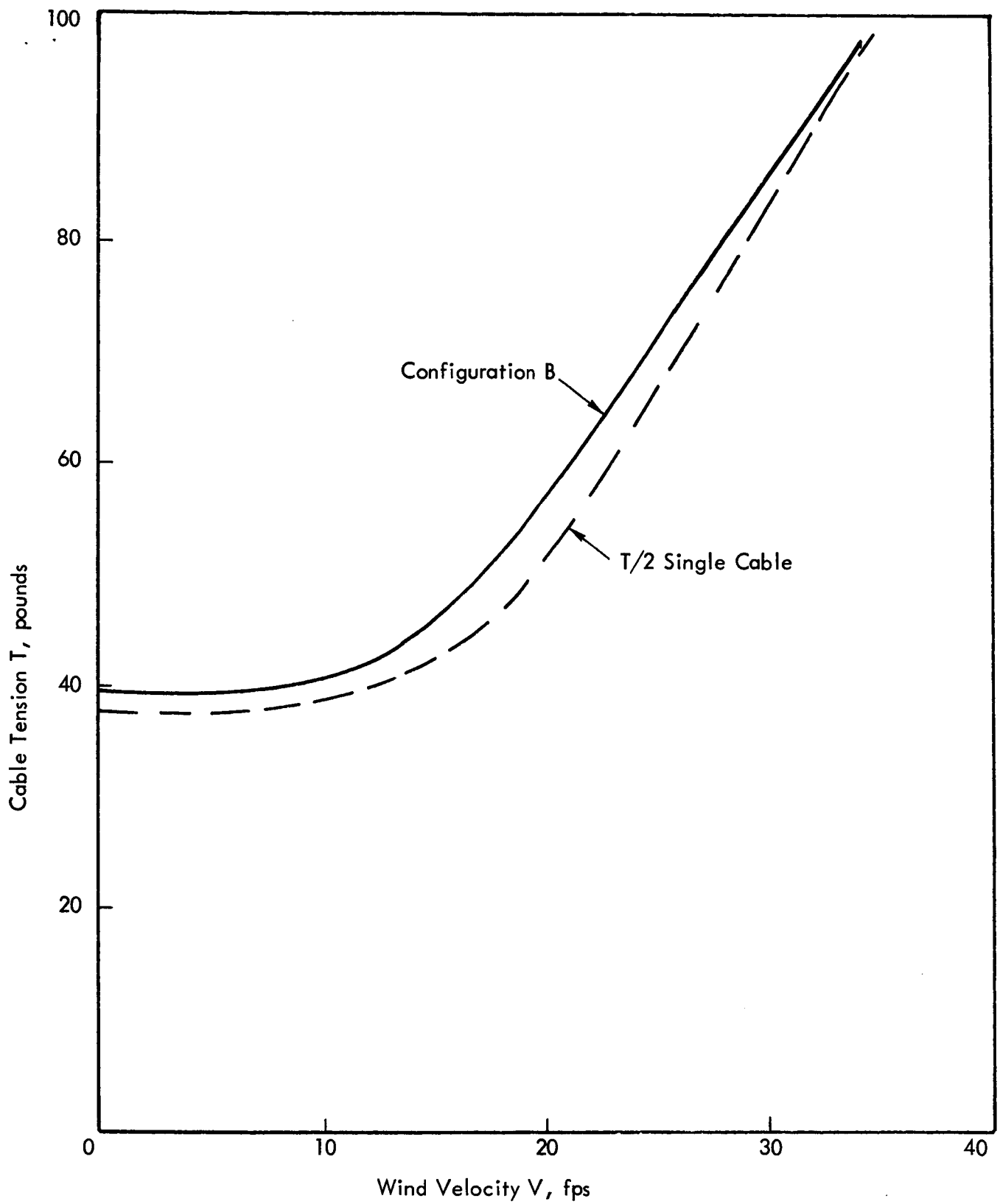
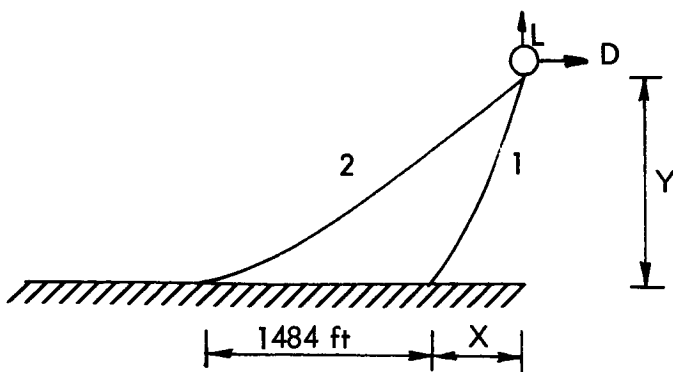
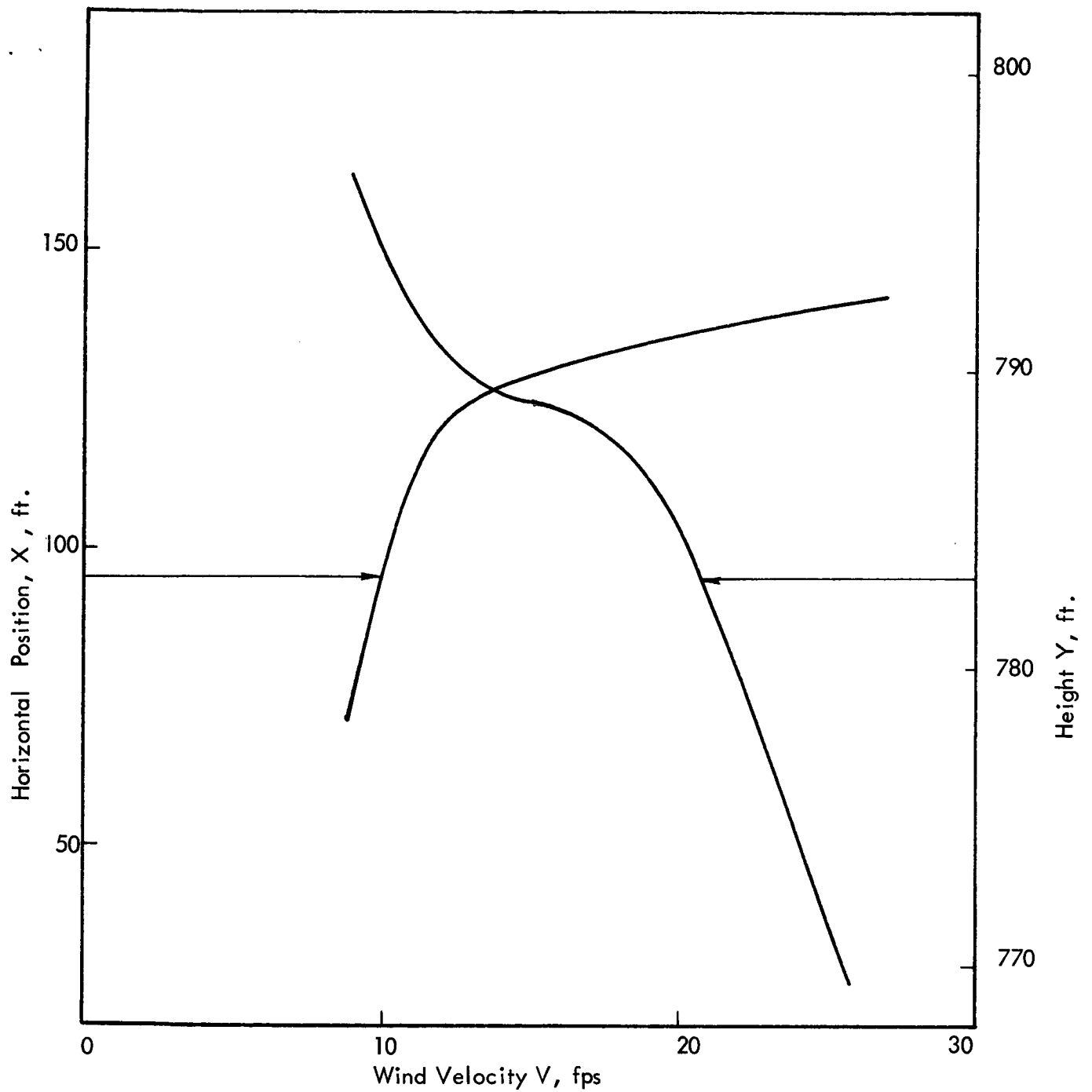


Figure 20. Cable Tension at Balloon, Configuration B.



Configuration C

Cable 1, 800 ft long,
0.04 pound/ft

Cable 2, 1800 ft long,
0.005 pound/ft

$L = 75$ pounds

Figure 21. Two Cable Balloon Stability, Configuration C.

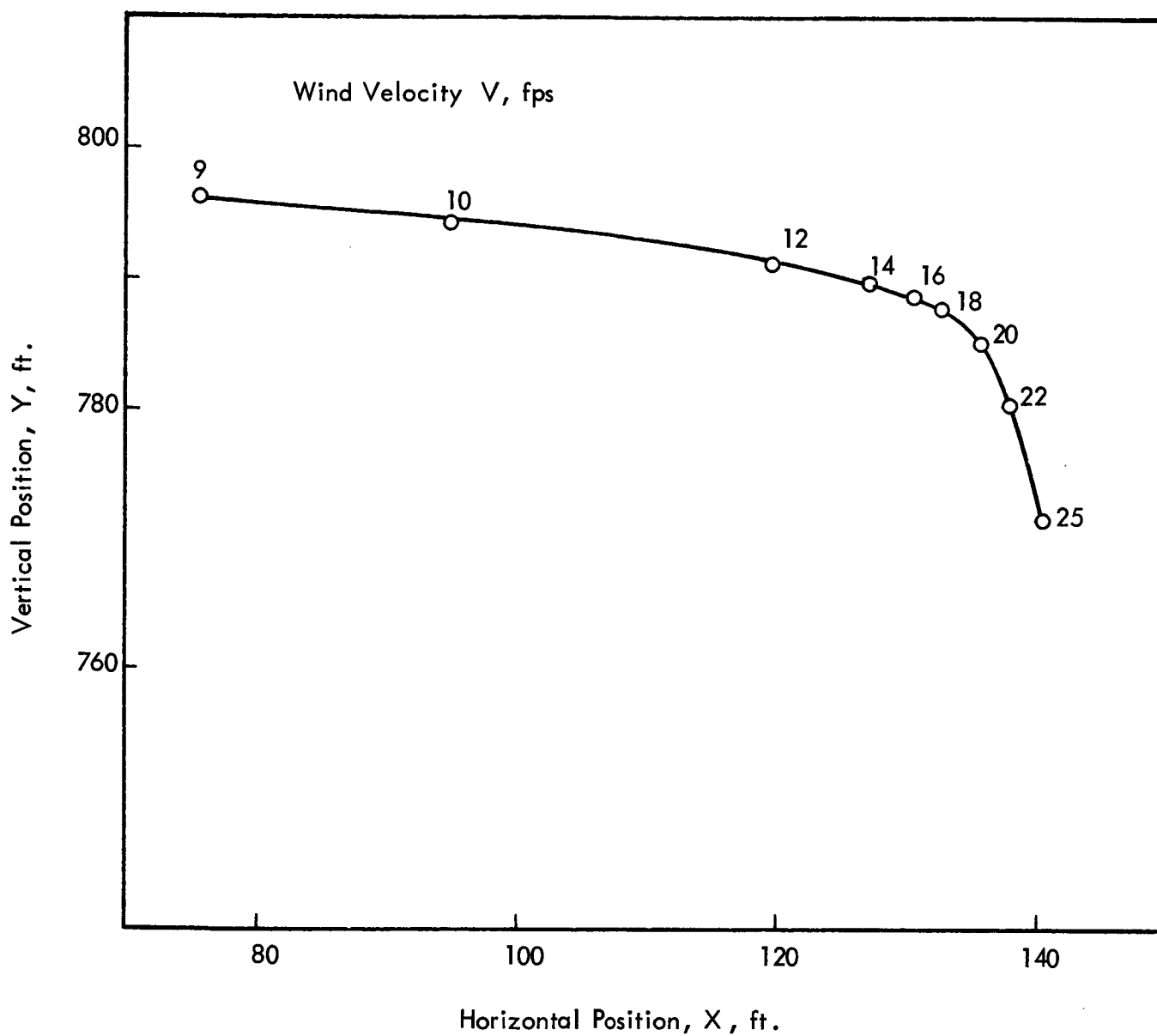


Figure 22. Two Cable Balloon Stability, Configuration C.

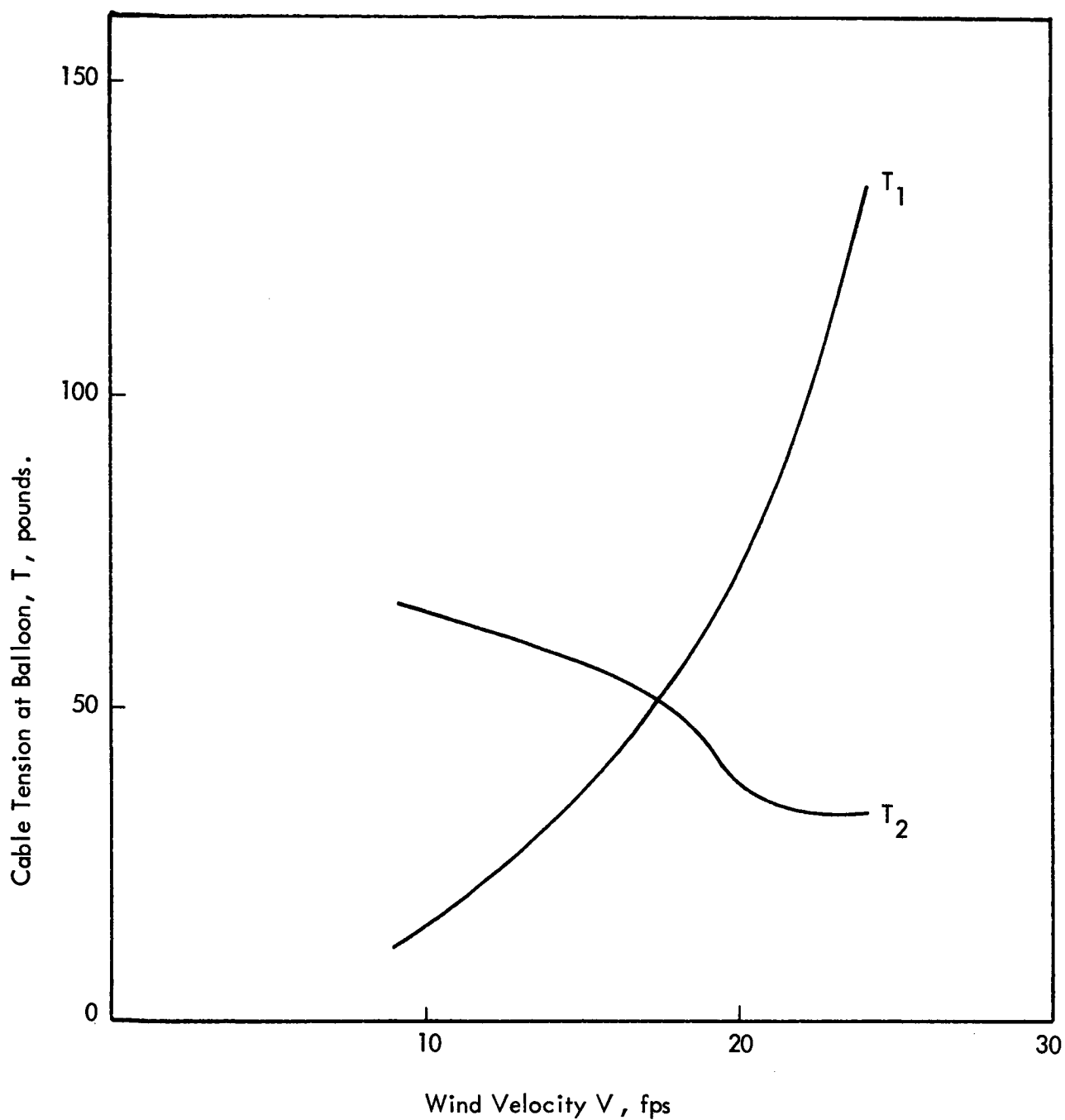


Figure 23. Cable Tension at Balloon, Configuration C.

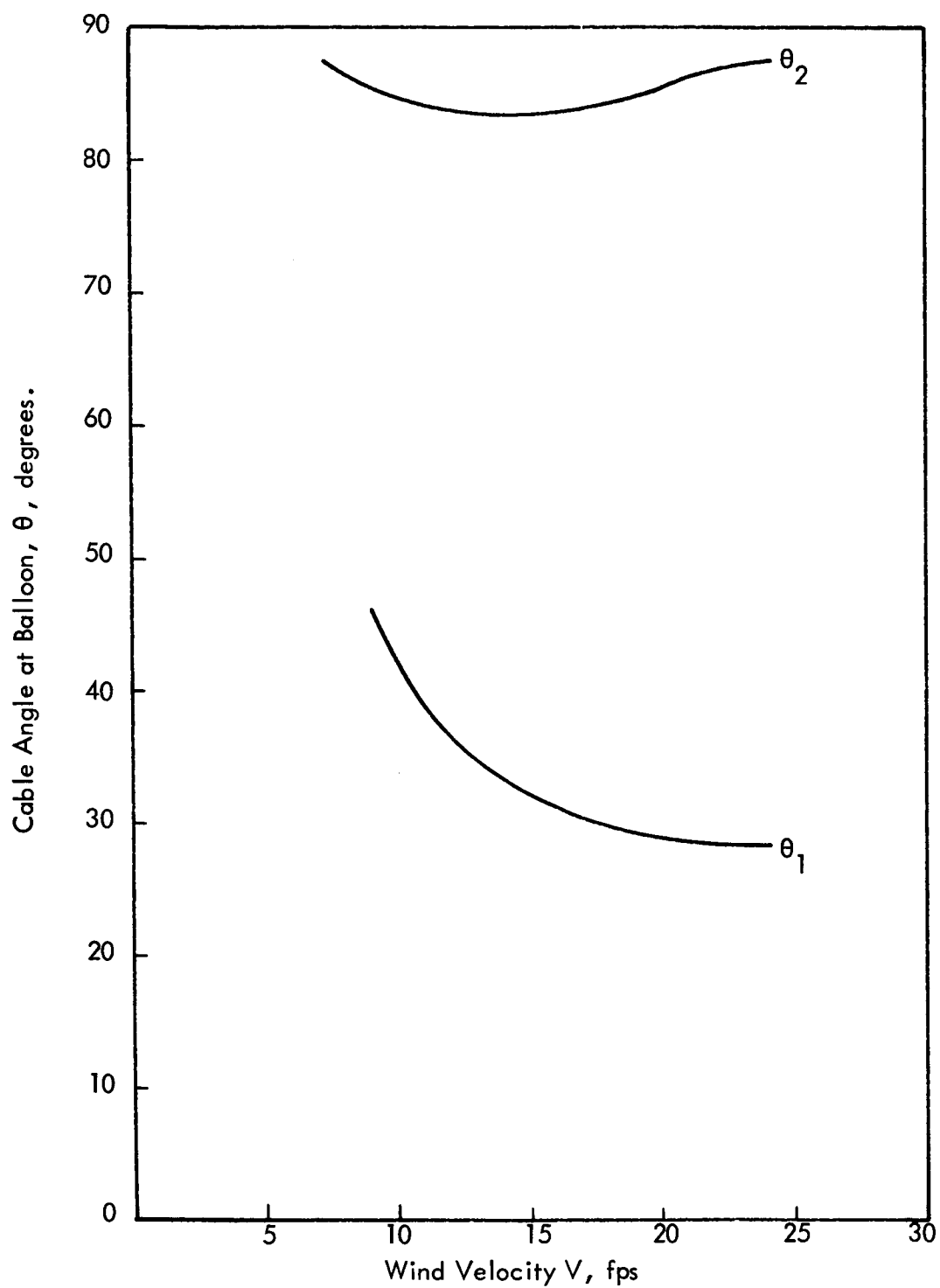
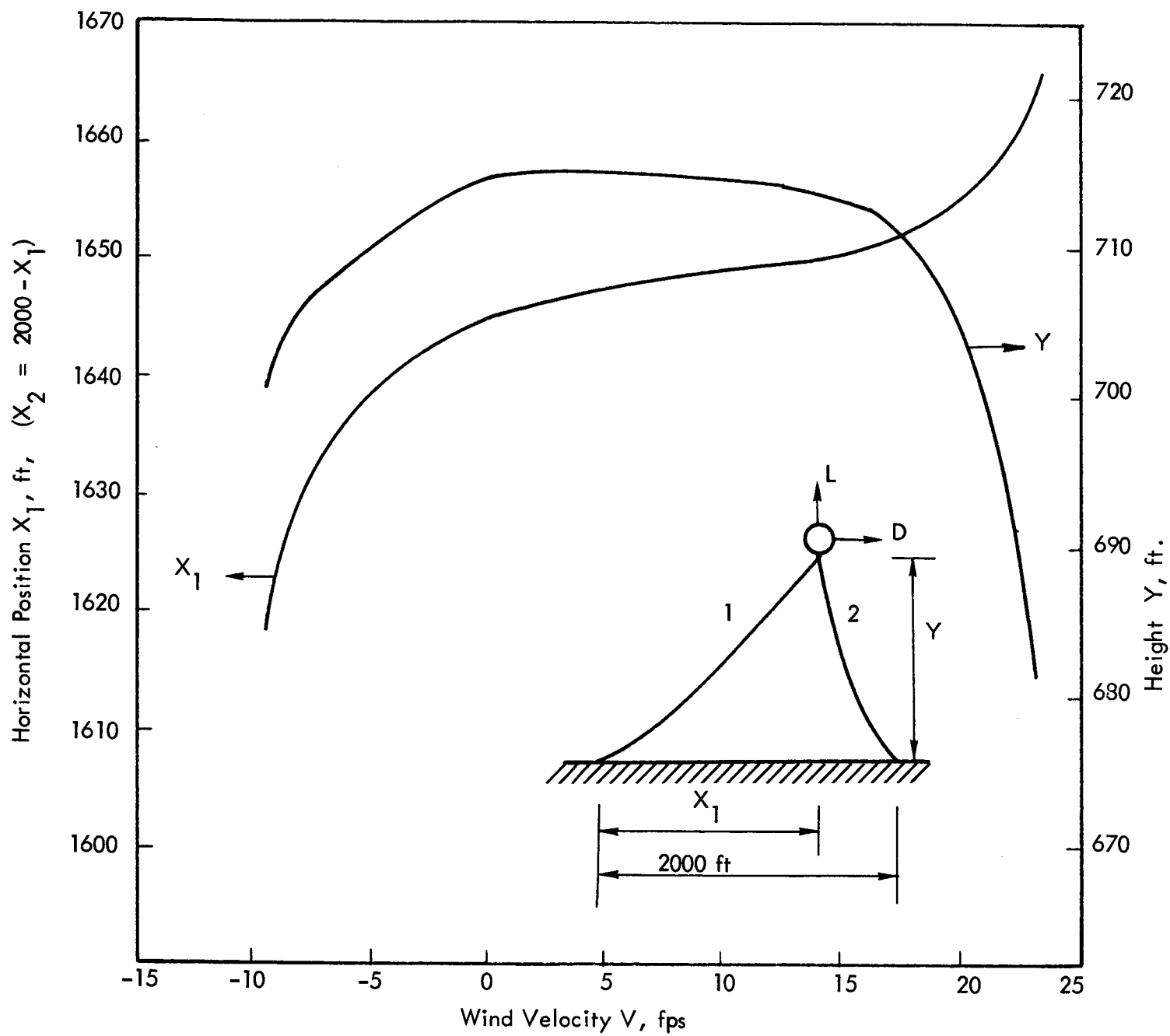


Figure 24. Cable Angle at Balloon, Configuration C.



Cable 1, 800 ft long, 0.04 pound/ft
 Cable 2, 1800 ft long, 0.005 pound/ft

Figure 25. Two Cable Balloon Stability, Configuration D.

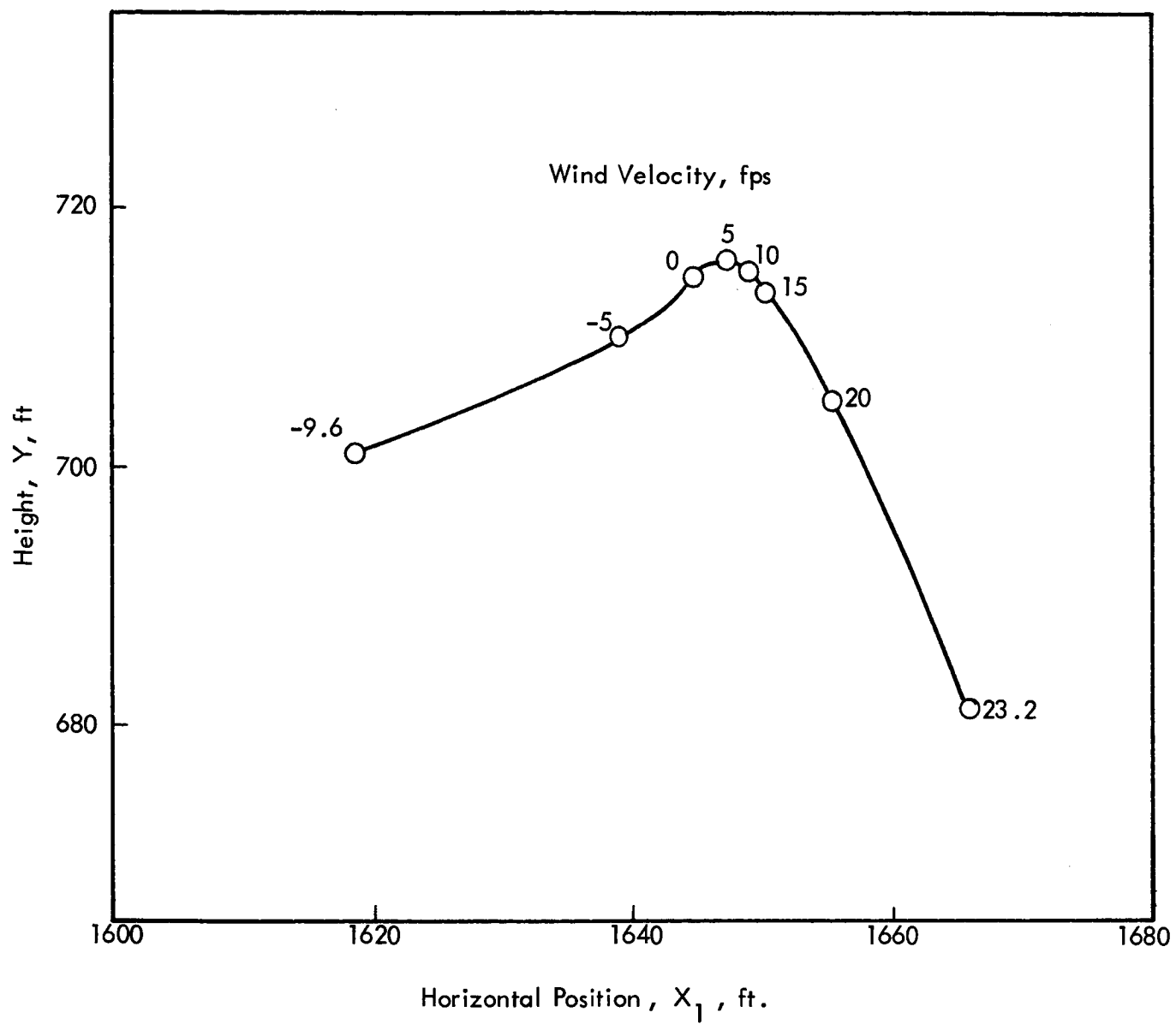


Figure 26. Two Cable Balloon Stability, Configuration D.

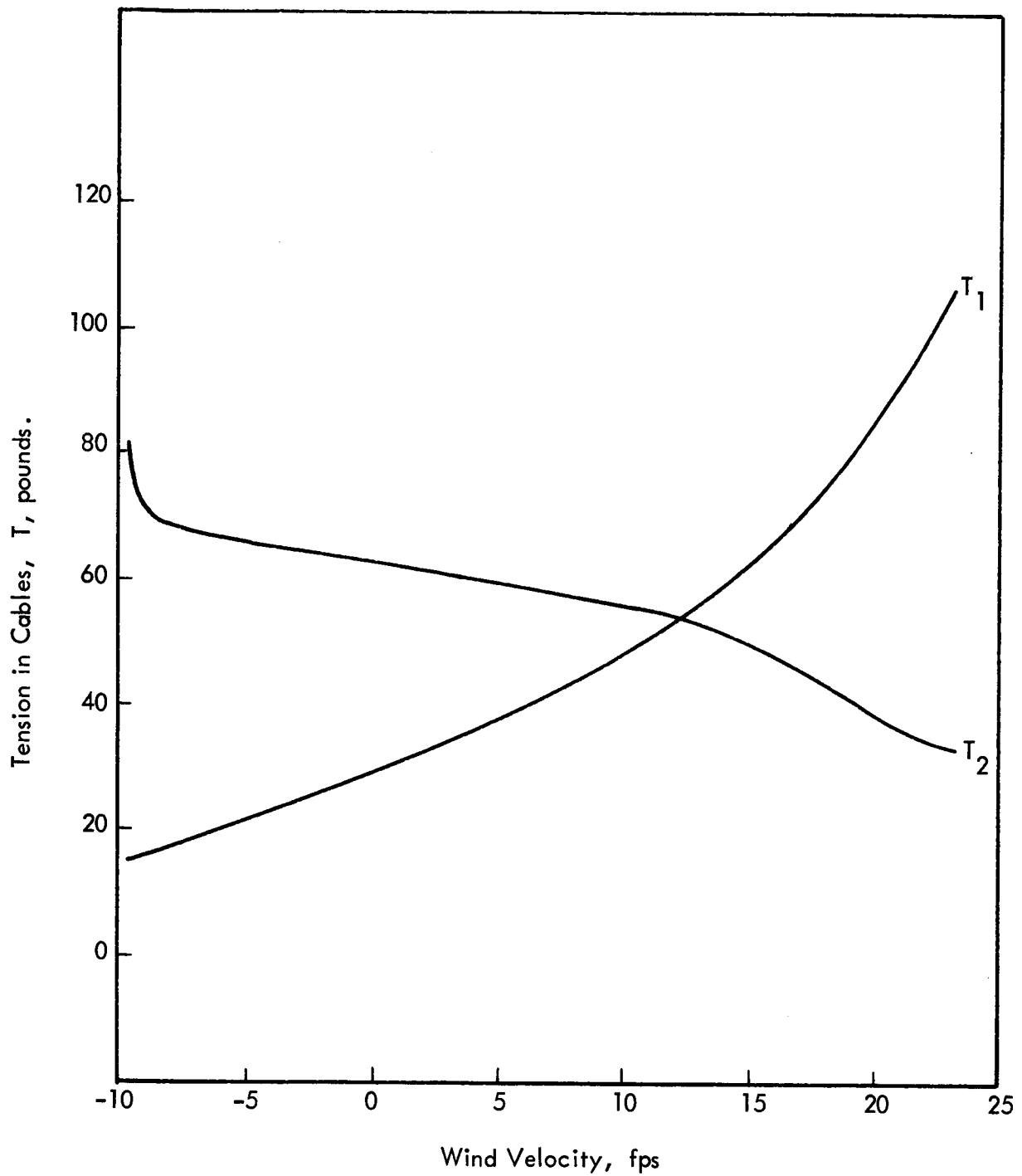


Figure 27. Balloon Configuration D, Cable Tension at Balloon.

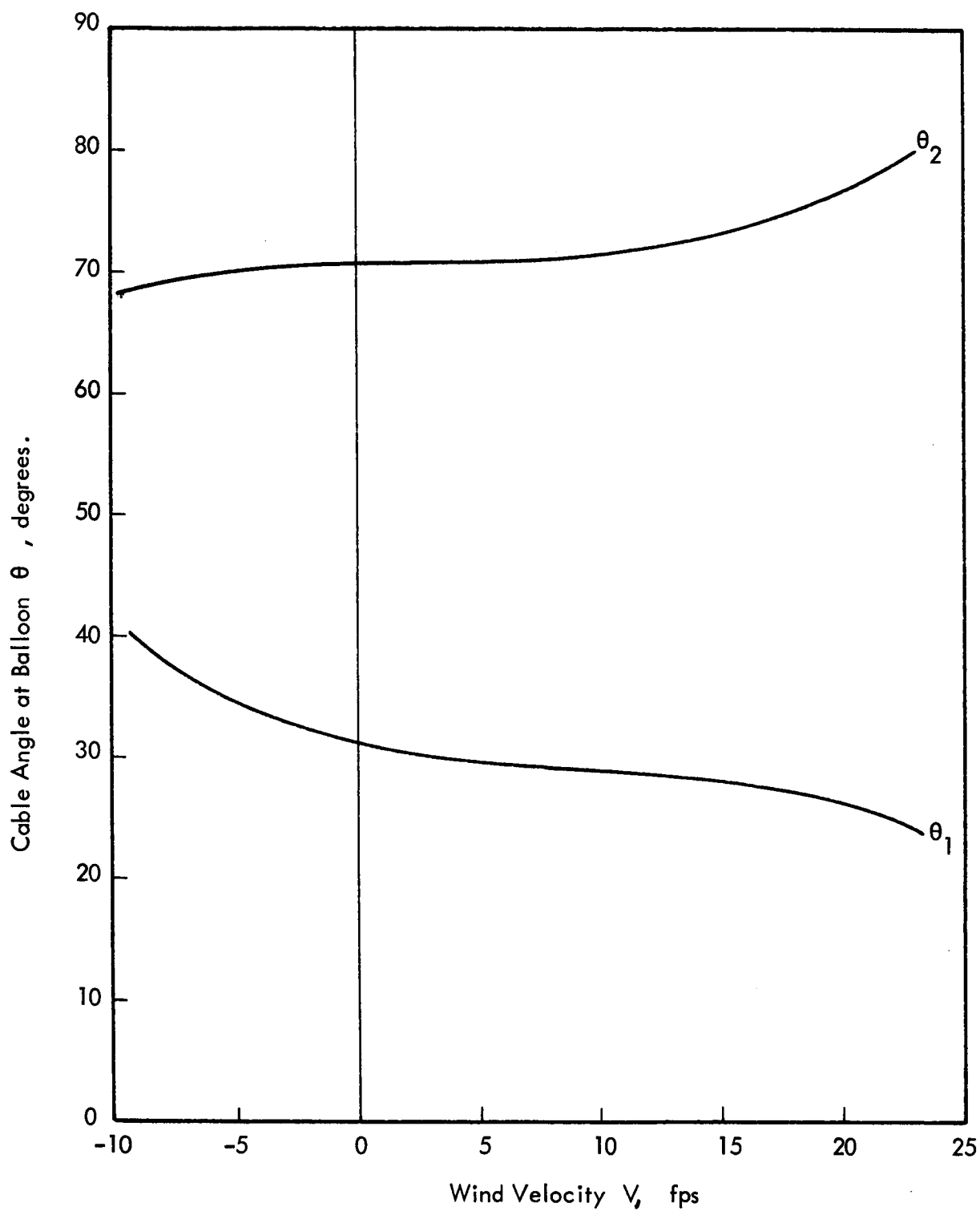


Figure 28. Configuration D, Cable Angles at Balloon .

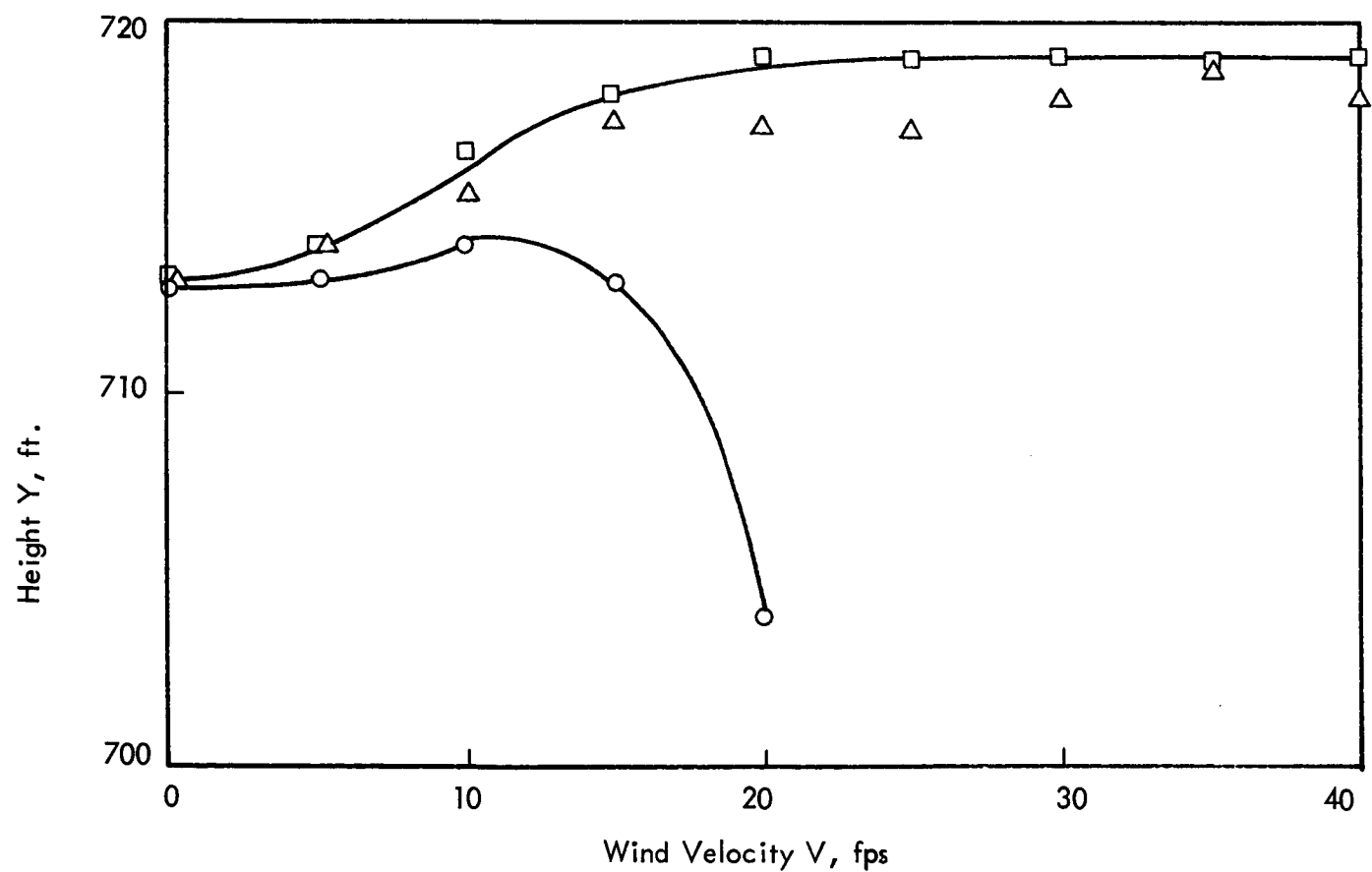
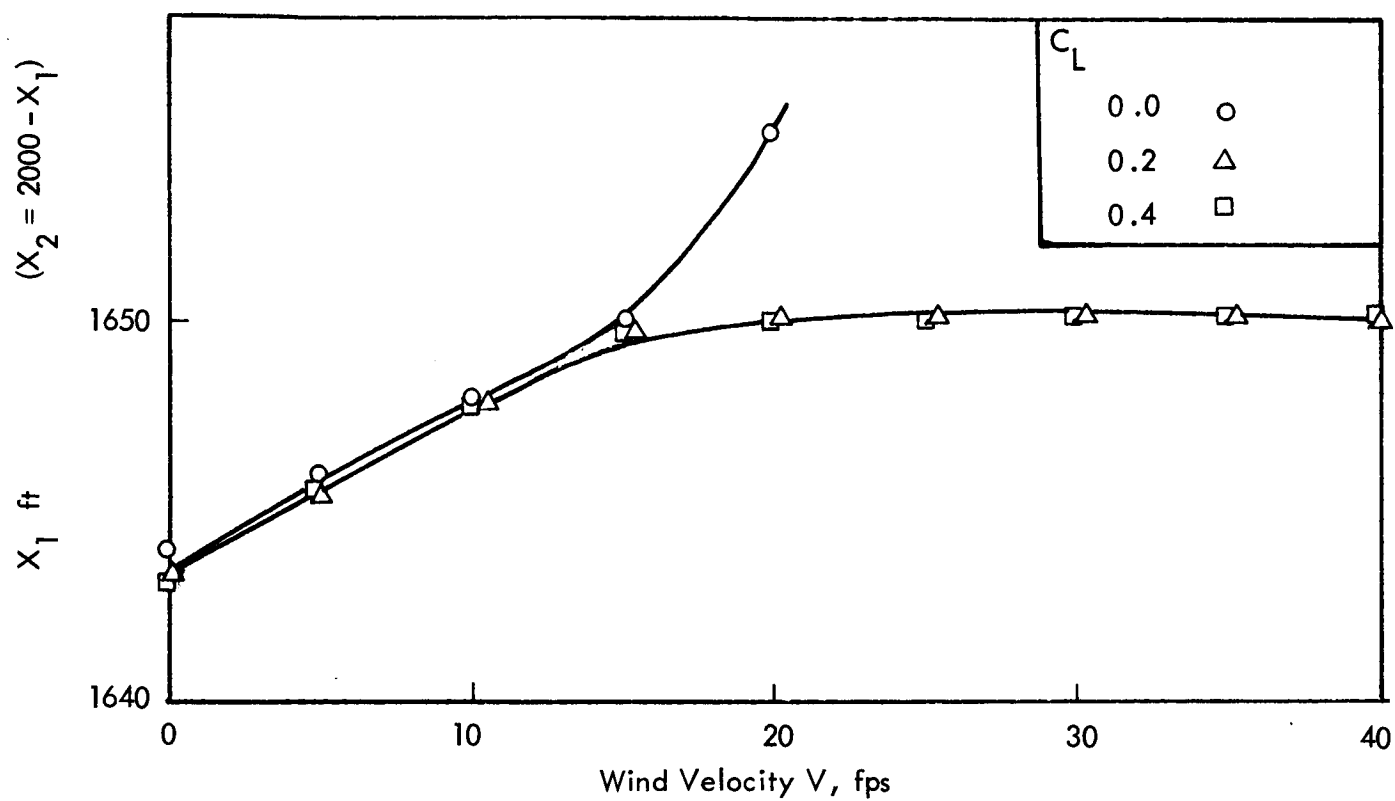
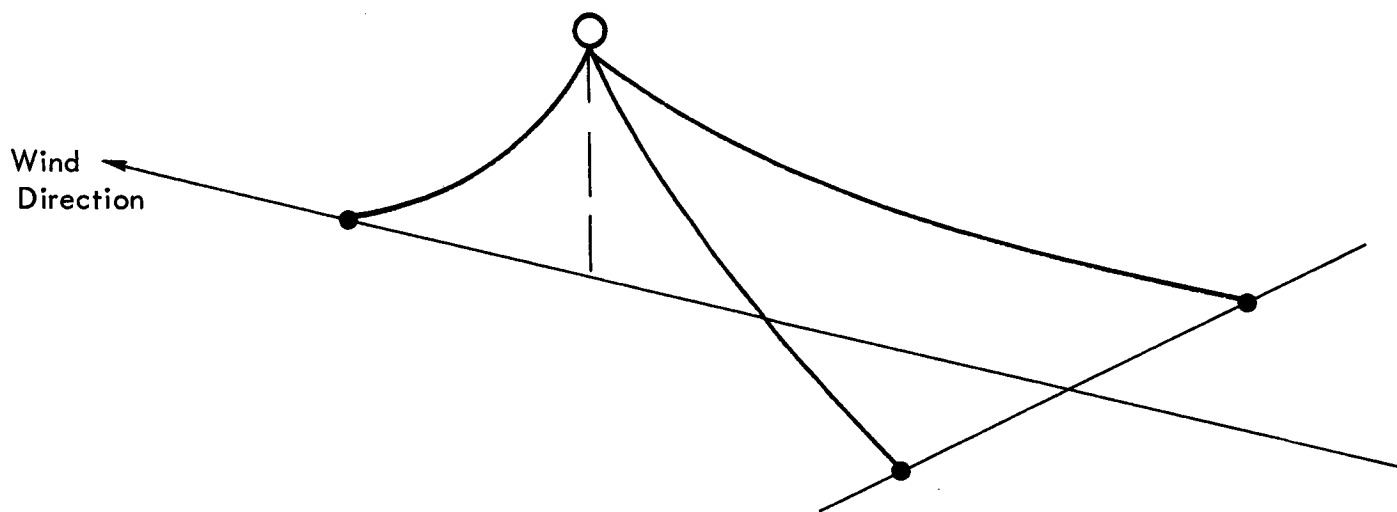
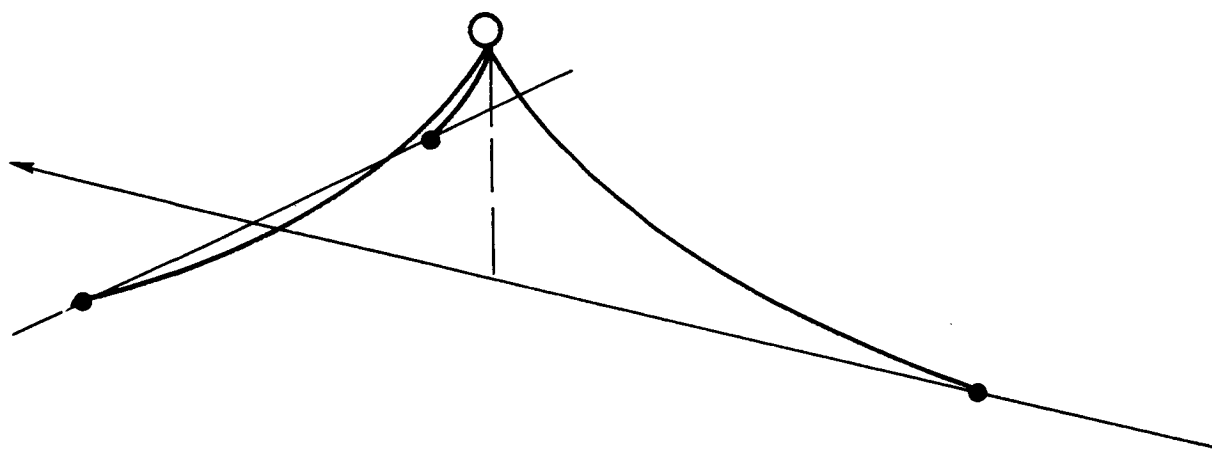


Figure 29. Effect of Aerodynamic Lift of Balloon, Configuration D.



a) Two Long Upstream Cables .



b) Two Short Downstream Cables .

Figure 30. Three Cable Configurations .

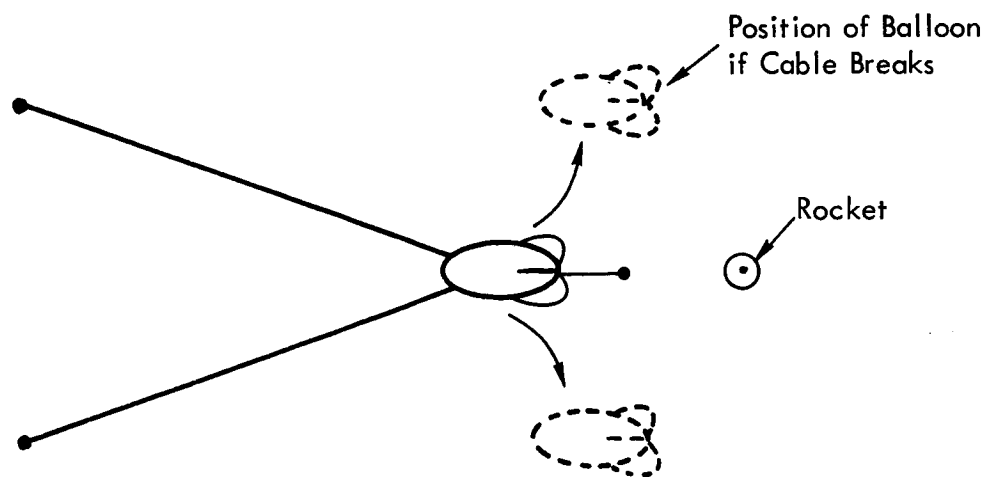
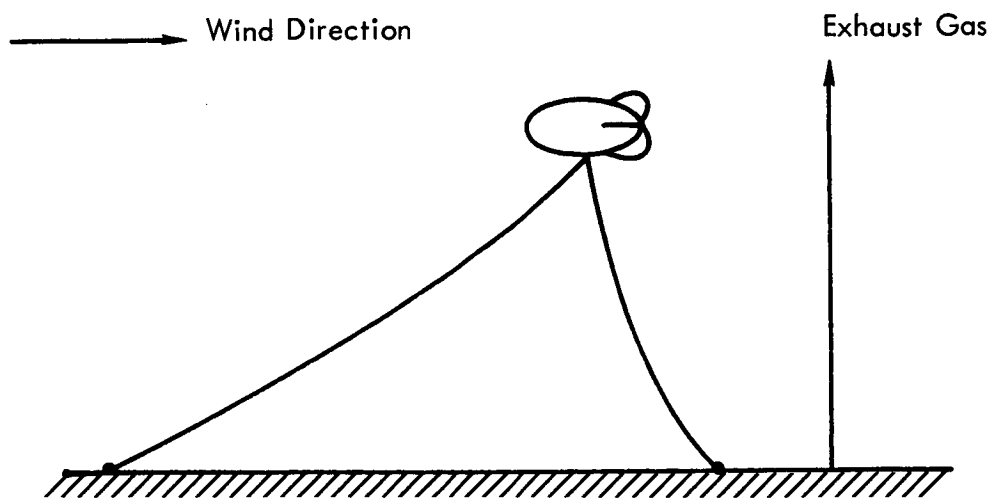


Figure 31. Balloon Positioned Upstream of Rocket.

```

PROGRAM POT21
C  MSEC BALLOON ITERATIVE PROCESS
C  WYLE LABORATORIES RESEARCH STAFF
C  AUGUST 1965
C  PROGRAMMER - DICK
  READ(60,1)AR,CL,CD,W1,W2
  READ(60,1)AL,CW1,CW2,CL1,CL2
1  FORMAT(5(F10,3))
  READ(60,15)THETA,N
15  FORMAT(F10,1,11U)
  WRITE(61,2)AR,CL,CD,W1,W2
2  FORMAT(1H1,2X,5HAREA=F10,2,5X,3HCL=F5,2,5X,3HCD=F5,2,5X,3HW1=,
1F8,2,5X,3HW2=F8,2)
  WRITE(61,3)AL,CW1,CW2,CL1,CL2
3  FORMAT(5X,5HLIFT=F5,1,5X,4HCW1=F8,4,5X,4HCW2=F8,4,5X,
14HCL1=F8,1,5X,4HCL2=F8,1)
  ALIT=CW1*CL1
  BLIT=CW2*CL2
  CLIT=CL1
  DLIT=CL2
  V=0.0
  DO 40 K=1,9
    EL=AL-W1-W2+0.00119*V*V*AR*CL
    DR=0.00119*V*V*AR*CD
    WRITE(61,4)V,DR,EL
4  FORMAT(1H1,5X,9HVELOCITY=F10,1,6HFT/SEC,/,2X,5HDRAG=F10,3,6HPOUN
1DS,/,5X,12HEXCESS LIFT=F10,3,6HPOUNDS,////)
    WRITE(61,14)
14  FORMAT(1X,10HTOTAL BASE,1X,10HFIRST BASE,3X,8HHEIGHT 1,3X,8HHEIGHT
1 2,5X,6HDRAG,1X,7HANGLE 1,3X,4HETA1,3X,4HETA2,4X,3HX11,4X,3HX12)
    TCOS=15.0
    FAC=1.011
    DO 50 I=1,400
      ETA1=TCOS/ALIT
      ETA2=(ALIT+ETA1-DR)/BLIT
      IF(ETA2)50,50,59
59  DO 60 J=1,N
        Z=J-1
        TH=(THETA-0.5*Z)/57.296
        XI1=SINF(TH)/COSF(TH)
        XI2=(EL-ALIT*XI1+ETA1)/(BLIT+ETA2)
        F1=XI1-1.0/ETA1
        IF(F1)60,60,51
51  F2=XI2-1.0/ETA2
        IF(F2)60,60,52
52  Y1=CLIT+ETA1*(SQRTF(1.0+XI1*XI1)-SQRTF(1.0+F1*F1))
        IF(Y1-CLIT*SINF(TH))50,58,60
58  Y2=DLIT+ETA2*(SQRTF(1.0+XI2*XI2)-SQRTF(1.0+F2*F2))
        IF(Y1-Y2+25.0)60,60,53
53  IF(Y1-Y2-25.0)54,60,60
54  X1=ETA1+CLIT*(ALOG(XI1+SQRTF(XI1*XI1+1.0))-ALOG(F1+SQRTF(F1*F1+1.0
1)))
        X2=ETA2+DLIT*(ALOG(XI2+SQRTF(XI2*XI2+1.0))-ALOG(F2+SQRTF(F2*F2+1.0
1)))
        X=X1+X2
        IF(X-1975.0)60,60,55
55  IF(X-2025.0)56,60,60
56  TH=TH+57.296
        WRITE(61,13)X,X1,Y1,Y2,TCOS,TH,ETA1,ETA2,XI1,XI2
13  FORMAT(4(3X,F8.1),3X,F8.2,2X,F6.1,4(1X,F6.3))
60  CONTINUE
50  TCOS=TCOS*FAC
40  V=V+5.0
    PAUSE1
  END

```

Figure 32. Computer Program POT 21, for Solution of Two-Cable Configuration with Aerodynamic Lift.

AREA= 468.00 CL= .40 CD= .37 W1= 220.00 W2= 205.00
LIFT=500.0 CL1= .0050 CW2= .0400 CL1= 1000.0 CL2= 800.0

VELOCITY= 0 FT/SEC
DRAG= 0 POUNDS
EXCESS LIFT= 75.00 POUNDS

TOTAL BASE	FIRST BASE	HEIGHT 1	HEIGHT 2	DRAG.1	ANGLE 1	ETA1	ETA2	X11	X12
1976.6	1641.1	714.2	723.4	23.38	33.5	2.264	.637	.662	3.019
1979.3	1640.9	717.7	721.5	21.60	33.5	2.289	.644	.662	2.979
1984.9	1647.1	700.5	722.3	20.60	33.0	2.289	.644	.649	2.991
1976.2	1631.1	738.4	718.7	23.83	34.0	2.314	.651	.675	2.927
1982.0	1638.6	721.2	719.6	20.63	33.5	2.314	.651	.662	2.939
1987.6	1645.9	704.1	720.4	20.83	33.0	2.314	.651	.649	2.952
1984.7	1637.3	724.7	717.6	21.06	33.5	2.340	.658	.662	2.900
1990.3	1644.3	707.6	718.4	21.26	33.0	2.340	.658	.649	2.913
1987.5	1636.1	728.1	713.5	21.29	33.5	2.365	.665	.662	2.861
1993.1	1643.4	711.0	716.4	21.29	33.0	2.365	.665	.649	2.874
1998.5	1650.5	693.9	717.3	21.29	32.5	2.365	.665	.637	2.886
1990.3	1634.8	731.5	713.4	21.92	33.5	2.391	.673	.662	2.823
1995.9	1642.2	714.4	714.4	21.92	33.0	2.391	.673	.649	2.835
2001.3	1643.3	697.4	715.3	21.92	32.5	2.391	.673	.637	2.848
1993.2	1633.6	734.8	711.3	21.76	33.5	2.418	.680	.662	2.785
1998.7	1641.0	717.8	712.3	21.76	33.0	2.418	.680	.649	2.798
2004.1	1648.1	708.8	713.2	21.76	32.5	2.418	.680	.637	2.810
2001.6	1639.7	721.1	710.1	22.00	33.0	2.444	.687	.649	2.760
2007.0	1646.9	704.1	711.1	22.00	32.5	2.444	.687	.637	2.772
2012.2	1653.9	687.1	712.1	22.00	32.0	2.444	.687	.625	2.785
2004.5	1638.5	724.4	707.9	22.24	33.0	2.471	.695	.649	2.723
2009.9	1645.8	707.4	708.9	22.24	32.5	2.471	.695	.637	2.735
2015.2	1652.8	690.4	709.4	22.24	32.0	2.471	.695	.625	2.747
2007.5	1637.3	727.6	705.6	22.48	33.0	2.498	.703	.649	2.686
2012.9	1644.6	719.7	706.7	22.48	32.5	2.498	.703	.637	2.699
2018.1	1651.6	694.7	707.7	22.48	32.0	2.498	.703	.625	2.711
2015.9	1643.4	713.4	704.4	22.73	32.5	2.526	.710	.637	2.662
2021.1	1650.2	697.0	705.5	22.73	32.0	2.526	.710	.625	2.674
2019.0	1642.3	717.1	702.1	22.98	32.5	2.554	.718	.637	2.626
2024.2	1649.4	700.2	703.2	22.98	32.0	2.554	.718	.625	2.639
2022.0	1641.1	720.2	699.7	23.23	32.5	2.582	.726	.637	2.591

X₁ = 1643 ft
Y = 713 ft

VELOCITY= 20.0 FT/SEC
DRAG= 66.83 POUNDS
EXCESS LIFT= 75.00 POUNDS

TOTAL BASE	FIRST BASE	HEIGHT 1	HEIGHT 2	DRAG.1	ANGLE 1	ETA1	ETA2	X11	X12
1999.0	1547.7	722.9	599.1	75.73	26.5	8.414	.278	.499	4.185
1992.9	1634.2	707.8	708.1	73.23	26.0	8.414	.278	.488	4.278
1987.4	1540.6	692.7	715.9	75.73	25.5	8.414	.278	.477	4.369
2021.1	1653.8	708.7	691.0	76.56	26.0	8.507	.304	.488	3.870
2015.1	1640.2	693.6	700.3	76.56	25.5	8.507	.304	.477	3.954

X₁ = 1655 ft
Y = 704 ft

VELOCITY= 20.0 FT/SEC
DRAG= 66.83 POUNDS
EXCESS LIFT= 164.10 POUNDS

TOTAL BASE	FIRST BASE	HEIGHT 1	HEIGHT 2	DRAG.1	ANGLE 1	ETA1	ETA2	X11	X12
1976.6	1643.2	733.8	720.6	109.85	26.0	12.206	1.344	.488	2.569
1979.7	1649.8	719.0	728.2	109.85	25.5	12.206	1.344	.477	2.597
1985.7	1643.0	734.4	722.2	111.06	26.0	12.340	1.382	.488	2.486
1988.7	1649.5	719.6	725.9	111.06	25.5	12.340	1.382	.477	2.513
1991.6	1655.9	704.7	725.6	111.06	25.0	12.340	1.382	.466	2.540
1994.9	1642.7	735.0	717.0	112.28	26.0	12.476	1.420	.488	2.406
1997.8	1649.3	720.2	719.4	112.28	25.5	12.476	1.420	.477	2.432
2000.6	1655.7	705.4	721.2	112.28	25.0	12.476	1.420	.466	2.459
2004.1	1642.5	735.6	712.8	113.52	26.0	12.613	1.459	.488	2.329
2006.9	1649.0	720.8	714.8	113.52	25.5	12.613	1.459	.477	2.355
2009.6	1655.4	706.0	716.6	113.52	25.0	12.613	1.459	.466	2.381
2016.1	1646.7	721.4	709.9	114.76	26.5	12.752	1.498	.477	2.282
2018.7	1655.2	706.6	711.9	114.76	26.0	12.752	1.498	.466	2.307
2021.2	1661.4	691.7	713.8	114.76	24.5	12.752	1.498	.426	2.333

X₁ = 1650 ft
Y = 719 ft

Figure 33. Typical Results for POT 21.

3200 FORTRAN (2.0)

```

PROGRAM POT15
C BASIC BALLOON CABLE - NO DRAG
C WYLE LABORATORIES RESEARCH STAFF
C APRIL 1965
C PROGRAMMER - MOOSE
C
COMMON/ DATA / XY(10)
DATA (XY=1.0,.995,.99,.985,.98,.975,.97,.965,.96,.955)
COMMON W(1),XL(1),Y(1),YX(1),TEMP(6),T(1),X(1),THD(1),THR(1)
1 READ (60,2) NN
2 FORMAT (I2)
IF (NN)999,999,3
3 READ(60,4)EXA,W,XL,Y
4 FORMAT(4F10.0)
5 DO 50 I=1,10
YX=Y*XY(I)
WRITE (61,40) YX
40 FORMAT (1H1,2X,29HBASIC BALLOON CABLE - NO DRAG,/,10X,2HY=,
1E16.9,/)
WRITE(61,15)EXA,W,XL,Y
15 FORMAT(5X,7HEXAMPLE,F10.4,5X,6HWEIGHT,F10.4,5X,6HLENGTH,F10.4,5X,6
1HHEIGHT,F10.4/)
L=7
WRITE (61,12)
L=L+2
THD=89.0
500 THR=THD*.01/453293
TEMP=YX/XL
TEMP(2)=SINF(THR)-TEMP
IF (TEMP(2))50,6,6
6 TEMP(3)=1.0-TEMP*TEMP
T=W*XL*TEMP(3)/(2.0*TEMP(2))
TEMP=1*SINF(THR)
TEMP(2)=T*COSF(THR)
TEMP(3)=TEMP-W*XL
IF (TEMP(3))/,8,8
8 TEMP(3)=TEMP(3)/TEMP(2)
TEMP(4)=TEMP/TEMP(2)
TEMP(5)=TEMP(2)/W
X=TEMP(5)*(SINH1(TEMP(4))-SINH1(TEMP(3)))
9 WRITE (61,10) THD,T,TEMP(1),TEMP(2),X
10 FORMAT (2X,E16.9,4X,E16.9,4X,E16.9,4X,E16.9,4X,E16.9)
L=L+1
IF(L-60)13,13,11
11 WRITE (61,61)
61 FORMAT (1H1)
WRITE (61,12)
12 FORMAT (7X,5HTHETA,17X,1HT,18X,4HTSIN,16X,4HTCOS,17X,1HX,/)
L=2
7 CONTINUE
13 THD=THD-1.0
IF (THD-14.8)50,50,500
50 CONTINUE
GO TO 1
999 STOP
END

```

3200 FORTRAN (2.0)

```

FUNCTION SINH1(X)
TEMP=X
TEMP=TEMP+SQRIF(TEMP*TEMP+1.0)
SINH1=ALOG(TEMP)
RETURN
END

```

Figure 34. Computer Program POT 15, for Solution of Single Cable.

BASIC BALLOON CABLE - NO DRAG

Y= 8,560000000E 02

EXAMPLE	10.5100	WEIGHT	.0200	LENGTH 1200.0000	HEIGHT 856.0000		
THETA	T	TSIN	TCOS	X			
7.100000000E 01	2.538432817E 01	2.400135409E 01	8.264328056E 00	7.386442674E 02			
7.000000000E 01	2.603766089E 01	2.446739810E 01	8.905403689E 00	7.493694841E 02			
6.900000000E 01	2.676024580E 01	2.498284200E 01	9.590013588E 00	7.591747863E 02			
6.800000000E 01	2.756068255E 01	2.555382022E 01	1.032441257E 01	7.681371057E 02			
6.700000000E 01	2.844921110E 01	2.618763725E 01	1.111599151E 01	7.763250628E 02			
6.600000000E 01	2.943810874E 01	2.689305090E 01	1.197355667E 01	7.838000918E 02			
6.500000000E 01	3.054220986E 01	2.768064304E 01	1.290769478E 01	7.906173791E 02			
6.400000000E 01	3.17959441E 01	2.856331068E 01	1.393125637E 01	7.968266531E 02			
6.300000000E 01	3.317251287E 01	2.955692585E 01	1.506000480E 01	8.024728510E 02			
6.200000000E 01	3.474864788E 01	3.068123549E 01	1.631350111E 01	8.075966878E 02			
6.100000000E 01	3.654286477E 01	3.196111020E 01	1.771633146E 01	8.122351429E 02			
6.000000000E 01	3.859968689E 01	3.342830998E 01	1.929984248E 01	8.164218788E 02			
5.900000000E 01	4.097687199E 01	3.512403535E 01	2.110464827E 01	8.201876028E 02			
5.800000000E 01	4.375070628E 01	3.710270381E 01	2.318434105E 01	8.235603823E 02			
5.700000000E 01	4.702406259E 01	3.943769798E 01	2.561113900E 01	8.265659183E 02			
5.600000000E 01	5.093906619E 01	4.223040055E 01	2.848476319E 01	8.292277860E 02			
5.500000000E 01	5.569776620E 01	4.562493989E 01	3.194692505E 01	8.315676452E 02			
5.400000000E 01	6.159741030E 01	4.983335268E 01	3.620604806E 01	8.336054265E 02			
5.300000000E 01	6.909396496E 01	5.518089501E 01	4.158178472E 01	8.353594953E 02			
5.200000000E 01	7.892433124E 01	6.219322295E 01	4.859066866E 01	8.368467974E 02			
5.100000000E 01	9.236205149E 01	7.177879673E 01	5.812532060E 01	8.380829898E 02			
5.000000000E 01	1.118144726E 02	8.565485715E 01	7.187295554E 01	8.390825545E 02			
4.900000000E 01	1.424456037E 02	1.075050640E 02	9.345272194E 01	8.398589017E 02			
4.800000000E 01	1.977044152E 02	1.469230161E 02	1.322900718E 02	8.404244642E 02			
4.700000000E 01	3.270666580E 02	2.392014161E 02	2.230589190E 02	8.407907775E 02			
4.600000000E 01	9.812509784E 02	7.058528979E 02	6.816341900E 02	8.409685583E 02			

Figure 35. Typical Results for POT 15.

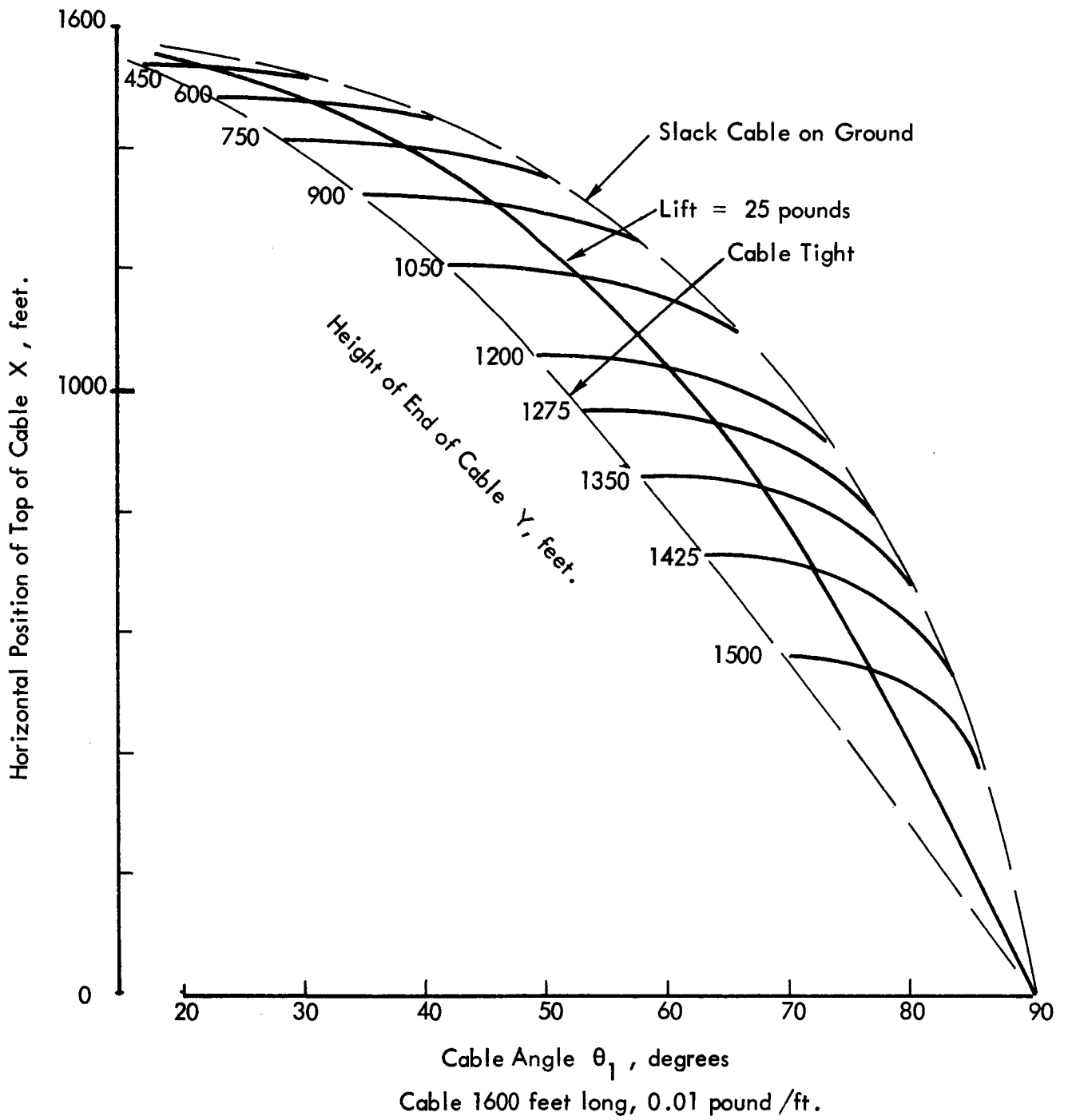


Figure 36. Single Cable Analysis

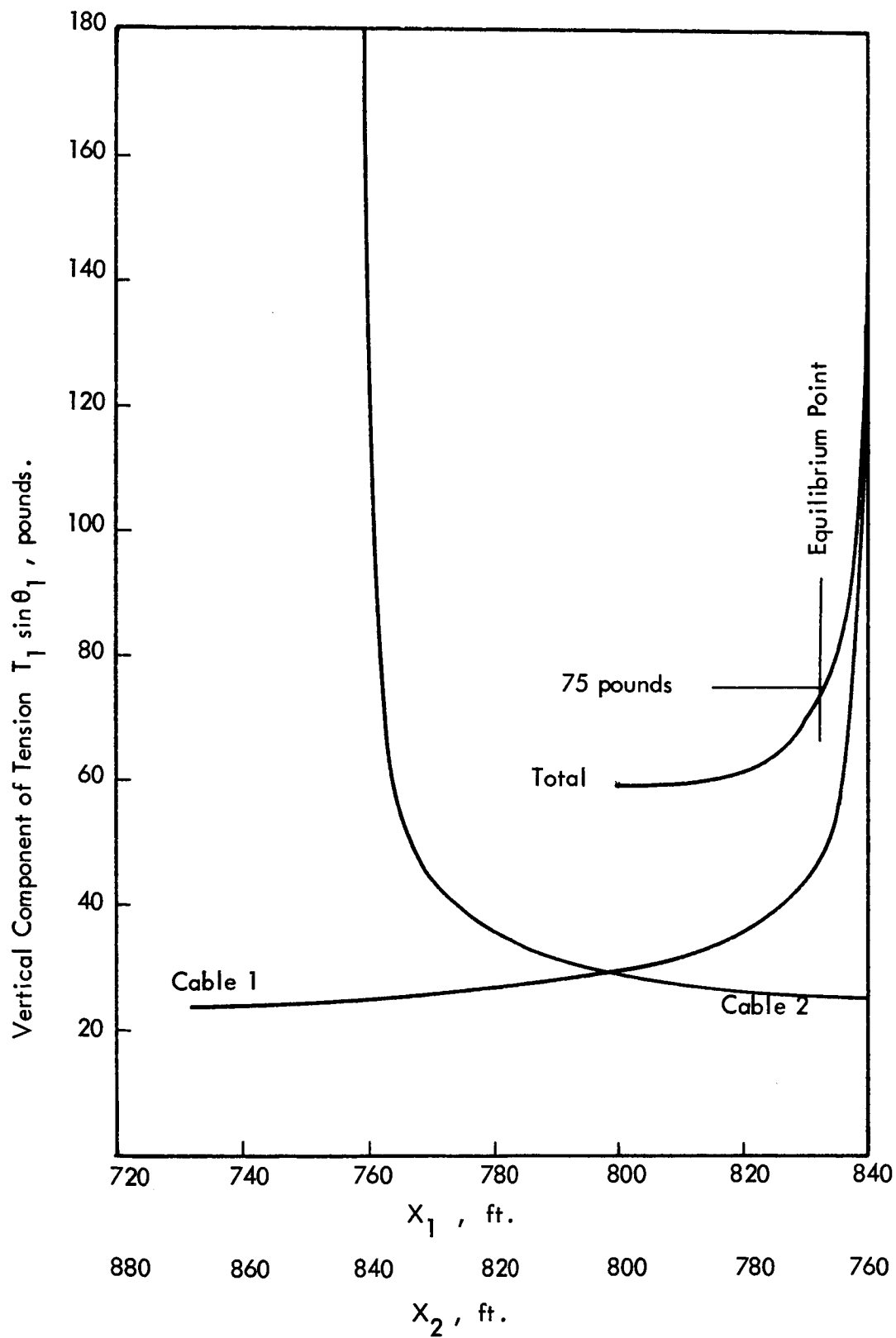


Figure 37. Vertical Components of Tension Configuration A2, $Y = 856$ ft.

<p>Example 10.51</p> <p>Both cables</p> <p>$\ell = 1200$ ft</p> <p>$w = 0.02$ pound/ft</p> <p>$Y = 856$ ft</p>									
X_1	X_2	L_1	L_2	$L_{tot.}$					
ft		pounds							
841	759	730	25	755					
841	759	242	25	267					
840	760	148	25	173					
840	760	108	25	133					
839	761	86	25	111					
838	762	72	25	97					
837	763	62	25	87					
835	765	55	25	80					
833	767	50	26	76					
831	769	46	26	72					
829	771	42	26	68					
826	774	39	26	65					
					<p>At $L_{tot} = 75$</p> <p>$X_1 = 833$</p> <p>$X_2 = 767$</p> <p>$L_1 = 49$</p> <p>$L_2 = 26$</p> <p>$\theta_1 = 54^\circ$</p> <p>$\theta_2 = 68^\circ$</p> <p>$T_1 = 60.6$</p> <p>$T_2 = 28.1$</p> <p>$D_1 = 35.6$</p> <p>$D_2 = 10.5$</p> <p>$D_{tot} = 25.1$</p> <p>$V = 12.2$ fps</p>				

Figure 38. Sample Tabulation to Solve for Balloon Position.

- a, 5/32 in. dia stabilizing cable
- b, 0.25 in. dia launch cable
- c, 0.25 in. dia microphone cable
- d, 5/32 in. dia ripcord

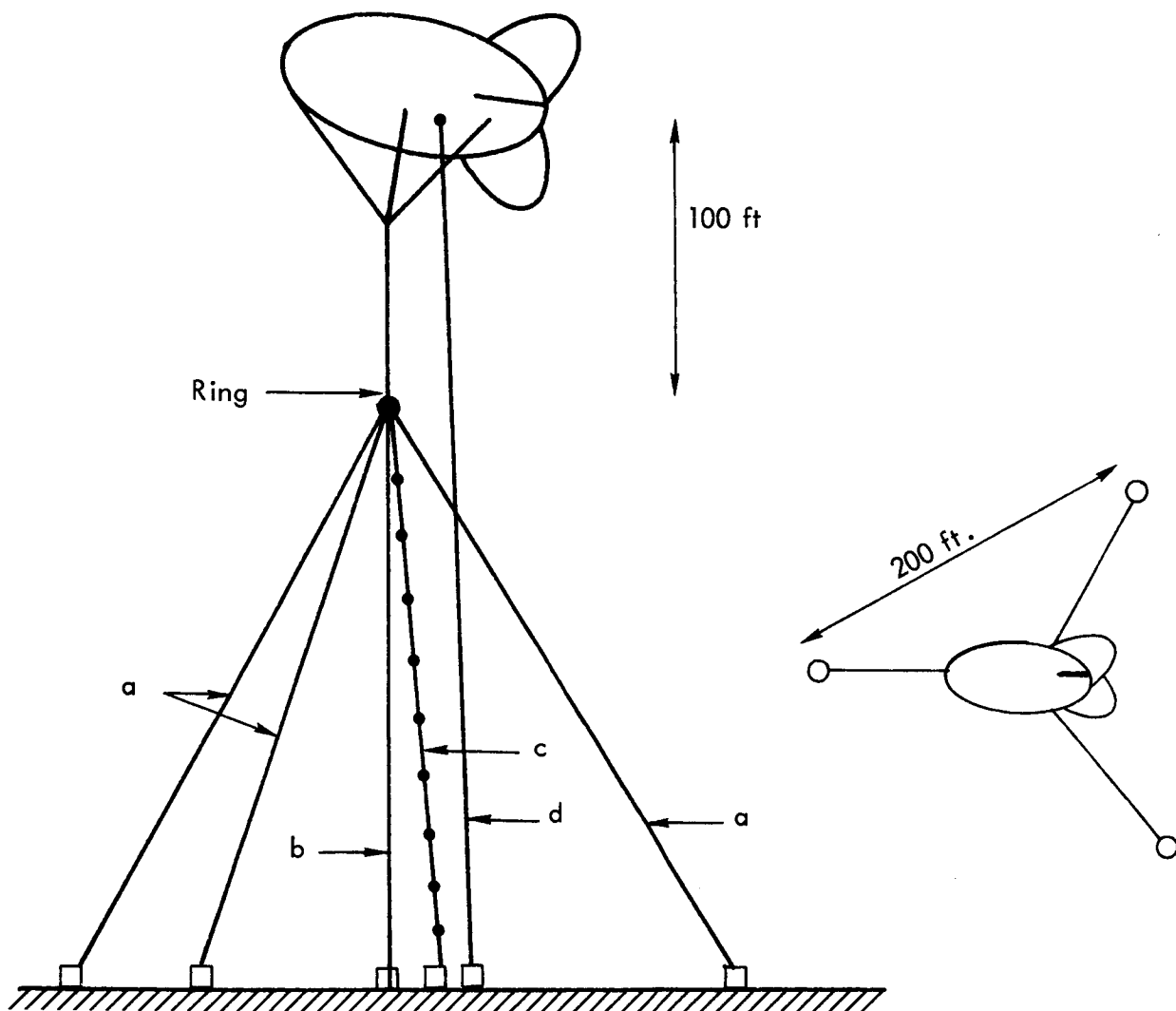


Figure 39. MSFC Balloon Rigging.

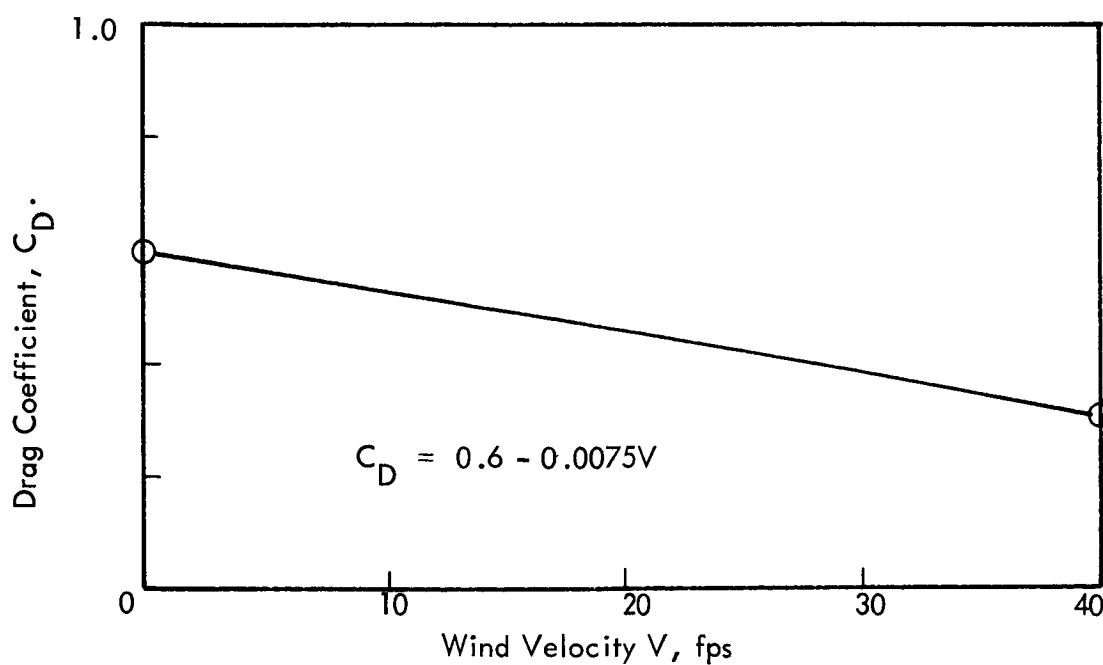
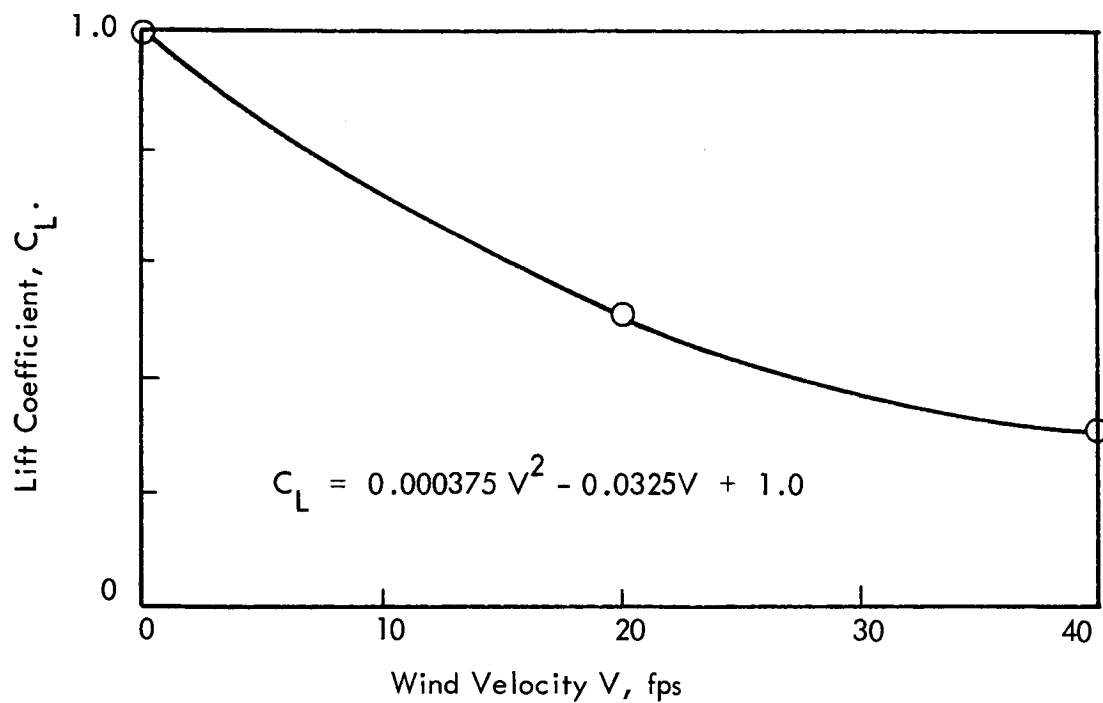


Figure 40. Estimated Aerodynamic Lift and Drag Coefficients for MSFC Balloon.

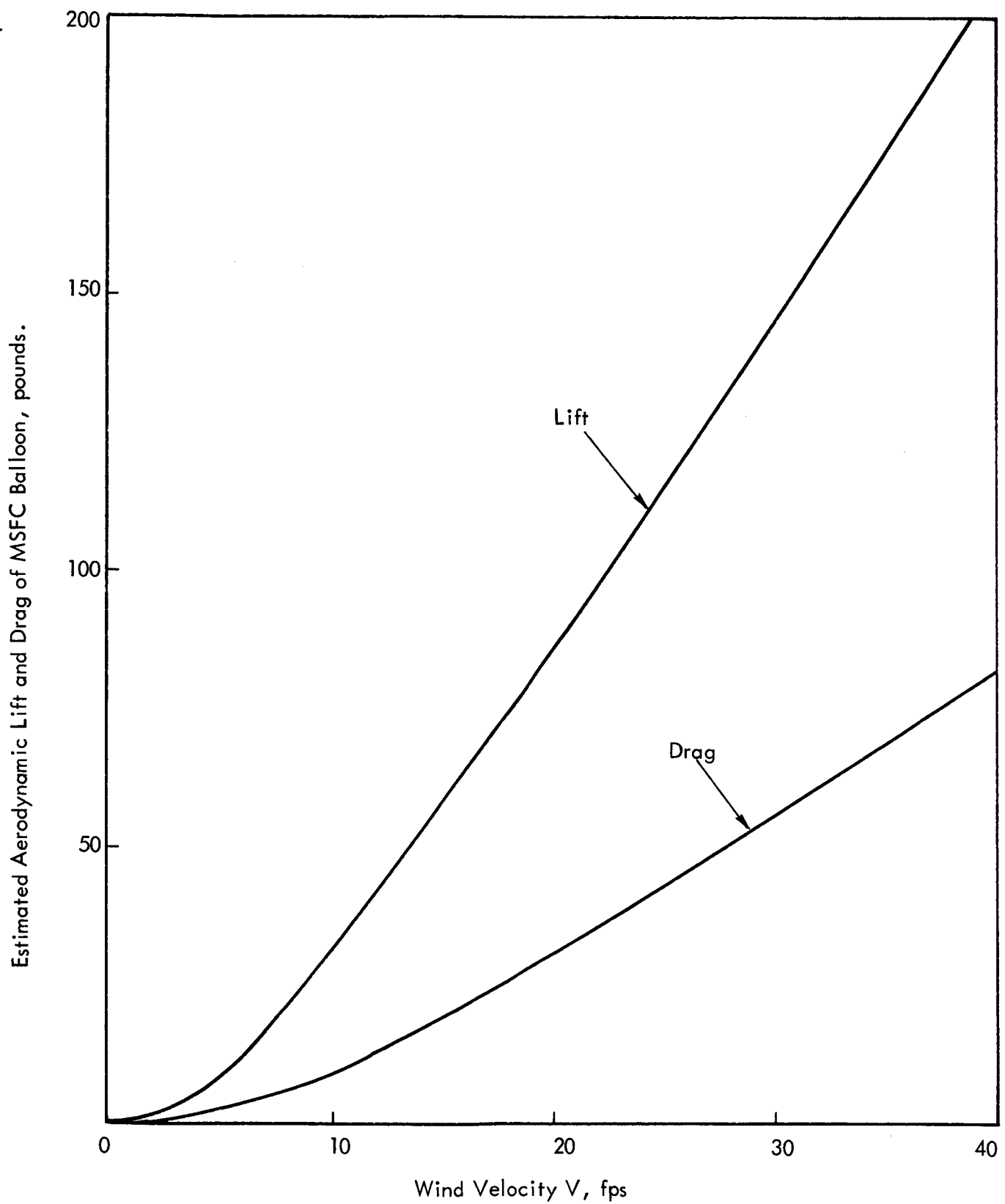


Figure 41. Estimated Aerodynamic Forces of MSFC Balloon.

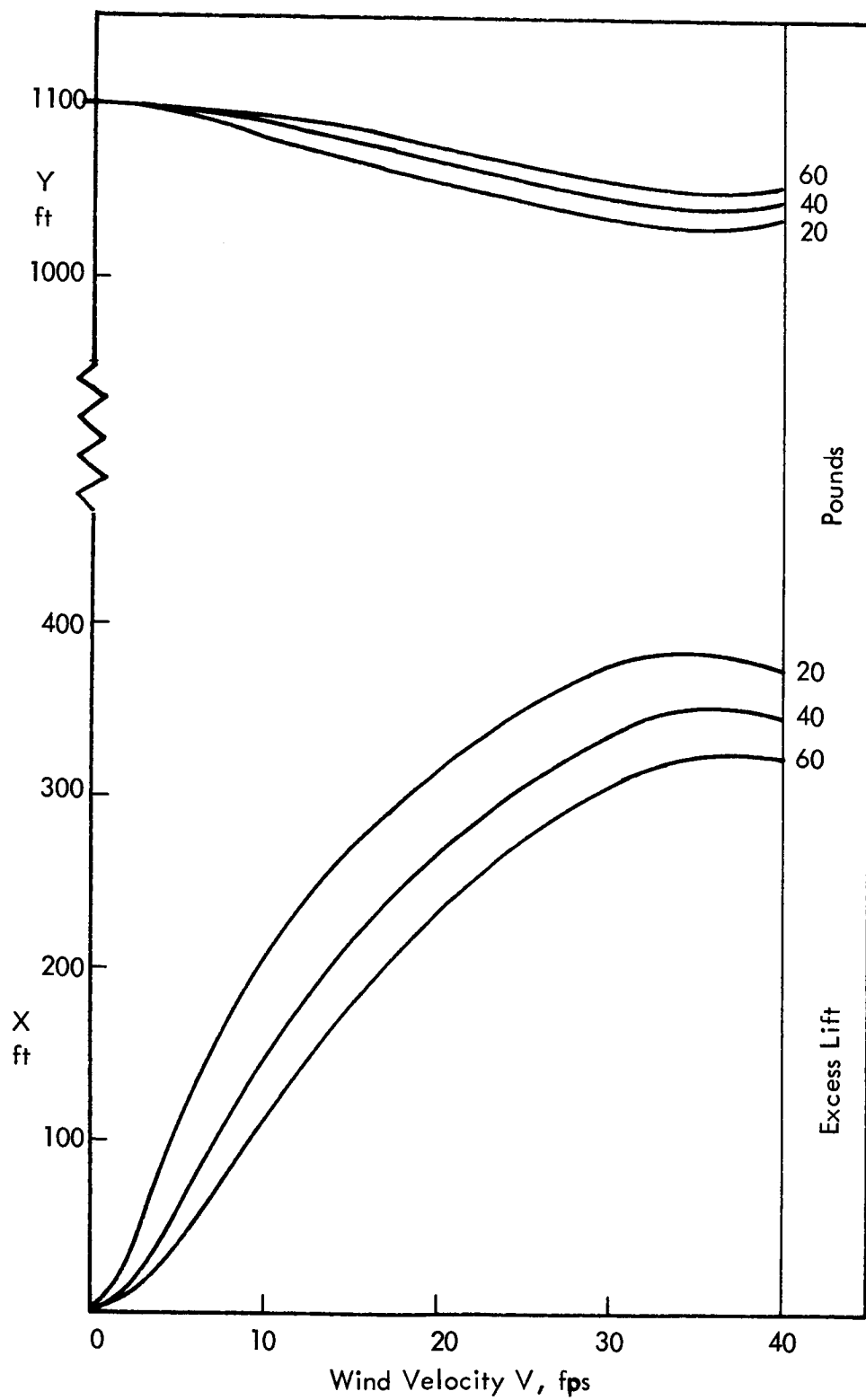
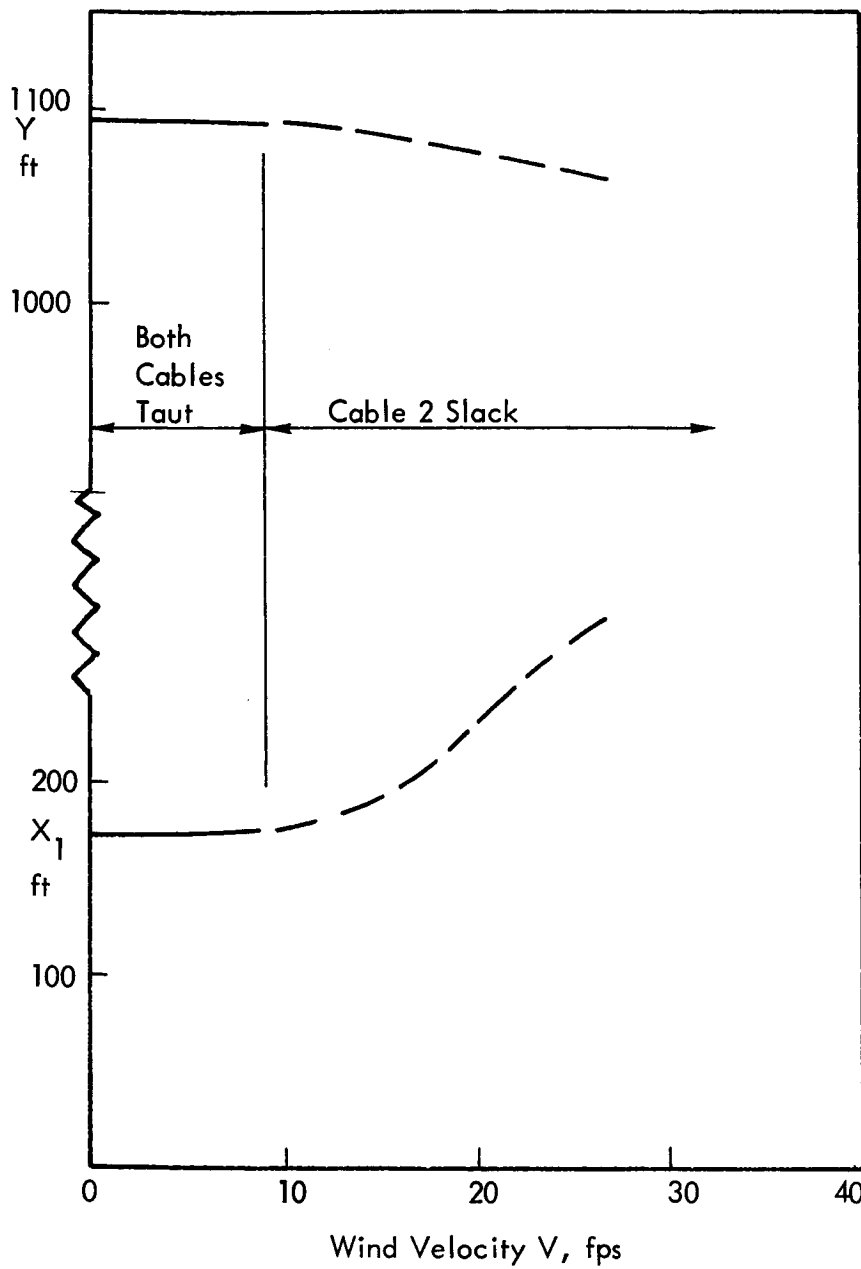


Figure 42. Calculated Behavior of MSFC Balloon on a Single Cable.



Cable 1
1100 ft long
0.006 pound/ft

Cable 2
1095 ft long
0.012 pound/ft

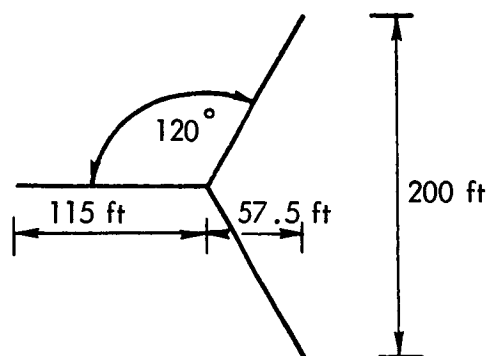
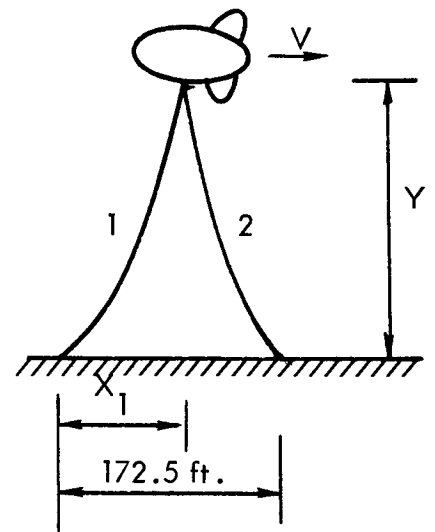


Diagram of
Tethering points

Figure 43. MSFC Balloon, 172.5 ft base.

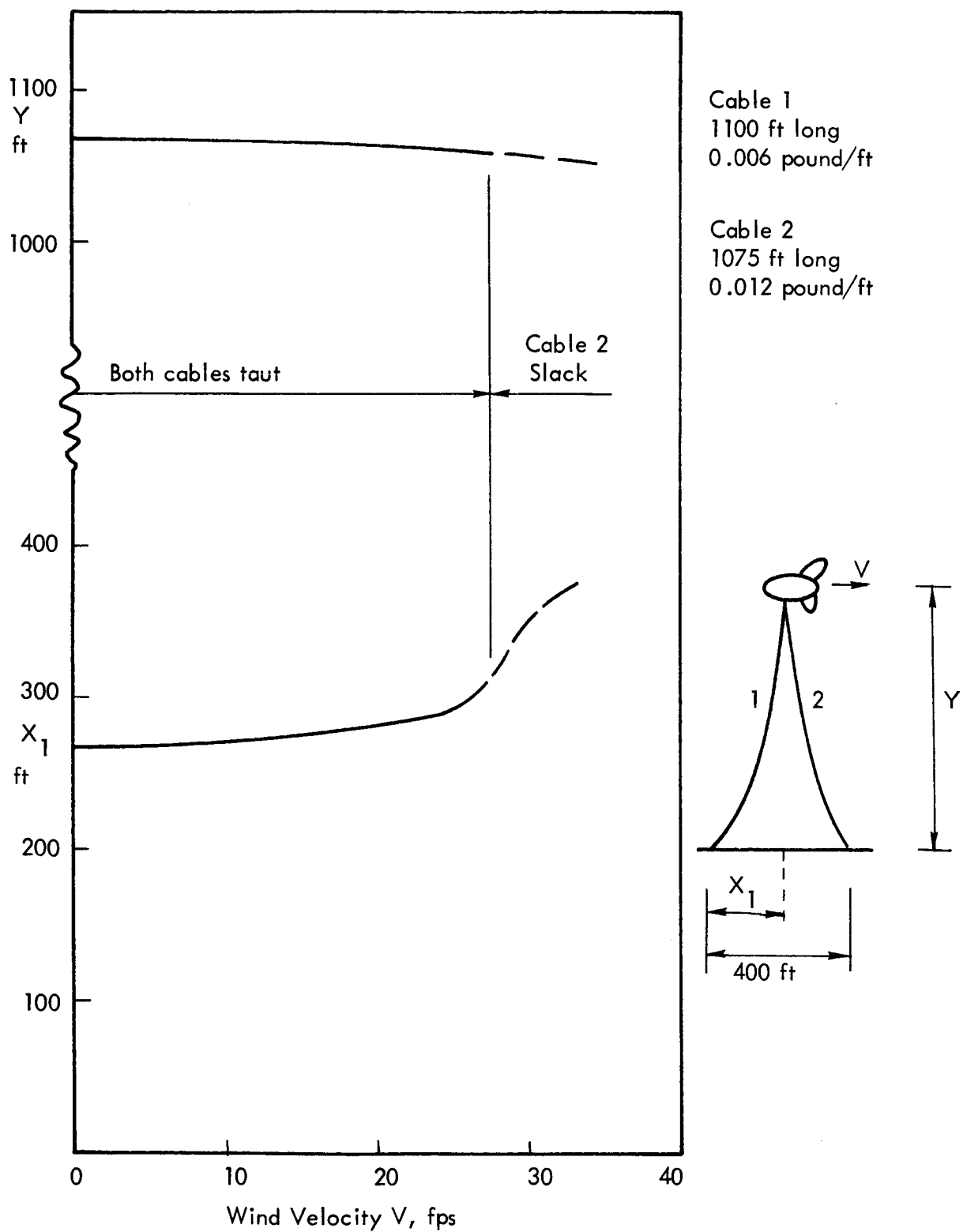


Figure 44. MSFC Balloon, 400 ft base.

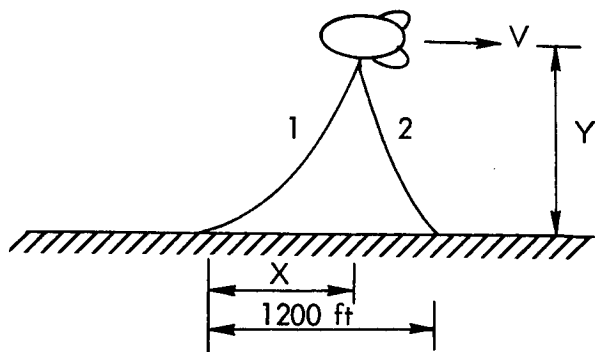
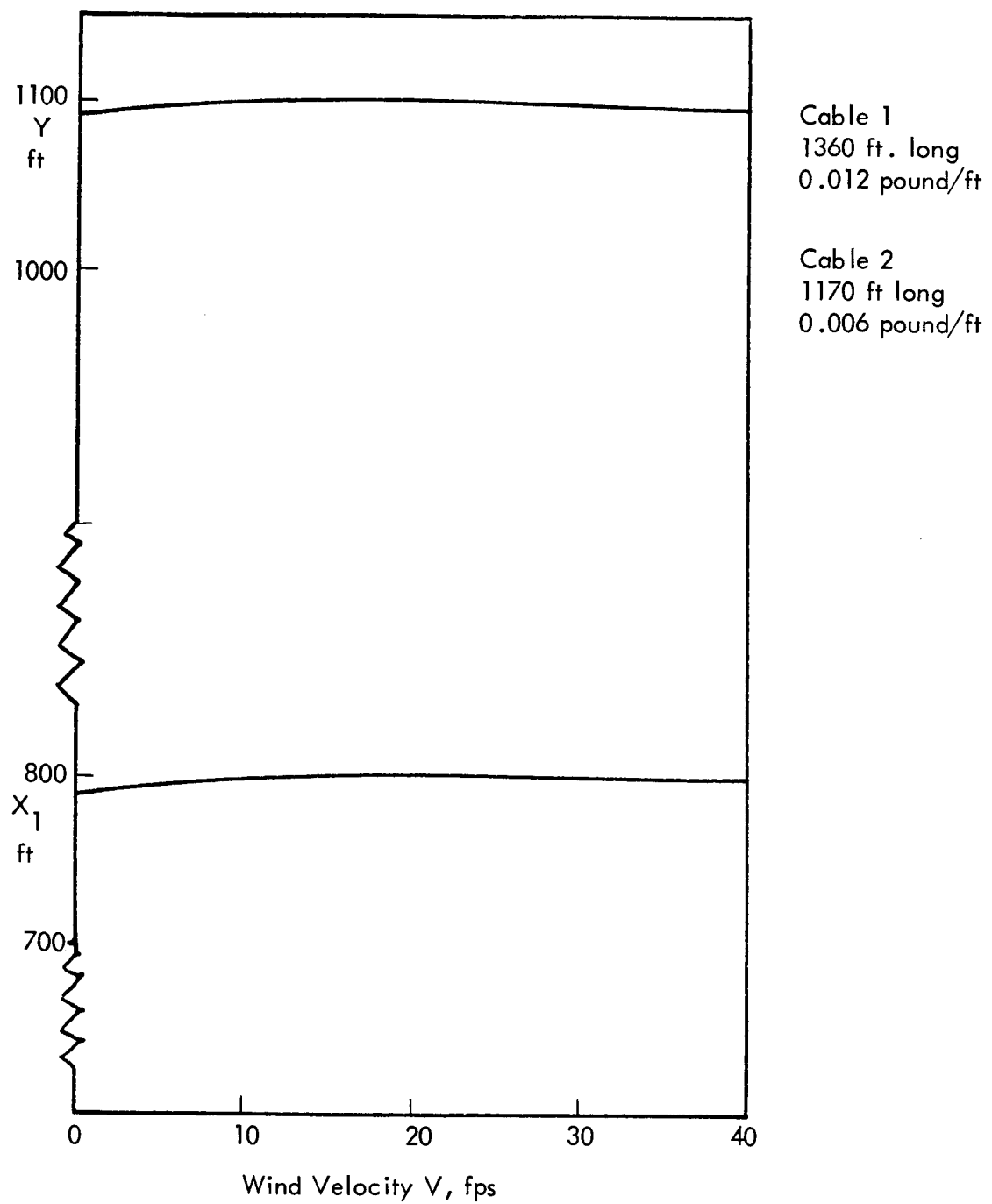


Figure 45. MSFC Balloon, 1200 ft base.